MODELLING STRUCTURE AND PROCESSING CHARACTERISTICS OF A RANDOMLY-FORMED WOOD-FLAKE COMPOSITE MAT

by

CHUNPING DAI

B.Sc., M.Sc., Nanjing Forestry University, 1986.

A THESIS SUBMITTED IN PARTIAL FULFILMENT OF

THE REQUIREMENTS FOR THE DEGREE OF

DOCTOR OF PHILOSOPHY

in

THE FACULTY OF GRADUATE STUDIES

DEPARTMENT OF FORESTRY

We accept this thesis as conforming
to the required standard

THE UNIVERSITY OF BRITISH COLUMBIA

January, 1994

ABSTRACT

The subject of modelling the wood composite manufacturing process has recently attracted more research attention due to the increasing need for a quantitative understanding of the product formation process. The existing models provide little information about wood composite mat structure, which is, like that of any other material, very important to the material properties. In this study, a mathematical model of wood flake mat formation has been developed using geometric probability theory. This model has been applied to further predict the compression behaviour of a wood flake mat during pressing. The model is verified through both experimental observations and computer simulations.

The results show that flake mat formation approximately follows a random process with random flake positions and orientations. This allows a flake mat structure to be fully characterized on a probability basis. Mat structural parameters such as flake centroids, flake coverage and between-flake void sizes are random variables, which are in essence Poisson distributed. Non-uniform flake coverage distribution is an inherent feature of a randomly-formed flake mat. This is why a horizontal density variation always exists in a random flakeboard panel. Due to point-to-point spatial correlation of local flake coverage, the variation of flakeboard density averages in finite sampling zones depends on the zone size, flake size, flakeboard thickness and compaction ratio. Such a relationship is known rigorously through the derivation of a mathematical model and through the visual presentation of the density variation image created by a computer simulation program.

The structural model of mat compression behaviour shows that the pressure applied in a mat during pressing is mainly supported by areas with higher wood coverage. Because of the random distribution of local flake coverage, a wide stress variation exists among the constituent wood elements from location to location in the mat field. Considering wood as a porous material, the void volume in a mat is composed of two components: within- and between-flake voids. Their relative volumetric change during mat compression is considerably different. Equations derived for calculating inter-flake bonded area change indicate a highly nonlinear relationship between the relative bonded area and mat compaction ratio. Because of the viscoelasticity of wood, a wood flake mat also exhibits time-dependent compression behaviour during pressing. Using the structure model developed, the stress relaxation of a flake mat has been explicitly related to that of wood. To correlate the creep response of a flake mat to that of wood, a new creep evaluation terminology -- relative creep compaction ratio, should be employed instead of the more common relative creep strain. The creep of a flake mat seems to be affected by its constituents through their average viscoelastic responses.

TABLE OF CONTENTS

ABSTRACT vi

TABLE OF CONTENTS iv

ACKNOWLEDGEMENT vii

PREFACE viii

CHAPTER I.
RATIONALE, CONCEPTS AND RESEARCH OUTLINE 1
- 1.1 INTRODUCTION 1
- 1.2 CHARACTERIZING THE MAT STRUCTURE 2
  - Mat Formation as a Random Process 2
  - Mat Structure and its Importance to Composite Manufacture 3
- 1.3 THEORETICAL BACKGROUND 5
  - Random Coverage Process 5
  - Statistical Geometry of a Fibrous Network 6
- 1.4 OUTLINE OF THE MODEL DEVELOPMENT 7
- REFERENCES 9

CHAPTER II.
FUNDAMENTALS OF A RANDOMLY-FORMED MULTI-LAYERED FLAKE MAT STRUCTURE 11
- ABSTRACT 11
- 2.1 INTRODUCTION 11
- 2.2 MODEL DEVELOPMENT 12
  - 2.2.1 Distribution of Flake Centroids 14
  - 2.2.2 Distribution of Flake Areal Coverage 15
  - 2.2.3 Void Volume Content and Size Distribution 17
    - Between-flake Void Volume Content 17
    - Distribution of Between-flake Void Sizes 18
  - 2.2.4 Inter-flake Bonded Area 22
- 2.3 METHODOLOGY 23
  - 2.3.1 Monte Carlo Simulation 23
  - 2.3.2 Experimental Measurements 24
- 2.4 RESULTS AND DISCUSSION 26
  - 2.4.1 Randomness of the Flake Deposition Process 26
  - 2.4.2 Distribution of Structural Properties 27
    - Poisson Distribution of Flake coverage 27
    - Exponential Distribution of Void Sizes 28

Overall and Average Geometric Properties 28
2.5 CONCLUSIONS 29
REFERENCES 30

CHAPTER III.
HORIZONTAL DENSITY VARIATION IN RANDOMLY-FORMED FLAKEBOARDS 44
ABSTRACT 44
3.1 INTRODUCTION 44
3.2 MATHEMATICAL MODEL 46
3.2.1 Variation of Point Density 47
3.2.2 Point-to-point Spatial Correlation 49
3.2.3 Distribution of Local Density Averages 52
3.3 RESULTS AND DISCUSSION 54
3.3.1 Computer Simulated Images of Flakeboard Density 54
3.3.2 Distribution of Flakeboard Density 55
3.3.3 Typical Predicted Results 57
Effect of Flake Sizes 57
Effect of Flakeboard Thickness 58
3.4 SUMMARY AND CONCLUSIONS 58
REFERENCES 60

CHAPTER IV.
COMPRESSION BEHAVIOUR OF RANDOMLY-FORMED WOOD FLAKE MATS 77
ABSTRACT 77
4.1 INTRODUCTION 77
4.2 THEORY 80
4.2.1 Compression Stress-strain Relationship of Flakes 81
4.2.2 Pressure-thickness Relationship of Flake Mats 82
4.2.3 Void Volume Change 83
4.2.4 Inter-flake Bonded Area Change 85
4.3 EXPERIMENT 85
4.3.1 Materials 86
4.3.2 Procedures 86
4.4 RESULTS AND DISCUSSION 87
4.4.1 Flake Compression Modulus and Strain Function 87
4.4.2 Compression Response of Flake Mats 88
Validation of the Model 88
Effect of Flake Properties 89
Local Stress Distribution 90
4.4.3 Predicted Results of Internal Structure Change 91

Void Volume Content 91
Relative Inter-flake Bonded area 91
4.5 SUMMARY AND CONCLUSIONS 92
REFERENCES 94

CHAPTER V.
VISCOELASTICITY OF RANDOM WOOD-FLAKE MATS DURING PRESSING 106
5.1 INTRODUCTION 106
5.2 BACKGROUND 107
5.2.1 Viscoelasticity of Wood and Other Cellular Materials 107
5.2.2 Rheological Behaviour of Wood Composite Mats 109
5.3 A STRUCTURAL MODEL OF MAT STRESS RELAXATION 110
5.4 MATERIALS AND EXPERIMENTAL PROCEDURE 114
5.5 RESULTS AND DISCUSSION 115
5.5.1 Flake Stress Relaxation 115
5.5.2 Mat Stress Relaxation 116
5.5.3 Creep 118
5.6 CONCLUSIONS 119
REFERENCES 121

CHAPTER VI.
CONCLUDING REMARKS 137
6.1 GENERAL REMARKS 137
6.2 NATURE AND CONTRIBUTIONS OF THE MODEL 137
6.3 FURTHER RESEARCH WORK 139
Model Modification and Development 139
Experimental Tests 140

APPENDIX: NOMENCLATURE 141

ACKNOWLEDGEMENT

I would like to thank my supervisor - Dr Paul Steiner, Faculty of Forestry, UBC, for his invaluable advise and help throughout this research. Thanks also go to Dr. David Barrett and other committee members: Dr. Simon Ellis and Dr. Stavros Avramidis, Faculty of Forestry, UBC, and Dr. Suezone Chow, Canfor Research and Development Centre. I wish to thank Dr. David Tait for his help in discussions on mathematical problems.

I would like to thank Rob Johnson, Bob Myronuk and Avtar Sidhu for laboratory assistance. Other help from Pingbo Xiong, Qiyi He and Andrew Goodison is also readily acknowledged.

Financial support from Weyerheauser Canada for my Ph. D studies is gratefully acknowledged.

Finally, my greatest gratitude goes to my wife - Linyun for her patience, understanding and support for my educational studies.

PREFACE

Part of the material in this thesis has been prepared in manuscript form and accepted for publication. It includes the following papers:

1. Dai, C. and P. R. Steiner. 1994. Spatial structure of wood composites in relation to processing and performance characteristics: Part II. Modelling and simulation of a randomly-formed flake layer network. Wood Sci. and Technol. No.3 (in press).
2. _____ and ____. 1994. Spatial structure of wood composites in relation to processing and performance characteristics: Part III. Modelling the formation of multi-layered random flake mats. Wood Sci. and Technol. No.4 (in press).
3. _____ and ______. 1993. Compression behaviour of randomly-formed wood flake mats. Wood and Fibre Sci. Vol.25, No.5 (in press).

The above papers have been prepared by the thesis author under the supervision of Dr. Paul R. Steiner.

CHAPTER I. RATIONALE, CONCEPTS AND RESEARCH OUTLINE

1.1 INTRODUCTION

The changing world forest resources and challenges from other materials have forced wood researchers and manufacturers to improve the existing product quality and develop more value added wood composites from a lower quality wood base. This requires a profound understanding of the wood composite manufacturing process, which is a combination of physical, mechanical and chemical processes involving a number of variables. For a long time, wood composite manufacture technology has been investigated predominantly on an empirical basis and a large body of experimental results have been reported (e.g., Kelly, 1977). These investigations provide some general knowledge about the relationship between the production variables and the product properties. However, empirical approaches are usually expensive and time-consuming, and the results are sometimes inconclusive. Moreover, the limited number of parameters allowed in an individual test may effectively prevent a systematic analysis of a full manufacturing process. Realization of these deficiencies has suggested the importance of analytical approaches. Thus the subject of modelling the wood composite formation process has recently attracted more research attention (Harless et al, 1987; Humphrey and Bolton, 1989; Kamke and Wolcott, 1991; Wolcott, 1990; Suchsland and Xu, 1989, 1991).

These models, although still in their development stages, seem to be classified into three different categories. Firstly, phenomenological models have been presented to predict the hot-pressing behaviour by treating discrete wood composite mat as a continuum

(Humphrey and Bolton, 1989; Kamke and Wolcott, 1991; Harless, et al, 1987). Secondly, fundamental compression properties of solid wood flakes have been modelled to simulate the consolidation response of wood composite mats during pressing (Wolcott, 1990). Finally, narrow veneer strips have been used to simulate the effect of mat structure in flakeboard manufacture (Suchsland and Xu, 1989, 1991). These models appear generally complementary to each other, since the macro-behaviour of a wood composite mat should be ultimately related to the mechanical properties of individual wood elements and their spatial configuration. However, a quantitative analysis of this relationship requires an explicit model of wood element arrangement in the mat structure. In fact, an appreciation of the structure of a mat, is definitely a prerequisite for fully understanding the processing and performance characteristics of wood composites.

The general working hypothesis is that the behaviour of wood composites can be adequately predicted if the properties of raw wood elements, mat structure, adhesive and hot-pressing parameters are known. Therefore, the specific objectives in this study are to develop a mathematical model of a flake mat structure and to further demonstrate how this structural model can be used to predict other wood composite properties based on the knowledge of solid wood.

1.2 CHARACTERIZING THE MAT STRUCTURE

Mat Formation as a Random Process

Depending on end-uses, there are many criteria that govern the design of a wood composite manufacturing process. No matter what type of products are being made, one criterion which always affects the way a mat is formed is that wood elements should be deposited as uniformly as possible. It would be desirable that wood mass content at any point throughout the mat area is identical. Such an ideal, uniform mat structure may only be achieved by precisely positioning and orienting each wood element in a pre-determined arrangement during the formation process. This procedure may not be practically viable.

In real life, a "uniform" mat is produced by randomly dispersing wood elements into a mat plane whereby individual elements can drop independently and have an equal chance to be placed at any spot in the mat area, with identical probability to be oriented at any angle. Thus practical mat formation is essentially a random process, in which the individual element deposition is not carefully controlled but occurs on a uniformly-random probability basis. As a result, the whole mat is a random structure with its local geometric properties being random variables, which, like those in any other random system, are not identical. For example, as one could imagine the number of wood elements intercepted by a infinitely thin needle passing vertically through a random mat varies from location to location. This type of non-uniformity is an inherent feature of a randomly-formed wood composite mat.

Mat Structure and its Importance to Composite Manufacture

In relating wood composite mat formation to processing and the resultant product performance, three major structural aspects need to be characterized: point-to-point wood element coverage, inside-mat void volume and inter-element contact area. As mentioned previously, the most noticeable structural feature of a random mat is the non-uniform wood element coverage, i.e., the varying number of elements overlapping at different locations in the mat area. First of all, non-uniform element coverage contributes structurally to unique mat consolidation behaviour as the applied pressure is mainly supported by higher wood coverage areas. The more wood elements a local mat area contains, the greater stress it shares. Secondly, since the hot-pressing may have little effect on the horizontal mat configuration, the non-uniform wood distribution will be retained after pressing and govern the horizontal density variation in the resulting product. Finally, heat and mass transfer in a mat during hot-pressing may also depend on local wood coverage variation since heat and moisture movement is affected by mat density.

A loose wood mat contains a large portion of void volume. Considering wood itself is a porous material, the total void volume may be classified into two parts: between- and within-element voids. While the characteristic of within-element void volume reflects that of the solid wood structure, the variation of between-element void determines the heat convectivity and conductivity and moisture permeability in a mat. Therefore, knowledge about the void volume inside a mat will help to more fully understand the mechanism of the heat and mass transfer during the hot-pressing.

One of the most important parts of the wood composite manufacturing process is to promote bonding through developing intimate element-to-element contact by compacting the mat structure. The relationship between inter-element contact and the mat compaction ratio depends on the initial mat formation. Due to the random variation of wood element coverage, a wide distribution of local inter-element contact is expected in a composite panel. Hence, characterization of the inter-element contact behaviour in a mat can provide insight into how internal bond strength is developed during the wood composite manufacturing process.

1.3 THEORETICAL BACKGROUND

In seeking a theory to develop a mathematical model of a wood composite mat structure, probability, or specifically, geometric probability theory is found to be very useful. This theory is suitable for wood composites because the localized structural properties in a randomly-formed mat are random variables, which can best be characterized on a probability basis. Conventional probability theory is created for describing random events independently occurring in one-dimensional space, for example, time. When it comes to multi-dimensional space problems, the spatial geometry becomes a factor. In this regard, such common terms as "geometric probability", "statistical geometry", "coverage process" and "random fields" may be referred to as more or less the same mathematical domain. Since a wood composite mat is a multi-layered structure with elements being placed in a plane parallel to each other, a two-dimensional model is considered to be adequate for this study.

Random Coverage Process

A two-dimensional stochastic coverage process is thought of as any random mechanism governing the positioning and configuration of random flat sets in the plane (Hall, 1988). Coverage process theory states that if the centroids of the sets are randomly placed in the plane, the number of the centroids contained in any sampling zone in the plane area is Poisson distributed.

If more than one set randomly drop into the plane, random overlap between the sets will occur. Thus some areas will contain more sets than other areas. Such non-uniform random set coverage over the plane is characterized by a Poisson distribution, as well. This distribution describes the relationship between the number of sets overlapping and its corresponding relative coverage area. Such two-dimensional coverage process is analogous to our wood composite mat formation process. Therefore, the theory can be applied to the random mat structure.

Statistical Geometry of a Fibrous Network

The theory on the geometry of a fibrous network, specifically, paper, has also been found to be closely relevant to the structure of a wood composite mat. This statistical geometric theory was developed first by Kallmes and Corte (1960), Kallmes et al (1961), Corte and Lloyd (1966) and later by Dodson (1971).

A random fibre deposition was generally assumed for a paper making process. Under this assumption, a number of structural parameters of the fibrous network including fibre coverage were found to follow the Poisson distribution (Kallmes and Corte, 1960), which is a feature also seen in the random set coverage process (Hall, 1988) as described previously. A very important structural property in paper is the void size variation in the fibrous network. Based on the probability geometry of polygons formed by random lines in a plane (Miles, 1964 a, b), a modified exponential distribution model was developed for characterizing the sizes of voids in a paper layer (Kallmes and Corte, 1960; Corte and

Lloyd, 1966).

The formation of paper has often been characterized quantitatively by one parameter -- the variation of areal density (total fibrous mass in a finite sampling zone divided by zone area). An analytical model for predicting the spatial variation of areal density has been developed by Dodson (1971). His analysis was based on the derivation of the isotropic point autocorrelation function of fibre coverage. Then the variance partition technique by Matern (1960) was employed to relate the density variance in a finite sampling zone to that at a point which was known by a Poisson distribution. This analysis suggests a very promising approach to characterizing the horizontal density distribution in a randomly-formed wood composite panel.

1.4 OUTLINE OF THE MODEL DEVELOPMENT

For our initial model development, uniform flake-type wood geometry is assumed with all elements in a mat of the same length, width and thickness. A basic assumption made during the analysis is that the flake deposition follows a random process, with each flake being randomly placed at any point in the mat area and randomly oriented at any angle with respect to an arbitrarily chosen direction. This allows the mat structure to be fully characterized on a probability basis.

The complete analysis, with the ultimate objective of modelling the flake-type wood composite manufacturing process, is presented in two parts: mat structure and mat compression behaviour. In the first part, a number of fundamental structural aspects of a random flake mat are characterized in Chapter II. Then Chapter III focuses on the development of a horizontal density variation model in a random flakeboard panel based on the concepts of probability geometry. At the same time, a computer program is developed using the Monte Carlo simulation technique. This program provides a rapid and comprehensive evaluation of a mat structure using inputs from simple experimental observations or on a pure simulation basis. The outcomes from the experimentally formed, computer simulated and mathematically modelled mats are compared.

The second part of the analysis demonstrates how to use the mat structure model to further simulate the consolidation behaviour of a flake mat during pressing. In Chapter IV, a theoretical model for predicting instantaneous response of a random flake mat during pressing is developed based on the mat structure and the mechanical properties of wood flakes. Equations are also derived for the calculation of structural changes, such as void volume changes, inter-flake contact area development during mat pressing process. Chapter V deals with the viscoelasticity behaviour of a flake mat in pressing. A structural model is developed to predict the time-dependent mat responses.

Finally, a brief summary on the general approach and nature of the proposed model and the major conclusions drawn from the analysis, as well as the further research work concerning this area is presented in Chapter VI.

REFERENCES

1. Corte, H. and E. H. Lloyd. 1966. Fluid flow through paper and sheet structure. In: Bolam, F. (ED.): Consolidation of the paper web. 2: 981-1010. London: Tech. Sect. British Paper and Board Makers Association.

2. Dodson, C. T. J. 1971. Spatial variability and theory of sampling in random fibrous networks. J. Roy. Statist. Soc. B. 33(1): 88-94.

3. Kelly, M. 1977. Critical review of relationships between processing parameters and physical properties of particleboard. General Technical Report FPL-10. pp 65. U.S. Forest Product Lab: Madison, Wisconsin.

5. Hall, P. 1988. Introduction to the theory of coverage processes. New York: John Wiley & Sons.

6. Harless, P. E., F. G. Wagner, P. H. Short, R. D. Seale, P. H. Mitchell, and D. S. Ladd. 1987. A model to predict the density profile of particleboard. Wood Fiber Sci. 19: 81-92.

7. Humphrey, P. E. and A. J. Bolton. 1989. The hot pressing of dry-formed wood-based composites: Part II. A simulation model for heat and moisture transfer, and typical results. Holzforschung. 43(3): 199-206.

8. Kallmes, O. and H. Corte. 1960. The structure of paper, I. The statistical geometry of an ideal two dimensional fiber network. Tappi. 43(9): 737-752.

9. ____ , ______ and G. Bernier. 1961. The structure of paper, II. The statistical geometry of a multiplanar fiber network. Tappi. 44(7): 519-528.

10. Kamke, F. A. and M. P. Wolcott. 1991. Fundamentals of flakeboard manufacture: wood-moisture relationships. Wood Sci. Technol. 25: 57-71.

11. Matern, B. 1960. Spatial variation. Stochastic models and their application to some problems in forest surveys and other sampling investigations. Meddelanden Fran Statens Skogsforskningsinstitut, Band 49, Nr 5. Stockholm.

12. Miles, R. E. 1964a. Random polygons determined by random lines in a plane. I. Pro. Natl. Acad, Sci. USA 52: 901-907.

13. ____ . 1964b. Random polygons determined by random lines in a plane. II. Pro. Natl. Acad, Sci. USA 52: 1157-1160.

14. Wolcott, M. P. 1990. Modelling viscoelastic cellular materials for the pressing of wood composite. Ph.D. dissertation, VPI&SU. Blacksburg, VA.

15. Suchsland, O. and H. Xu. 1989. A simulation of the horizontal density distribution in a flakeboard. For. Prod. J. 39(5): 29-33.

16. ____ and ______. 1991. Model analysis of flakeboard variables. For. Prod. J. 41(11/12): 55-60.

CHAPTER II. FUNDAMENTALS OF A RANDOMLY-FORMED MULTI-LAYERED FLAKE MAT STRUCTURE

ABSTRACT. A mathematical model for describing the structure of a randomly-formed multi-layered flake mat network is presented. The structural properties of the flake network are random variables which are, in essence, characterized by the Poisson and exponential distributions. The model predicts distribution of: flake centres, flake areal coverage, free flake length, and void size in the multi-layer flake network. A computer program for simulating the random flake network and rapidly evaluating structural properties is developed as well. In addition, the structural properties of hand-formed flake mats are experimentally measured. Close agreement is found between mathematical model prediction, computer simulation and experimental measurements.

2.1 INTRODUCTION

The previous chapter has discussed the rationale for developing a mathematical model of wood composite mat structure. In this chapter, such a model for describing the structure of a random flake mat will be developed along with the presentation of a computer simulation program. The specific objectives are:

1. To explicitly define the random flake deposition process and the nature of multi-layered mat formation;
2. To apply geometric probability theory to mathematically characterize the flake-type wood mat structure;

3. To develop a computer program to simulate the mat formation process and to evaluate the mat structural properties;

4. To compare the mathematical predictions with the computer simulations and experimental observations to verify the proposed model.

2.2 MODEL DEVELOPMENT

A randomly-formed flake mat has more or less a layered structure since all flakes essentially lie parallel to the horizontal plane of the mat. Such a structural feature best manifests itself in a two, rather than three dimensional geometric model. The approach of using a two-dimensional model to describe the mat structure has the following advantages:

1). Structure of the geometric model becomes more mathematically tractable. A complete three-dimensional description of voids inside the mat, for instance, would encounter almost insurmountable mathematical difficulties;

2). A constituent layer can be prepared in laboratory and the flake arrangement can be directly measured. This makes it possible to appreciate the nature of the problems and to experimentally test the mathematical model.

For this descriptive model a multi-layered random flake mat is defined herein as a summation of N_L two-dimensional randomly-arranged flake layers. A random flake layer is defined here as a plane of area A where a limited number N_f/N_L (N_f: total number of flakes in the mat) of flakes with length λ, width ω and thickness τ are independently and identically placed by a random process. Thickness τ is so thin that all flakes lie parallel to the plane, with coverage area (i.e., projected area) of each flake equal to $\lambda\omega$. The number of layers N_L in a mat is determined in such a way that total flake coverage area in each layer, $\lambda\omega N_f/N_L \leq A$. A random flake mat formation process is explicitly defined as follows:

1). Each flake is deposited independently of another;

2). Each flake has an equal opportunity of being placed at any point in the mat area, i.e., the flake centroid position (or any specified point on the flake) is randomly distributed in the mat plane; and

3). Each flake has an equal probability of being oriented at any angle in the mat plane, i.e., the angle between flake length axis (or any specified axis along the flake surface) and any given reference axis along the mat plane is uniform randomly valued in range [0, 180].

Because of its stochastic nature the structure of such a randomly arranged flake network can be best theoretically characterized by applying geometric probability theory. As mentioned in Section 1.3, this theory has been successfully utilized to model the structure of fibrous paper sheets (e.g., Kallmes and Corte, 1960; Kallmes et al, 1961; Kallmes and Bernier, 1963; Dodson, 1971).

To analyze random systems, mathematicians have created many special distributions for characterizing the random variables. Thus it is the first step to determine which distribution form suits the random variables that are of interest in this modelling process. The one that is most suitable for a random flake deposition process is the Poisson process, which is an approximation of the well known binomial distribution. In the field of stochastic processes, the Poisson distribution is preferably used due to the fact that it is well documented and easy to manipulate.

2.2.1 Distribution of Flake Centroids

As far as flake position is concerned, a random mat formation means an independent and uniformly-random distribution of flake centroid points in a two dimensional plane. To characterize such random point distribution, one could divide the mat plane of area A into a number of non-overlapping congruent zones with area of s, and evaluate the flake centroid counts in s and their corresponding probabilities. Let us first consider the simplest case where only one flake randomly drops onto the plane. Then the chance for an arbitrarily chosen zone s to contain this flake centroid will equal the zone-to-plane areal ratio, i.e., s/A. In other words, the probability that the flake centroid does not lie within this zone is $1-s/A$. Therefore, this random-flake-drop case is essentially one trial of a random experiment which has only two possible outcomes, i.e., "success" which means s contains the flake centroid, or "failure" which means s does not contain the flake centroid.

For N_f uniformly random distributed flakes (i.e., N_f trials) over the area A as shown in Fig.2.1, the actual number of flake centers (i.e., number of successes) contained in a zone s is a random variable. The probability that any zone s contains exactly j flake centres, $p_c(j)$, is given by the binomial distribution, which can be approximated using the Poisson distribution when N_f increases and s/A becomes very small together in such manner that $N_f/A \rightarrow \gamma$ $(0 < \gamma < \infty)$, i.e. (Hall, 1988),

$$
\begin{aligned}
p_c(j) &= \binom{N_f}{j}\left(\frac{s}{A}\right)^j\left(1-\frac{s}{A}\right)^{N_f-j} \\
&= \left(\frac{N_f}{A}s\right)^j\frac{1}{j!}\left(1-\frac{s}{A}\right)^{N_f}\frac{N_f!}{(N_f-j)!\,N_f^{\,j}}\left(1-\frac{s}{A}\right)^{-j} \\
&= \frac{(\gamma s)^j}{j!}\left(1-\frac{s}{A}\right)^{N_f}\left[\left(\frac{N_f}{N_f}\right)\left(\frac{N_f-1}{N_f}\right)\ldots\left(\frac{N_f-j+1}{N_f}\right)\right]\left(1-\frac{s}{A}\right)^{-j} \\
&\approx \frac{(\gamma s)^j\, e^{-\gamma s}}{j!} \qquad (2.1)
\end{aligned}
$$

since $(1\text{-}s/A)^{N_f}$ approaches $e^{-\gamma s}$ and both $(1\text{-}s/A)^j$ and term in square brackets approach. Hence, the number of flake centers contained in a zone s is Poisson distributed with mean $\mu_c = \gamma s$. The parameter γ, namely, the mean number of flake centers per unit area content of A, is defined as the intensity of the point Poisson process.

2.2.2 Distribution of Flake Areal Coverage

Another way of applying the Poisson process to mat formation is to use it to describe the distribution of flake coverage over the mat area. As will be seen in the following chapters, the non-uniform flake coverage distribution is an extremely important structural characteristic of a randomly formed flake mat, which is directly related to a number of processing and performance properties of wood composites.

Suppose only one flake of length λ and width ω randomly drops onto and remains within the plane of area A. The probability that any point in A is covered by this flake is merely given by $\lambda\omega/A$, or the chance for the chosen point not being covered by this flake is $1\text{-}\lambda\omega/A$. The situation, however, becomes much more complicated in case of N_f such flakes, because of the likelihood of flakes overlapping (Fig.2.2). Thus, various numbers of flakes could pile up over each point in the plane. If the flake centroid is Poisson distributed with intensity γ, the probability that any arbitrarily chosen point contains i flakes, $p_f(i)$, is given by the Poisson distribution as well, i.e.(Hall, 1988),

$$p_f(i) = \binom{N_f}{i} \left(\frac{\lambda\omega}{A}\right)^i \left(1-\frac{\lambda\omega}{A}\right)^{N_f-i} \approx \frac{(\gamma\lambda\omega)^i \, e^{-\gamma\lambda\omega}}{i!} \tag{2.2}$$

as N_f increases and $\lambda\omega/A$ becomes very small but finite. The approximation is justified because the total number of flakes N_f in a full mat is indeed large (usually >1000) and the flake-to-mat areal ratio $\lambda\omega/A$ for non-veneer wood composites is very small (usually <0.01). Thus the number of flakes covering any point over the mat area A is Poisson distributed with mean $\mu_f = \gamma\lambda\omega$. In fact, the mean flake coverage is always equal to the total coverage area of all flakes divided by the total mat area, no matter how the flakes are distributed, i.e.,

$$\mu_f = \gamma\lambda\omega = \frac{\lambda\omega N_f}{A} \tag{2.3}$$

It is instructive to note that the probability $p_f(i)$ is also interpreted as the fraction of mat area containing i flakes. Therefore, the Poisson distribution (Eq.2.2) can easily provide a quick calculation of fractional area $p_f(i)$ corresponding to flake coverage number i for a given average μ_f, which is, in turn, readily determined (Eq.2.3) if the total flake coverage area $N_f\lambda\omega$ and mat area A are known.

2.2.3 Void Volume Content and Size Distribution

One feature that makes a randomly formed flake mat a unique material is that it is extremely porous. Since wood itself is a porous material, void volume inside the mat is comprised of two parts, i.e., between- and within-flake voids. For a uncompressed flake mat, the inside-flake void volume can be easily calculated if the solid flake density is known. Thus the following concerns only the between-flake void volume.

Between-flake Void Volume Content

To calculate the between-flake void volume content in a flake mat, one must know the mat height. Because of the random distribution of flake coverage, the apparent height of a mat varies locally from point to point. In addition, flakes are not always flat, therefore, measurements of overall mat height could be rather arbitrary. The overall mat height H_0 is defined here as the height of mat where the probability of the flake coverage is approximately 0.001. This permits an analytical approach to estimating H_0 by using Eq. (2.2), i.e.,

$$\frac{(\gamma\lambda\omega)^{H_0/\tau} e^{-\gamma\lambda\omega}}{(H_0/\tau)!} \approx 0.001 \tag{2.4}$$

where τ is the flake thickness.

The between-flake void volume is the difference between the bulk mat volume and total flake volume. Thus the between-flake void volume content, VC_{bf}, is then given by:

$$\begin{aligned} VC_{bf} &= \frac{AH_0 - N_f \lambda \omega \tau}{AH_0} \\ &= 1 - \frac{\gamma \lambda \omega \tau}{H_0} \end{aligned} \tag{2.5}$$

Distribution of between-flake void sizes

To mathematically characterize the true shape of voids between flakes in a three-dimensional mat system can be an extremely difficult task. However, the voids defined by the uncovered areas in two-dimensional flake layer networks in a multi-layered mat system, are of much more describable shapes as they are merely various polygons formed by flake boundaries (Fig.2.2). Therefore, the following analysis will focus on determining how the uncovered polygon areas are distributed. To do so, the distance between adjacent flake crossings, i.e., the free flake length (Fig.2.2), needs to be characterized first.

If a straight line of length L is drawn across the random flake network and intersects N_l flakes (long axes of flakes), the distribution of the number of flakes intersected per unit length of the line will be also Poisson distributed with the mean N_l/L (Kallmes and Corte, 1960). As a result, the probability that the distance m between adjacent intersects is between m and $m+dm$, $p_l(m)$, is given by the exponential distribution, i.e. (Hall, 1988; Kallmes and Corte, 1960; Kallmes and Bernier, 1963),

$$p_l(m) = \frac{e^{-\frac{m}{\mu_l}}}{\mu_l} \tag{2.6}$$

where μ_l is the mean distance, obtained by: $\mu_l = L/N_l$. If the scanning line is viewed as a long axis of a flake, the distance m and, therefore, the distribution $p_f(m)$ will reflect the dimension and distribution of free flake length. Total number of crossings N_c between N_f/N_L (total number of flakes in a layer, N_L: number of layers in a mat) flakes of length λ is given by (Miles, 1964a, 1964b; Kallmes and Corte, 1960):

$$N_c = \frac{(\lambda N_f/N_L)^2}{\pi A} \tag{2.7}$$

As each crossing is shared by two flakes, the average number of crossings of a flake, n_c, is then obtained by:

$$n_c = \frac{2N_c}{N_f/N_L} = \frac{2\gamma\lambda^2}{\pi N_L} \tag{2.8}$$

where N_c is given by Eq.(2.7) and γ is the flake deposition indensity given by N_f/A.

Because n_c crossings separate a flake with n_c+1 segments, the mean free flake length, μ_l, is given by:

$$\mu_l = \frac{\lambda}{n_c+1} = \frac{\pi N_L \lambda}{2\gamma\lambda^2+\pi N_L} \tag{2.9}$$

since n_c is known by Eq.(2.8).

Even for a two-dimensional flake network, exact distribution of void size is usually prohibitively complex, although some progress can be made in working out its properties for the case of one dimension (Hall, 1988). An approximate solution reached by Kallmes and Corte (1960) for two-dimensional fibre network can be modified for the flake layer structure in this work. Assuming the area of individual void, a_v, is proportional, on the average, to square of the free flake length m, i.e.,

$$a_v = \alpha m^2 \tag{2.10}$$

where α is a constant of coefficient. Thus, the distribution of a_v can be obtained through the following transformation:

$$p_v(a_v) = \frac{dm}{da_v} p_l(a_v) = \frac{e^{-\frac{1}{\mu_l}\sqrt{\frac{a_v}{\alpha}}}}{2\mu_l\sqrt{\alpha a_v}} \tag{2.11}$$

since the distribution of m is known by Eq.(2.6).

The mean size of void areas, μ_v, is obtained by:

$$\mu_v = \int_0^\infty a_v\, p_v(a_v)\, da_v = 2\alpha\mu_l^2 \tag{2.12}$$

An equation for calculating the total number of polygons formed by infinitely long lines (Miles, 1964a, 1964b), N_{vo}, was modified for predicting that of voids in a fibre network of paper sheet (Kallmes and Corte, 1960), namely,

$$N_{vo} = (N_{co} - N_{fo})\, e^{-\mu_{fo}} \tag{2.13}$$

where N_{co} is the total number of intersections between N_{fo} fibers or lines and μ_{fo} is the mean fiber coverage. During derivation of the above equation, the effect of fibre width was neglected. However, such effect needs to be incorporated into the equation for a flake network. Thus, a modified equation for calculating the total number of voids in a flake layer, N_v, is:

$$N_v = (N_c' - \frac{N_f}{N_L})\, e^{-\beta \frac{\mu_f}{N_L}} \tag{2.14}$$

where β is a constant, given by: $\beta = 1/(1+\omega/\lambda)$, and N'_c is given by extending λ to $\omega+\lambda$ in Eq.(2.7), namely:

$$N_c' = \frac{((\lambda+\omega)\, N_f/N_L)^2}{\pi A} \tag{2.15}$$

Note that by definition Eq.(2.15) should not invalidate Eq.(2.7) for computing total number of flake crossings.

According to Eq.(2.2), the total void area in a flake layer, A_v, is obtained by:

$$A_v = Ap_f(0) = Ae^{-\frac{\mu_f}{N_L}} \tag{2.16}$$

On the other hand, A_v is determined by: $A_v = N_v \mu_v$. Thus,

$$Ae^{\frac{-\mu_f}{N_L}} = N_v \mu_v \tag{2.17}$$

or combining with Eq.(2.14) and (2.15) so that

$$\mu_v = \frac{Ae^{-\frac{\mu_f}{N_L}}}{N_v} = \frac{\pi N_L^2 e^{(\beta-1)\frac{\mu_f}{N_L}}}{\gamma^2 (\lambda+\omega)^2 - \pi\gamma N_L} \tag{2.18}$$

Combining Eq.(2.18) with Eq.(2.12) and solving for α yield:

$$\alpha = \frac{\pi N_L^2 e^{(\beta-1)\frac{\mu_f}{N_L}}}{2\mu_l^2[\gamma^2(\lambda+\omega)^2-\pi\gamma N_L]} \tag{2.19}$$

2.2.4 Inter-flake Bonded Area

The flake areal coverage distribution as given by Eq.(2.2) can lead to the calculation of inter-flake bonded area, a parameter of interest for predicting the development of internal bond strength of wood composites during the hot-pressing. A potential bonded area results wherever an overlap can occur between a pair of flakes. As shown in Fig.2.3, there are *(i-1)* interfaces or potential bonded areas in a *i*-flake stack. The maximum bonded area in a random flake mat, BA_{max}, resulting from complete mat compression, is determined by:

$$\begin{aligned} BA_{\max} &= \sum_{i=2}^{N_f} (i-1)p_f(i)A \\ &= A[\ \sum_{i=2}^{N_f} ip_f(i) - \sum_{i=2}^{N_f} p_f(i)\ ] \\ &= A\{\ \sum_{i=0}^{N_f} ip_f(i) - [\ p_f(1) + \sum_{i=2}^{N_f} p_f(i) + p_f(0)\ ] + p_f(0)\ \} \\ &= A(\ \gamma\lambda\omega - 1 + e^{-\gamma\lambda\omega}\ ) \\ &\approx A(\ \gamma\lambda\omega - 1\ ) \end{aligned} \tag{2.20}$$

as $\gamma\lambda\omega$ increases. Note that a one-flake "stack" can not form any bonds. The actual bonded areas in wood composites are always less than BA_{max} and are controlled to a great extent by compaction ratio in addition to the effects of the initial mat formation.

2.3 METHODOLOGY

There are two ways to evaluate the structural properties of a flake network and verify the mathematical model developed previously: 1). computer simulation, i.e., the flake network is numerically simulated and the structural properties calculated. 2). direct experimental measurements, i.e., the flake mat is physically formed and its structural properties are measured.

2.3.1 Monte Carlo Simulation

A C x D mm^2 plane representing the area of a layer onto which flakes were to be deposited, was digitized to a resolution unit of 1x1 mm^2 in a two dimensional XY coordinate system. The higher the resolution, the more accurate the simulation. The flake deposition process was numerically simulated by three sets of random variables, x_{fj}, y_{fj}, θ_{fj} ($j=1,2,\ldots,N_f$). Variables x_{fj} and y_{fj} were real numbers generated from a random uniform distribution in the range $[0, C]$ and $[0, D]$ respectively and θ_{fj} in the orientation range $[0, \pi]$. A FORTRAN program for executing the whole simulation process was developed, with inputs to the program being: flake length λ, width ω and total flake number N_f and total mat area A. A typical output featuring a flake network is illustrated in Fig.2.4. In addition, a number of sub-programs for calculating the geometric properties of the structure were written. The calculations included: number of flake centres in a given area (e.g. 25x25 mm^2), total void area and total flake overlap areas, total number of flake crossings, free flake length and its distribution, size of voids and its distribution. The results of the outputs were compared with the experimental measurements and the mathematical model predictions.

2.3.2 Experimental Measurements

The experiments were conducted first by directly measuring the configuration of random flake layer networks and then indirectly evaluating the structure of a multi-layer flake mat using the computer simulation program described previously.

For testing a flake layer, in total 80 aspen flakes of length 83.8 ± 3.1 mm, width 9.31 ± 1.12 mm and thickness 0.8 ± 0.1 mm were prepared. The reason for choosing 80 flakes was to make the expected total flake coverage area 83.8x9.31x80 (=62414.24 mm^2) approximately equal to that of the layer, which was 62500 mm^2. Each flake was marked with its geometric centre and length-wise central axis. A layer area of 250x250 mm^2 was ruled on the surface of a clear plastic plate. Each sample was hand-formed. During the formation process, efforts were made to disperse flakes as randomly as possible and to keep all flake centres inside the ruled area.

A forming box was not used in this process, because the edges of the box could interfere with the randomness of flake deposition. It was not intended to consider this "edge effect" in the present study. However, this created another problem due to the fact that an undetermined portion of flakes would lie out of the defined layer area despite their centres being restricted to inside, resulting in less flake areal coverage than designed. To solve this problem the so-called "torus convention" concept (Hall, 1988) was introduced. Here one could imagined that each flake which protruded out one side of the layer area entered again from the opposite side (Fig.2.5). This concept became more logical when the present layer square was considered as a structural unit of a much larger network in which flakes protruding out of one unit inevitably entered another or vice-versa. It should be noted that the same treatment was made in the Monte Carlo simulation program.

Flake centre positions, flake orientations and some other structural properties were directly measured from the prepared samples with a ruler or angle gauge. To facilitate the determination of void area and regions of one-, two-, three-, four-flake overlap the whole layer network was projected onto a screen and flake outlines drawn onto a piece of paper. By determining the arrangement of overlapping flakes, the nature of individual polygons was differentiated in terms of voids, one-, two-, three-, and four-flake overlap area (see Fig.2.2). The area of each polygon was measured with a planimeter. Besides experimental errors this type of measurement was extremely tedious and time-consuming. To avoid it, the previously described simulation programs were extended to allow to input flake centre positions and orientations of the samples from direct measurements and to calculate the structural properties of interest. Comparison between direct measurements and calculations showed less than 10% discrepancy.

For the test of a 10-layer mat, a total of 800 flakes of the same size were prepared, each marked with a length-wise axis and a geometric centre. These flakes were deposited manually in a random fashion to form a mat (area: 250x250 mm^2). Their orientations and centre positions were measured. The data were entered into a computer program where the configuration of the mat was calculated.

2.4 RESULTS AND DISCUSSION

2.4.1 Randomness of the Flake Deposition Process

A key hypothesis made in the model development is that an ordinary flake mat formation mathematically follows a random process, in which flake centroid positions are regarded as the Poisson points in a two-dimensional field, and flake angle with any fixed reference axis is random. This assumption was tested first by directly counting the number of flake centres per 25x25 mm^2 zone area in five hand-felted flake layers, the distribution of which was then compared with the model prediction (Eq.2.1) and computer simulation results as shown in Fig.2.6a. The experimental results are correlated to those of the Monte Carlo simulations and both are reasonably well predicted by the Poisson distribution. The flake centroids become more closely Poisson distributed when the total number of flakes increased as seen from the comparison between Fig.2.6a (80 flakes) and Fig.2.6b (800 flakes).

The randomness of flake orientation was checked by comparing the number of flakes intersected respectively by two sets of mutually perpendicular scanning lines. The results from both hand-formed and computer-simulated layers (Fig.2.7) indicate no significant preferential flake alignment in either x-axis or y-axis direction. Thus the assumption of randomness of the flake deposition is verified.

2.4.2 Distribution of Structural Properties

Poisson Distribution of Flake Coverage

The distribution of flake areal coverage of 1-layer flake networks (80 flakes) and a 10-layer mat (800 flakes) were compared in Fig.2.8. Again the experimental observations for single layer are fairly well predicted by the computer simulations and mathematical calculations (Eq.2.2) and an excellent agreement is found as the number of layers increase to 10. Thus flake coverage in a random mat is a Poisson variable, which, for example, can vary from as small as 2 to as high as 20 with average of 10 (Fig.2.8b). As will be discussed in the following chapters, such structural variation directly results in a non-uniform horizontal density distribution in the final wood composite products (Chapter 3), and it is also responsible for a unique mechanical behavior of wood flake mats in pressing (Chapter 4 and 5).

According to Eqs.(2.2) and (2.3), the Poisson flake areal coverage distribution $p_f(i)$ depends on the distribution of flake size only through their total coverage area CA_t ($=\lambda\omega N_f$). Thus, it is not affected by changes in either flake length or width provided that CA_t is kept constant. In a real flakeboard manufacturing process, CA_t is usually controlled by the flake thickness τ. Therefore, τ is a determining factor on how flake elements are distributed in the random mat field.

Another interesting fact about the Poisson distributed flake coverage, according to Hall (1988), is that it is not influenced by the alignment of flakes, even though this may have a significant effect on pattern of voids and local flake covered areas. This statement stays true, of course, only if the flake alignment does not interfere with the randomness of flake position distribution during the mat formation process.

Exponential Distribution of Void Sizes

The distribution of void sizes in a two-dimensional flake layer was predicted through the transformation (Eq.2.11) of the exponential distribution of free flake length (Eq.2.6). The results from the experimental measurements and computer simulations were compared with those from the model predictions in Fig.2.9a for free flake length and in Fig.2.9b for void size, and satisfactory agreements between the three procedures exist.

Aside from being useful for estimating void size distribution, the exponential distribution of free flake length is also critical for evaluating the bending stresses of flakes which occur in a mat under pressing. As suggested in Eqs.(2.6) and (2.9), the free length distribution depends on flake length λ and flake deposition intensity γ, and is independent of flake width ω. However, void size distribution is affected by all three flake geometric factors.

Overall and Average Geometric Properties

The experimentally measured, computer-simulated and mathematically predicted overall and average geometric properties are presented in Table 2.1. The model predictions are in excellent agreement with Monte Carlo simulations, and both provide a good estimation of experimental data. This in general justifies the applicability of random probability theory to flake mat formation and verifies the distributional models developed in this work.

2.5 CONCLUSIONS

The geometric probabilistic structure of a randomly formed multi-layered flake mat including distribution of flake centroids, flake areal coverage, free flake length and void volumes was investigated by both mathematical and experimental procedures. A computer program for structural simulation and experimental data acquisition was also developed. The findings of this study are summarized as follows:

1. Formation of a flake mat can be approximated as a random process. A non-uniform distribution of flake coverage over the mat area is the inherent characteristic of such a process.
2. The expected geometric properties of a random flake mat can be adequately modelled by flake length λ and width ω, total flake number N_f and total mat area A.
3. The Poisson distribution and exponential distribution are the essence of all the structural mathematical models.
4. Monte Carlo simulation provides an effective technique for simulating flake networks and rapidly evaluating their structural arrangements.
5. The results of the experimental measurements, the computer simulation and the mathematical prediction are in good agreement. These concepts will be further extended to study the horizontal density ditribution in flakeboards and the structure-processing property relationship of a multi-layered flake mat.

REFERENCES

1. Corte, H. and Lloyd, E. H. 1966: Fluid flow through paper and sheet structure. In: Bolam, F. (Ed.): Consolidation of the paper web. Vol.2:981-1010. London: Tech. Sect. British Paper and Board Makers Association.
2. Dodson, C. T. J. 1971: Spatial variability and the theory of sampling in random fibrous networks. J. Roy. Statist. Soc. B. Vol.33, No.1: 88-94.
3. Hall, P. 1988. Introduction to the theory of coverage processes. New York:John Wiley & Sons.
4. Kallmes, O. and Corte, H. 1960: The structure of paper, I. The statistical geometry of an ideal two dimensional fibre network. Tappi. Vol.43, No.9: 737-752.
5. Kallmes, O.; Corte, H. and Bernier, G. 1961: The structure of paper, II. The statistical geometry of a multiplanar fibre network. Tappi. Vol.44, No.7: 519-528.
6. Kallmes, O. and Bernier, G. 1963: The structure of paper, IV. The free fibre length of a multiplaner sheet. Tappi. Vol.46, No.2: 108-114.
7. Miles, R. E. 1964a: Random polygons determined by random lines in a plane. I. Pro. Natl. Acad. Sci. U.S.A. No.52: 901-907.
8. Miles, R. E. 1964b: Random polygons determined by random lines in a plane. II. Pro. Natl. Acad. Sci. U.S.A. No.52: 1157-1160.
9. Suchsland, O. 1959: An analysis of the particle board process. Michigan Quarterly Bulletin. Vol.42, No.2: 350-372.

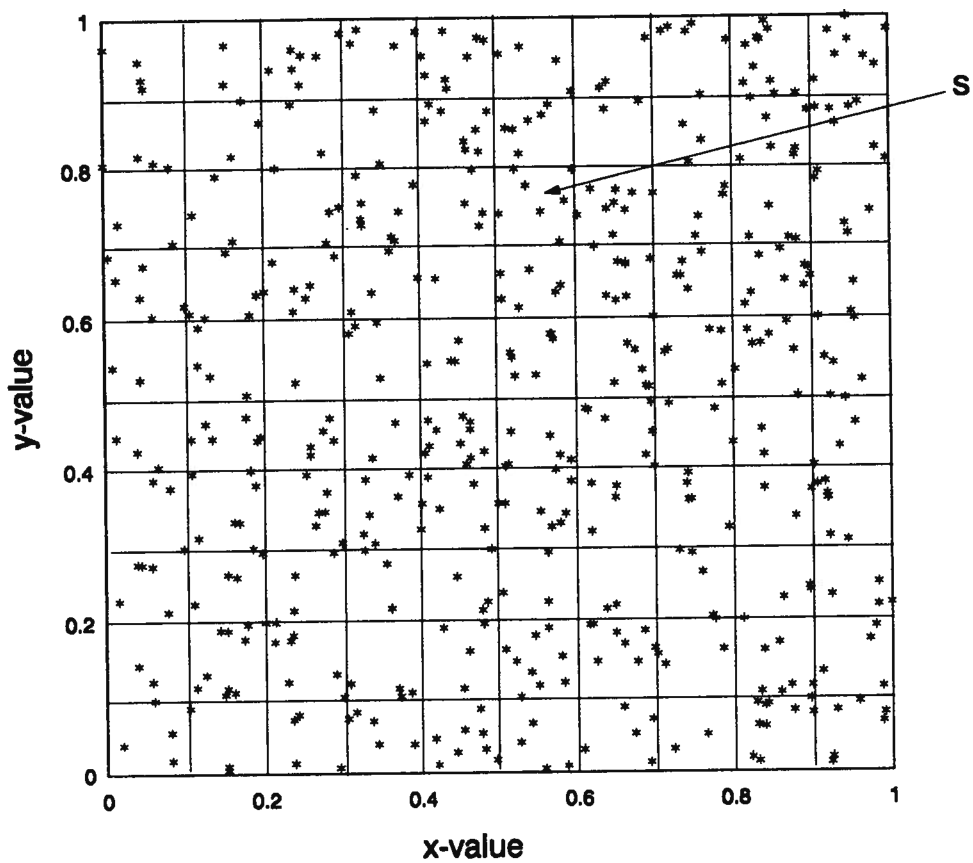

Figure 2.1. **Schematic diagram of uniformly random distribution of 500 flake centroids over 1x1 mat area.**

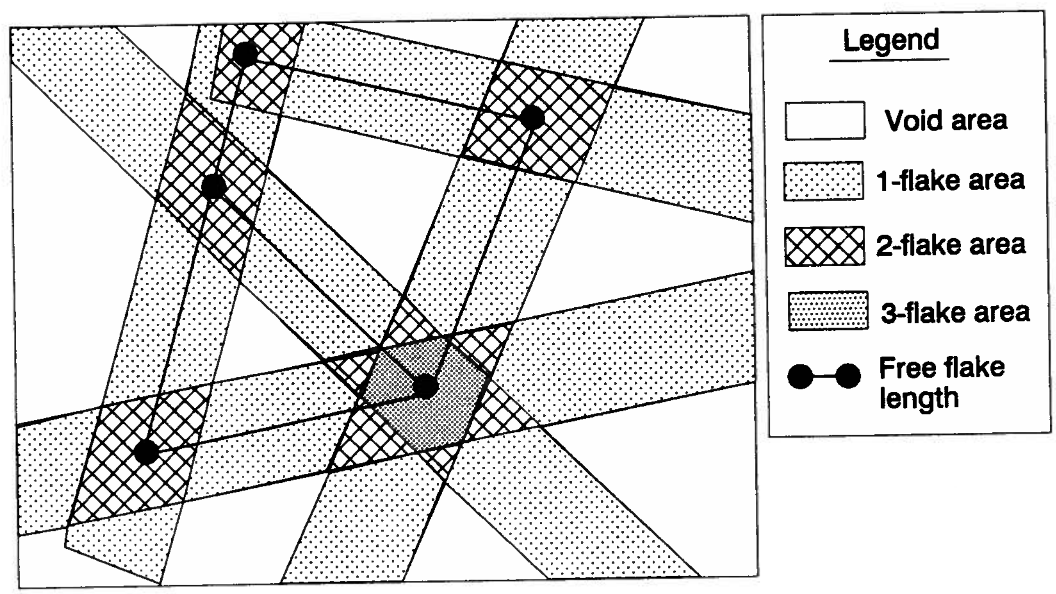

Figure 2.2 Schematic diagram of a two-dimensional randomly-formed flake network.

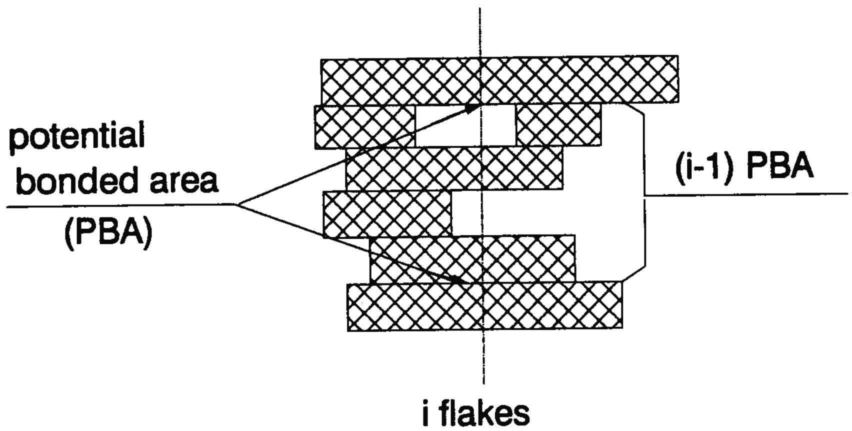

Figure 2.3 Schematic diagram of the potential flake-to-flake bonded interfaces in an i-flake stack.

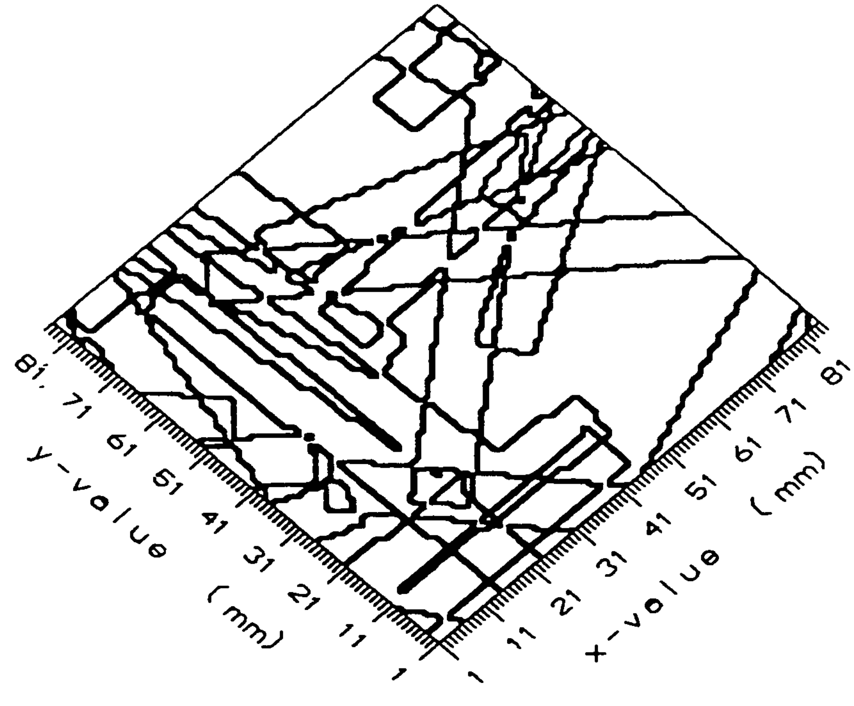

(a)

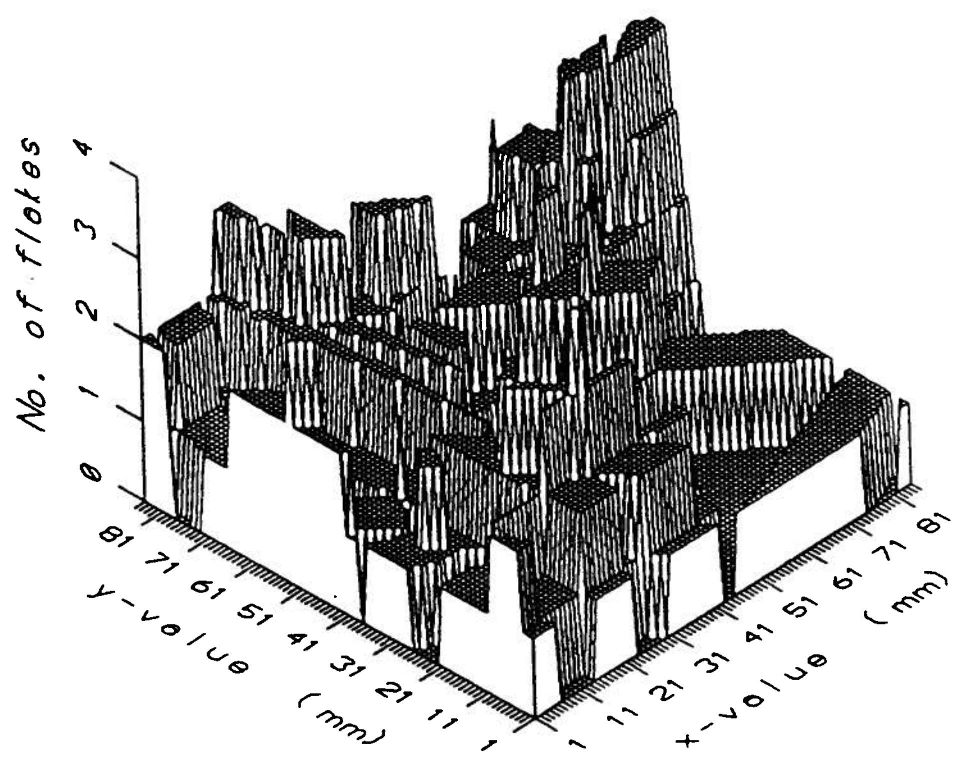

(b)

Figure 2.4 The image of a simulated random flake network illustrating overlap and void areas. a) two dimensional version and b) three dimensional version.

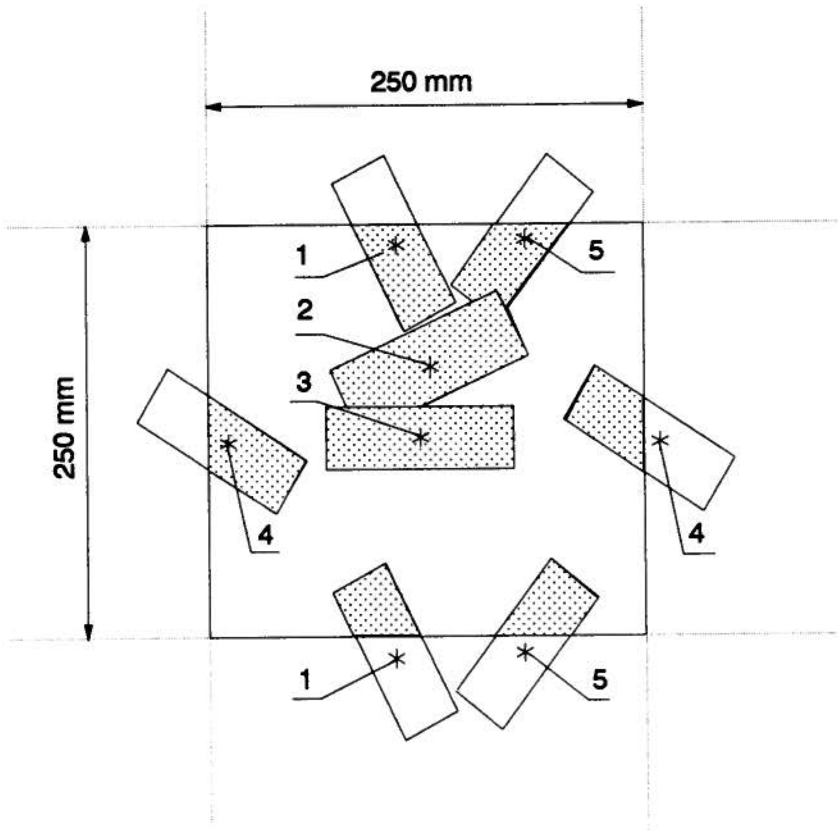

Figure 2.5 The torus convention in a random flake mat to keep the total flake coverage area constantly equal to $\lambda\omega N_f$.

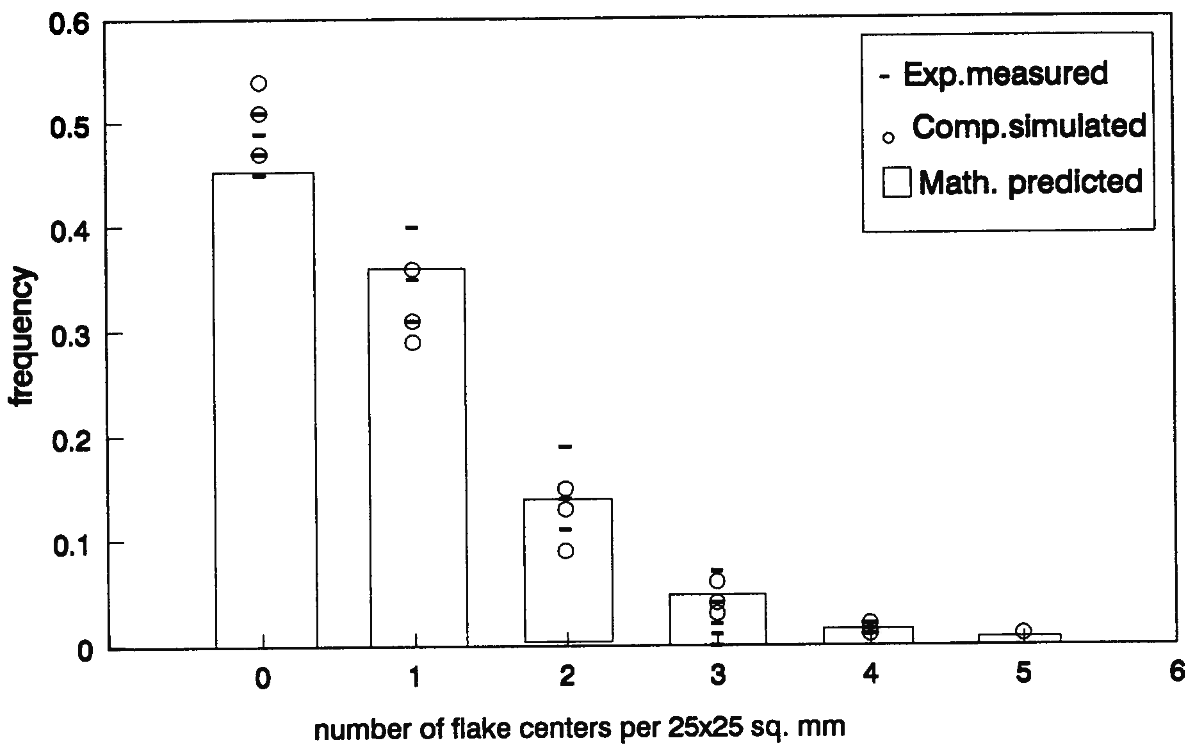

Figure 2.6a The distribution of number of flake centres per 25x25 mm^2 of layer area as experimentally measured, computer simulated and mathematically predicted. Total layer area A=250x250 mm^2; Flakes: N_f=80, λ=83.8 mm and ω=9.31 mm.

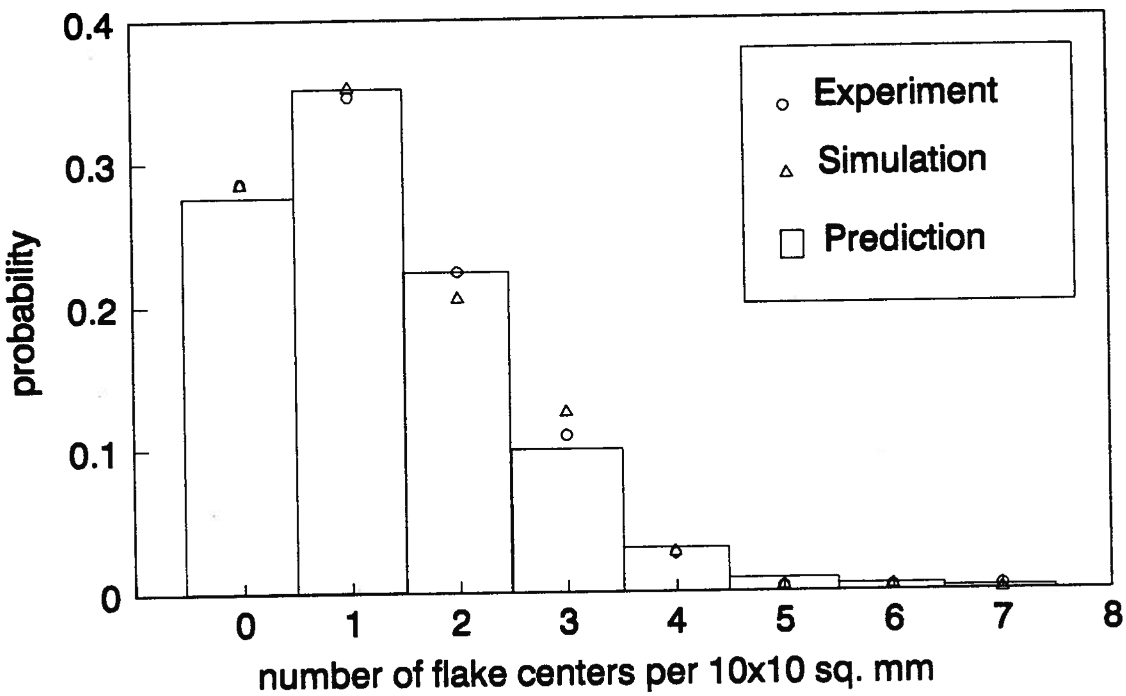

Figure 2.6b The distribution of number of flake centres per 10x10 mm^2 mat area as experimentally measured, computer simulated and mathematically predicted. N_f=800, other conditions as in Fig.2.6a.

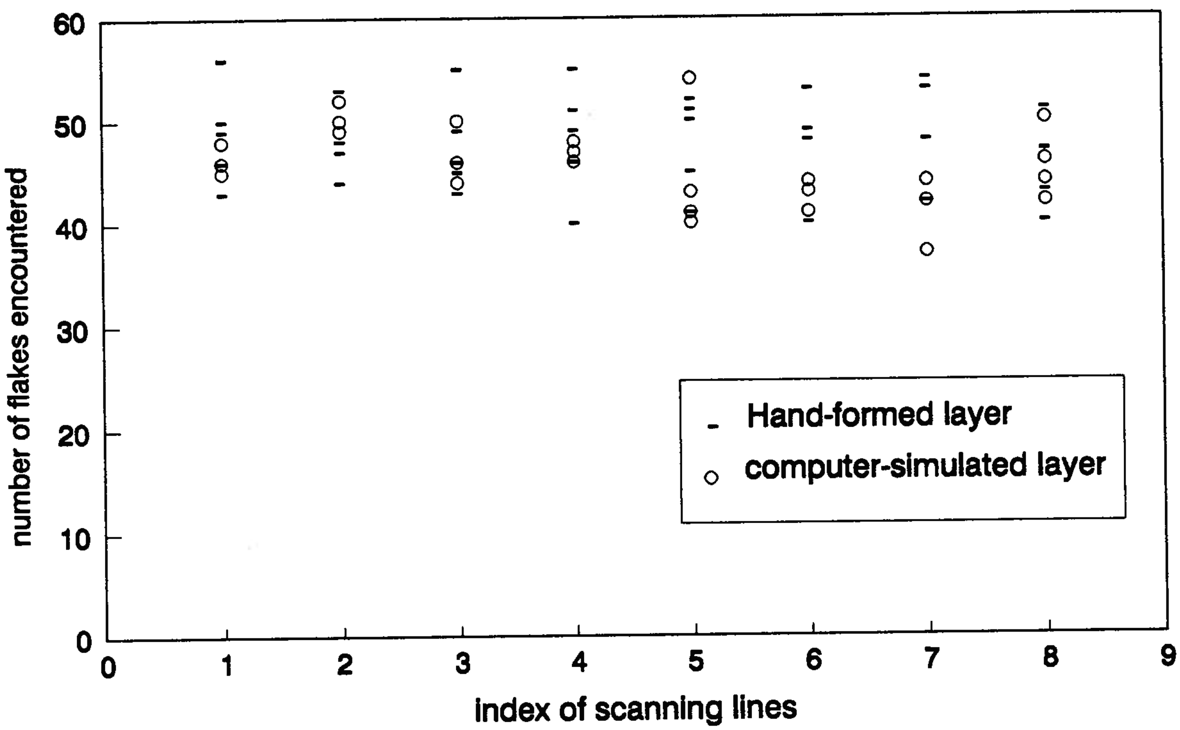

Figure 2.7 The distibution of number of flakes encountered by randomly selected scanning lines parallel to x-axis (line 1-4) and parallel to y-axis (line 5-8). Conditions as in Fig.2.6a.

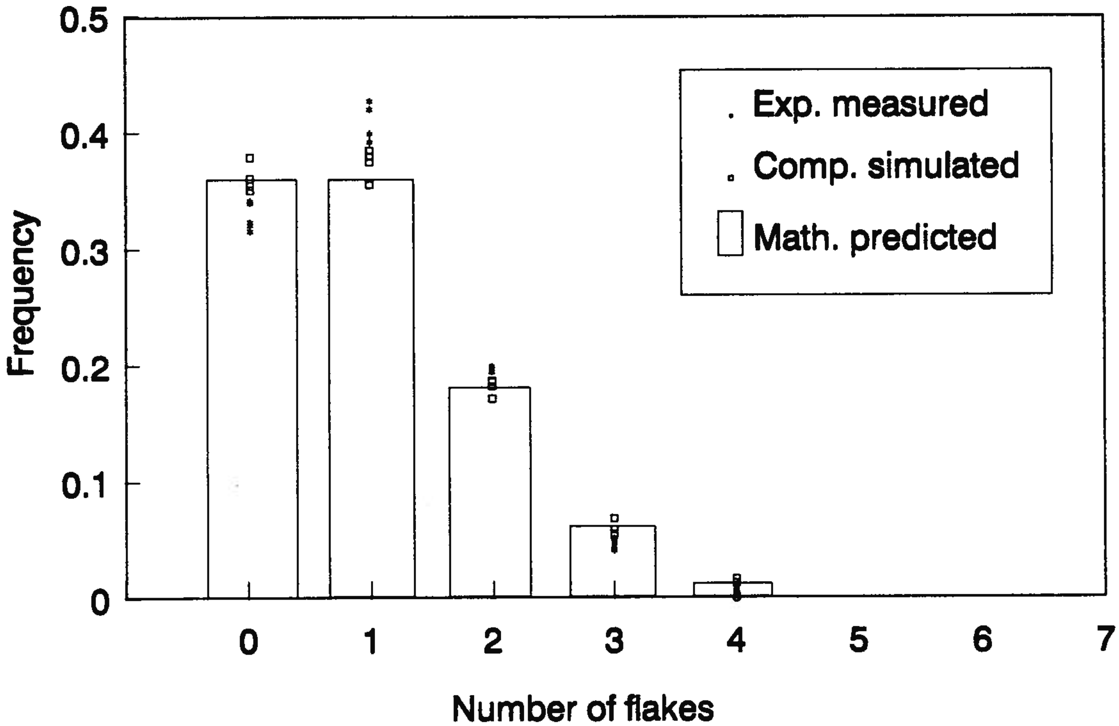

Figure 2.8a The distribution of number of flakes covered at any point in a layer as experimentally measured, computer simulated and mathematically predicted. Conditions as in Fig.2.6a.

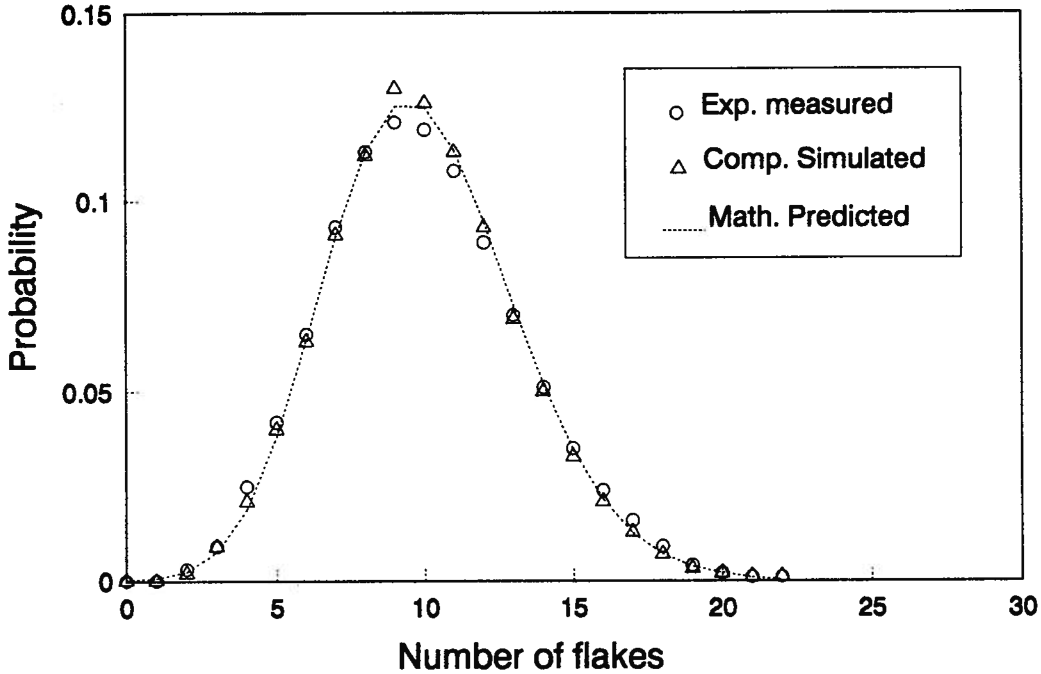

Figure 2.8b The distribution of number of flakes covered at any point in a multi-layered mat as experimentally measured, computer simulated and mathematically predicted. Conditions as in Fig.2.6b.

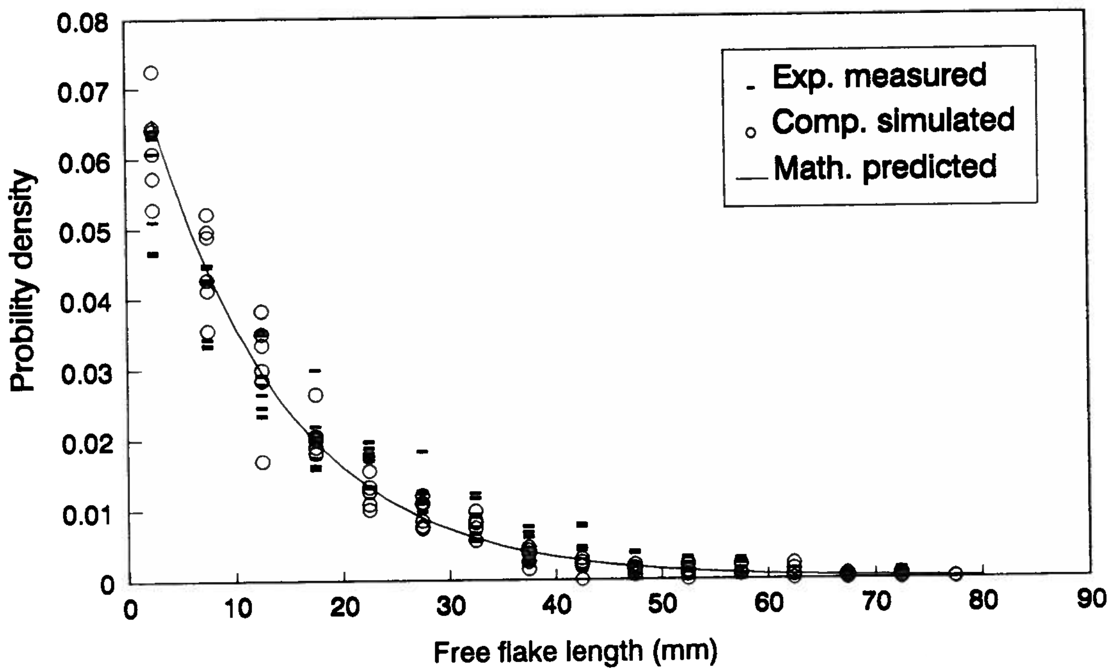

Figure 2.9a The distribution of free flake length in a flake layer as experimentally measured, computer simulated and mathematically predicted. Conditions as in Fig.2.6a.

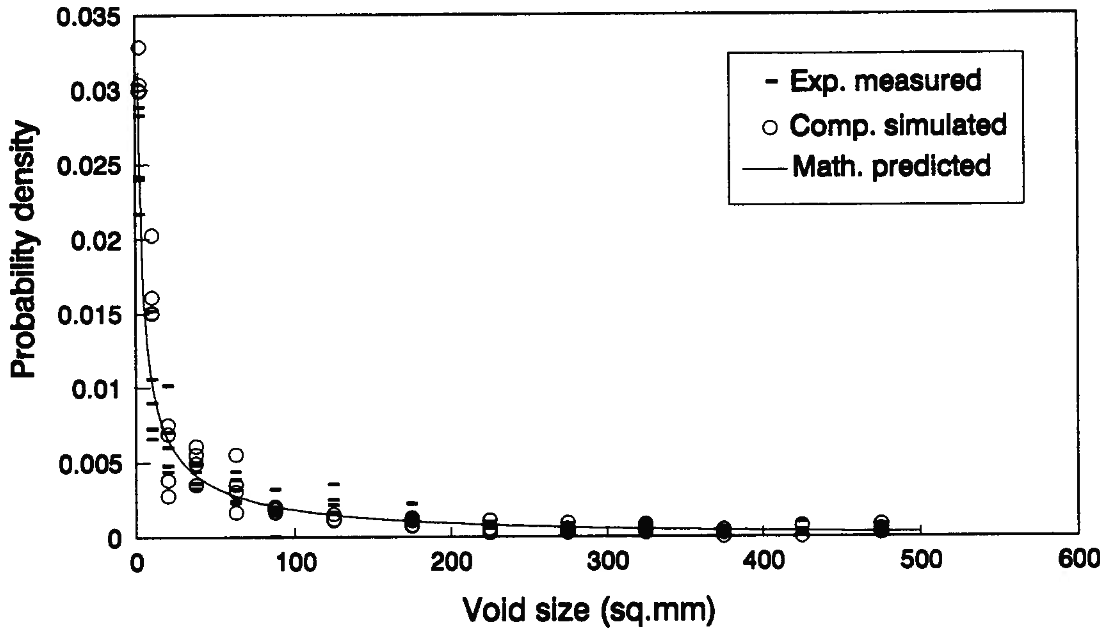

Figure 2.9b The distribution of void size in a flake layer as experimentally measured, computer simulated and mathematically predicted. Conditions as in Fig.2.6a.

Table 2.1. The expected structural properties of a random flake layer.

Properties	Symbol	Unit	Eq. No.	Values* Math.	Comp.	Expl.
Ave. flake length	$\bar{\lambda}$	mm		83.8	83.8	83.8
Ave. flake width	ω	mm		9.31	9.31	9.31
Total no. of flakes	N_f			80	80	80
Total area of layer	A	mm^2		62500	62500	62500
Total fraction of void area	$p_f(0)$		(2.2)	0.368	0.365	0.332
Total fraction of 1-flake area	$p_f(1)$		(2.2)	0.368	0.375	0.414
Total fraction of 2-flake area	$p_f(2)$		(2.2)	0.184	0.183	0.197
Total fraction of 3-flake area	$p_f(3)$		(2.2)	0.061	0.060	0.047
Total fraction of 4-flake area	$p_f(4)$		(2.2)	0.015	0.013	0.009
Ave. no. of flake coverage	μ_f		(2.3)	0.999	0.999	0.999
Total no. of flake crossings	N_c		(2.7)	229	222	194
Ave. no. of crossings per flake	n_c		(2.8)	5.73	5.55	4.85
Ave. free flake length	μ_l	mm	(2.9)	12.46	11.36	13.08
Total no. of voids	N_v		(2.14)	80	79	95
Ave. void area	μ_v	mm^2	(2.18)	285	288	218

* The values listed from computer simulation and experimental measurements are the averages of five samples, respectively.

CHAPTER III. HORIZONTAL DENSITY VARIATION IN RANDOMLY-FORMED FLAKEBOARDS

ABSTRACT. A probability-based mathematical model describing the formation of a flakeboard panel in terms of the variances of point density and zone density averages is presented. Due to within-zone spatial correlation of flake coverage, variance of horizontal density averages in any finite zone depends on the zone size, and is a function of such production variables as flake size, flake density, board compaction ratio and board thickness. With the development of the present model this relationship is explicitly known. In addition, typical flakeboard density variation patterns, in the forms of three-dimensional colour images produced by a computer simulation program, are also presented. This program is also capable of calculating flakeboard density statistics and therefore can be used to check the validity of the mathematical model. Close agreement is found between model prediction, computer simulation and experimental measurement.

3.1 INTRODUCTION

As pointed out in Chapter II, an ordinary flake mat formation in a wood composite manufacturing process follows a two-dimensional random process. As a result, flake coverage in the mat field is not uniform. In this chapter, a further step will be taken to examine how such non-uniform flake coverage contributes to horizontal density variation in flakeboards. This will be achieved by using random field theories to model the spatial correlation of flake coverage from one point to another and the random variation of local density averages in finite sampling zones in the two-dimensional flakeboard field.

Density is one of the most important physical characteristics of wood or wood-based composites, affecting nearly every other physical and mechanical property of the material. In the case of flakeboards, these properties are significantly affected not only by overall panel density, but also by the distribution of board density within the panel. For a conventionally pressed flakeboard, density variation can occur in both the vertical and horizontal plane of the panel, commonly known as vertical density distribution and horizontal density distribution.

While vertical density distribution results primarily from interactions between flake mat compression and temperature and moisture conditions during hot-pressing, horizontal density variation is determined by flake size and the mat formation process, in addition to the density variability of raw materials. In fact, density and its variations in flakeboards are both the cause of board properties and the effect of manufacturing variables.

To date, research to study the board density distribution has focused on the vertical density distribution. Only limited attention has been given to the horizontal density distribution, despite the increasing recognition of its importance in determining board manufacturing process and product performance (Smith, 1982; Bolton et al, 1989; Au and Gertjejansen, 1989; Liu and McNatt, 1991). Suchsland is a prominent researcher who has investigated the horizontal density distribution in flakeboards. His initial work (Suchsland, 1959, 1962) showed that the non-uniformity of density distribution was the inevitable consequence of the discontinuity of flake elements. He proposed a binomial distribution of local board density, the variance of which was further assumed to depend on flake size.

density variation and its effect on flakeboard properties. The results showed a significant effect of horizontal density variation on flakeboard properties, especially on internal bond strength and thickness swelling.

Suchsland's work has contributed to the recognition of horizontal density variation and its importance to product performance. However, to quantitatively analyze the flakeboard manufacturing process a more rigorous and systematic approach is needed.

Within this context, the objectives of the present work are:

1. To apply two-dimensional random field theory to mathematically model the horizontal density distribution in a flakeboard;
2. To demonstrate typical horizontal density variations in a flakeboard through computer generated images;
3. To compare the mathematical predictions with computer simulations and experimental measurements; and
4. To present the typical predictions on how horizontal density variation is affected by production variables.

3.2 MATHEMATICAL MODEL

In the following analysis, horizontal density variation in a flakeboard panel will be considered only to be a result of an idealized manufacturing process in which variation due to raw material quality, equipment limitations and other unpredictable factors are excluded. Flake elements with length λ, width ω, thickness τ and density δ are deposited in a random process, i.e., random positions and random orientations.

For flake-type wood composites, it can be reasonably assumed that the random flake configuration is retained after the hot-pressing operation, and the flake elements are parallel to the board surfaces in the layered panel structure. Under these assumptions, the flakeboard panel is essentially a two-dimensional random field. A key feature about the variation of random variable in this field is that it strongly depends on the spatial scale on which the variables are evaluated (Vanmarcke, 1983). In the case of flakeboard, it is intuitive that the board density averages in finite zones vary with the sampling zone sizes, namely, the smaller the sampling zones, the higher the density variations, or vice versa. To mathematically characterize this phenomena, one needs to formulate how local point flakeboard densities are distributed and how they spatially correlate with each other.

3.2.1 Variation of Point Density

If an infinitely thin needle passes vertically through a random flakeboard, the number of flakes it hits i will be equivalent to the number of flakes overlapping at a point over the panel field. Since the random flake configuration is presumably not affected by the hot pressing process, the flake overlaps i will be also Poisson distributed as given by Eq.(2.2).

A characteristic feature of a Poisson distribution is that the variance $Var[i]$ equals the mean $E[i]$, or:

$$Var[i] = E[i] = \mu_f = \frac{\lambda \omega N_f}{A} \tag{3.1}$$

For a flakeboard with thickness H and compaction ratio CR (ratio of overall board density to raw material density), the total number of flakes N_f is determined by:

$$N_f = \frac{A\ H\ CR}{\lambda\ \omega\ \tau} \tag{3.2}$$

and combining Eq.(3.1) with Eq.(3.2) yields:

$$Var[i] = E[i] = \mu_f = \frac{H\ CR}{\tau} \tag{3.3}$$

Thus the point flake coverage i is fully characterized by the Poisson distribution with mean and variance equal to the board-to-flake thickness ratio (H/τ) multiplied by the compaction ratio CR. It is independent of flake length λ and width ω.

Assume the flakeboard density at any point is D. Neglecting effect of resin and other additives, the overall (or mean) flakeboard density, $E[D]$, is then given by dividing total weight of flakes by total board volume, i.e.,

$$E[D] = \frac{\lambda\ \omega\ \tau\ \delta\ N_f}{A\ H} = \frac{\tau\ \delta}{H}\ E[i] \tag{3.4}$$

This equation allows a point density, D, to be defined as board density at a given point, where there are i flakes overlapping, i.e.,

$$D = \frac{\tau\ \delta}{H}\ i \tag{3.5}$$

Since distribution of flake coverage i is known by Eq.(2.2), the distribution of point flakeboard density D can then be obtained through linear transformation according to Eq. (3.5), i.e.,

$$p(D) = \frac{(\gamma\lambda\omega)^{\frac{H\,D}{\tau\,\delta}}\; e^{-\gamma\lambda\omega}}{\left(\frac{H\,D}{\tau\,\delta}\right)!} \tag{3.6}$$

Thus, the point board density also follows a Poisson distribution, with the variance *Var[D]* determined by:

$$\begin{aligned} Var[D] &= Var\left[\frac{\tau\,\delta}{H}\,i\right] \\ &= \frac{\tau^2\,\delta^2}{H^2}\,Var[i] \\ &= \frac{\tau\,CR\,\delta^2}{H} \end{aligned} \tag{3.7}$$

This point density variance, as given by the above equation, represents the maximum possible density variation of a flakeboard. It depends on flake thickness and is independent of flake length and width.

3.2.2 Point-to-point Spatial Correlation

Because of the Poisson distribution of flake coverage, the point flakeboard densities are random variables which are also characterized by a Poisson distribution. The fact that a flake of finite area content covered at one point can always contribute to the coverage of its neighbouring points make the random densities at different locations in the flakeboard field spatially correlated. The degree of such coverage contribution from one point to another depends on the distance between the two points. This feature is measured by the correlation coefficient of the flake coverage.

Consider the number of flakes covered at any arbitrarily chosen point e is i and i_{ef} at both point e and f which are r distance apart. Then the correlation coefficient at the two locations e and f is (Dodson, 1971),

$$\eta(r;\ \lambda, \omega) = \frac{Var[i_{ef}]}{Var[i]} \tag{3.8}$$

where $Var[i]$ and $Var[i_{ef}]$ are variance of flake coverage i and i_{ef}, respectively.

It is known that i is Poisson distributed with the mean μ_f and variance $Var[i]$ equal to $\gamma\lambda\omega$. An instructive explanation of the Poisson parameter $\gamma\lambda\omega$ for i is that it in fact equals the product of the flake centroid intensity γ and the centroid locus $\lambda\omega$ for a flake to cover location e, as shown in Fig.3.1a. Similarly, the calculation of the Poisson parameter for i_{ef} can be made, if the centroid locus area for a flake to cover both location e and f, a_c, is known.

As indicated in Fig.3.1b, the flake centroid locus a_c is a rectangle with side lengths equal to u and v. Assuming the angle between the line ef and flake length is ϕ, then $u=\lambda-r\cos(\phi)$ and $v=\omega-r\sin(\phi)$. Thus the locus area is

$$a_c = [\lambda - r\cos(\phi)]\,[\omega - r\sin(\phi)] \tag{3.9}$$

Since flake orientations are randomly distributed over the mat area, the variance $Var[i_{ef}]$ is

$$Var[i_{ef}] = \frac{2\gamma}{\pi}\int_{\Omega}[\lambda - r\cos(\phi)]\,[\omega - r\sin(\phi)]\,d\phi \tag{3.10}$$

or the correlation coefficient $\eta(r;\ \lambda,\omega)$ becomes

$$\eta(r;\ \lambda,\omega)=\frac{2}{\pi}\int_{\Omega}[1-\frac{r}{\lambda}\cos(\phi)]\,[1-\frac{r}{\omega}\sin(\phi)]\,d\phi \tag{3.11}$$

where Ω is the integral range. Depending on how far e and f separate in reference to the flake size and because the locus a_c is symmetrical with respect to the flake lengthwise direction (Fig.3.2), ϕ can fall into following three ranges:

1) when $0< r \le \omega$, $\Omega=\{\ 0< \phi \le \pi/2\ \}$;

2) when $\omega< r \le \lambda$, $\Omega=\{\ 0< \phi \le arc\ sin(\omega/r)\ \}$;

3) when $\lambda< r \le (\lambda^2+\omega^2)^{0.5}$, $\Omega=\{\ arc\ cos(\lambda/r)< \phi \le arc\ sin(\omega/r)\ \}$.

Accordingly, the correlation coefficient $\eta(r;\ \lambda,\omega)$ is obtained as follows (Dodson, 1971):

$$\begin{aligned}
\eta_1(r;\lambda,\omega) &= 1-\frac{2}{\pi}\left(\frac{r}{\lambda}+\frac{r}{\omega}-\frac{r^2}{2\lambda\omega}\right) \qquad (0<r\le\omega)\\
\eta_2(r;\lambda,\omega) &= \frac{2}{\pi}\left(\arcsin\left(\frac{\omega}{r}\right)-\frac{\omega}{2\lambda}-\frac{r}{\omega}+\left(\frac{r^2}{\omega^2}-1\right)^{0.5}\right) \qquad (\omega<r\le\lambda)\\
\eta_3(r;\lambda,\omega) &= \frac{2}{\pi}\left(\arcsin\left(\frac{\omega}{r}\right)-\arccos\left(\frac{\lambda}{r}\right)-\frac{\omega}{2\lambda}-\frac{\lambda}{2\omega}-\frac{r^2}{2\lambda\omega}\right.\\
&\qquad \left.+\left(\frac{r^2}{\lambda^2}-1\right)^{0.5}+\left(\frac{r^2}{\omega^2}-1\right)^{0.5}\right) \qquad (\lambda<r\le(\lambda^2+\omega^2)^{0.5})
\end{aligned} \tag{3.12}$$

and $\eta(r;\ \lambda,\omega)=0$ for $r\ge(\lambda^2+\omega^2)^{0.5}$. A typical calculated result of $\eta(r;\ \lambda,\omega)$ is plotted in Fig.3.3. The correlation coefficient is in value range of $0\le\ \eta(r;\ \lambda,\omega)\ \le 1$. It decreases with an increase in the distance and becomes nil as the distance r exceeds the maximum linear length of the flake $(\lambda^2+\omega^2)^{0.5}$. The maximum correlation occurs when r approaches 0.

3.2.3 Distribution of Local Density Averages

Although the point density distribution can provide in detail the local point-to-point variation occurring on a high level micro-scale in the horizontal plane of a flakeboard, it is usually more useful to model the distribution of local density averages. This is because point density is not observable in practice and details of the microstructure of the wood composites may affect behaviour on the macro-scale only through their effect on local average.

In modelling the variation of local density averages, the whole flakeboard area can be viewed as a two-dimensional random field provided that flakes are deposited in a random fashion. Thus, based on the known point variance the derivation of the local average variance model can be carried out through the application of random field theory (Vanmarcke, 1983). According to this theory, if the point is extended to a finite zone, say a rectangle with side length of a and b, the variance of regional density average in the zone, $Var[D_a]$, is expressed as:

$$\begin{aligned} Var[D_a] &= \rho(a,b)\ Var[D] \\ &= \frac{\rho(a,b)\ \tau\ CR\ \delta^2}{H} \end{aligned} \tag{3.13}$$

where $\varrho(a,b)$ is defined as the variance function of zone density average D_a, which measures the reduction of the point variance $Var[D]$ under regional averaging. It is a dimensionless function of value range: $0 \leq \varrho(a,b) \leq 1$. The upper limit occurs when the sampling zone shrinks to a point.

The reduction of variance of regional density average is merely due to the spatial correlation of the flake coverage between points within the zone. Assuming stationary and isotropic properties, the variance function $\rho(a,b)$ is given by (Matern, 1960; Dodson, 1971):

$$\rho(a,b) = \int_0^{\sqrt{a^2+b^2}} \eta(r;\ \lambda,\omega)\ p(r;\ a,b)\ dr \tag{3.14}$$

where $\eta(r;\ \lambda,\omega)$ is the correlation coefficient of flake coverage between pairs of points which are a distance r apart, given by Eq.(3.12). It depends only on the distance r, flake length λ and width ω. The function $p(r;\ a,b)$ is the probability density for the distance r between two points arbitrarily chosen in the rectangle, and depends only on the shape and size of the inspection zone.

The probability density function $p(r;\ a,b)$ for rectangular zone with side length a and b $(a \geq b)$ is given by (Ghosh, 1951):

$$\begin{aligned}
p_1(r;a,b) &= \left(\frac{4r}{a^2b^2}\right)\left(\frac{1}{2}\pi ab - r(a+b) + \frac{1}{2}r^2\right) \qquad (0 \leq r \leq b) \\
p_2(r;a,b) &= \left(\frac{4r}{a^2b^2}\right)\left(ab \arcsin\left(\frac{b}{r}\right) + a(r^2-b^2)^{0.5} - ar - \frac{b^2}{2}\right) \\
&\qquad (b \leq r \leq a) \\
p_3(r;a,b) &= \left(\frac{4r}{a^2b^2}\right)\left(ab\left(\arcsin\left(\frac{b}{r}\right) - \arccos\left(\frac{a}{r}\right)\right)\right. \\
&\qquad \left. + a(r^2-b^2)^{0.5} + b(r^2-a^2)^{0.5} - \frac{1}{2}(r^2+a^2+b^2)\right) \\
&\qquad (a \leq r \leq (a^2+b^2)^{0.5})
\end{aligned} \tag{3.15}$$

For square zones, $a=b$, and the central range for r is non-existent.

The density function p(r; 20,20) for a square 20x20 mm^2 is plotted in Fig.3.4. It should be noted that the exact solution to the integral (Eq.3.14) cannot be derived and the approximation can be obtained using numerical methods.

The distribution of board density averages in a finite zone can be obtained by fitting the mean density $E[D_a]$ (equal to $E[D]$) and its variance $Var[D_a]$ with a normal distribution.

The normal distribution of the zone density is assumed here as a result of a direct application of the Central Limit Theorem (Olkin *et al*, 1980). According to this theorem, the normal distribution can provide a good approximation for the probabilistic characterization of a Poisson associated distribution as the mean of the distribution increases. This mean is represented here by the average flake coverage μ_f.

3.3 RESULT AND DISCUSSION

3.3.1 Computer Simulated Images of Flakeboard Density

The previously described Monte Carlo simulation program was extended to allow for the calculation of flakeboard density based on the simulated local flake coverage i, flake density δ, board compaction ratio CR and board thickness H. Then the extended program was interfaced with an image program so that the digital data could be transferred into colour images. In addition, the density statistics associated with the images could also be obtained from the program. The input parameters allowed a quick visual and numerical evaluation of how flakeboard density distribution is affected by the production variables, such as flake length λ, width ω, thickness τ, density δ, board compaction ration CR, board thickness H, and even flake orientation.

Figure 3.5, for example, shows some typical computer simulated images of flakeboard density variation patterns as affected by changes of flake sizes. The random flake deposition in the initial mat formation makes it no surprise to see the mountain-like density variation with irregular "peak" and "valley" alternations. The spatial transition from the density "peaks" to "valleys" is gradual due to the nature of flake coverage correlation. If such density variation field is viewed as a two-dimensional fluctuation system, then the frequency (number of "peaks" per unit sampling distance) and scale (density difference between "peaks" and "valleys") of the variation change with the flake sizes. The frequency appears to related to the flake length λ and width ω, whereas the scale seems to depend on flake thickness τ. Comparison between Fig.3.5a and Fig.3.5b shows that greater slenderness ratio, λ/ω, results in higher variation frequency. The differences between Fig.3.5a and Fig.3.5c indicates a larger variation scale resulting from thicker flakes.

3.3.2 Distribution of Flakeboard Density

The density variation in a flakeboard was evaluated by calculating the density average statistics in finite zones using the computer program mentioned above. The calculations were based on the flake centroid position and orientation data either directly measured from an 800-flake mat as described in Sect.2.3.2 or simulated using Monte Carlo technique. The results for sampling zone size 1x1 and 5x5 mm^2, were compared in Fig.3.6 with mathematical predictions. The density of the hand-formed mat is close to that of the computer simulated mat, and both are nearly normally distributed with a slightly positive skewness, which stems from the Poisson distribution of the point density (Eq.2.6). Such skewness becomes more noticeable as the zone size and the mean flake coverage decrease and less so as they increase (compare (a) and (b) in Fig.3.6).

Nevertheless, the most characteristic parameter for describing variation of horizontal density in a flakeboard is numerically expressed as the variance of the density distribution, which is independent of the shape of the distribution. In Table 3.1 the variances of density averages of different sampling zone size are compared between experimental, simulated and predicted data. Again a close correlation is found between the three procedures. The results also show that density variance is a monotonically decreasing function of sampling zone size. This is generally true in practice that the measured density of smaller flakeboard samples always varies more than that of bigger ones. A decrease in between-zone variance with increase in zone size is due to the within-zone spatial correlation of flake coverage.

The slightly higher values for simulation compared to that of mathematical prediction in Table 1 are due to the digitization process from real numbers in practice to integers in simulation. This difference will decrease as digitization resolution is increased.

It is important to note that the variance of the hand-formed mat is slightly greater than that of both simulated and model mats (Table 1). This means less uniformity and, therefore, less randomness of the hand-formed mat structure. A similar scenario seems to occur for most machine-formed flake mats in wood composite manufacturing processes due to the likelihood of such non-random effects as flocculation and preferential orientation of flakes in the machine direction. Thus, completely random mat formation would provide the maximum uniform structure which could possibly be achieved by a practical flakeboard manufacturing process. This offers a standard of maximum uniformity to which present commercial flakeboards can be compared.

3.3.3 Typical Predicted Results

Effect of Flake Sizes

The maximum uniformity or the minimum density variance, as a function of sampling zone size, depends on such production variables as flake geometry (length λ, width ω and thickness τ), flake density D_f, board compaction ratio CR and board thickness T_b. With the development of the present model, the relationships are explicitly known. Figure 3.7, for example, exhibits markedly different effects of flake length λ, width ω and thickness τ, respectively, on the density variances of different zone sizes, with τ being the most significant factor followed by ω.

While an increase in flake size generally results in higher density variance, the sensitivities of the variance change with the flake dimension depend on the zone size. For example, changing flake thickness has little impact on the variance of bigger zone densities, but a considerable effect occurs when the sampling zone becomes small (Fig.3.7a). The relationship between density variance and flake width is highly nonlinear (Fig.3.7b). The small-zone variances increase very rapidly with flake width at the start and then level off, whereas more gradual relationships result as the zones becomes bigger. Flake length, in this case where flake width is not narrow, seems to have little influence on how the local densities vary (Fig.3.7c).

Understanding how flakeboard density variation is influenced by flake size and sampling zone size is without doubt of great significance for evaluating and controlling the quality of flake-type wood composites during the manufacturing processes. Firstly, it helps composite designers to choose the right flake size from the standpoint of optimizing the product uniformity. In this regard, thinner and narrower flake geometry, according to this model prediction, appear to be among the better choices. Secondly, this type of prior knowledge can be used to determine the right sampling zone size to more effectively evaluate flakeboard density uniformity, because the sensitivities of the board density variances changing with flake size depend on the zone size. For example, using 1x1 mm^2 zone is good for measuring the effect of flake thickness in any value range, but not so for detecting the influence of flake width with a value greater than 5 mm (compare Fig.3.7a with Fig3.7b).

Effect of Flakeboard Thickness

According to Eq.(3.13), flakeboard density variance is inversely proportional to the board thickness. As shown in Fig.3.8, the density variance can be very high on small scale if the board is not very thick. Therefore, it may not be suitable to manufacture too thin flakeboard, say less than 10 mm, unless a reduced flake thickness is also used.

3.4 SUMMARY AND CONCLUSIONS

The horizontal density variation in a random flakeboard is characterized in terms of local point density distribution, point-to-point flake coverage correlation coefficient and variance of density averages between finite sampling zones. The model has been developed using the prior knowledge about the Poisson flake mat formation process and the concepts of two-dimensional random field theory. In addition, computer simulated images of typical flakeboard density distribution have been presented. The program is also capable of calculating the flakeboard density statistics based simulated or experimentally obtained flake mat configuration. The model prediction agrees well with experimental results and computer simulation. This overall verifies the proposed theory and methodology, and leads to the following main findings:

1. Because of the Poisson flake coverage distribution, the point density of a randomly formed flakeboard is also Poisson distributed;
2. Due to the spatial correlation of flake coverage at neighbouring points, the variance of density averages between finite zones is always less than the point-to-point density variance, and the larger the zone size, the smaller the between-zone density variance;
3. The zone density variation depends on such production variables as flake geometry (length λ, width ω and thickness τ), flake density D_f, board compaction ratio CR and thickness H. With the development of the present model, such relationship is explicitly known;
4. A completely random flakeboard appears to provide a maximum product uniformity that a practical manufacturing process can possibly achieve. Therefore, it can establish a uniformity standard to which present commercial flakeboards can be compared.

REFERENCES

1. Au, K.C. and R.O. Gertjejansen. 1989. Influence of wafer thickness and resin spread on the properties of paper birch waferboard. For. Prod. J. 39(4):47-50

2. Bolton, A.J., P.E. Humphrey and P.K. Kavvouras. 1989. The hot pressing of dry-formed wood-based composites, Part VI. The importance of stresses in the pressed mattress and their relevance to the minimization of pressing time, and the variability of board properties. Holzforschung. 43:406-410.

3. Dodson, C. T. J. 1971. Spatial variability and the theory of sampling in random fibrous networks. J. Roy. Statist. Soc. B. 33(1):88-94.

4. Ghosh, B. 1951. Random distances within a rectangle and between two rectangles. Calcutta Math. Soc., 43: 17-24.

5. Liu, J.Y. and J.D. McNatt. 1991. Thickness swelling and density variation in aspen flakeboards. Wood Sci. Technol. 25:73-82.

6. Matern, B. 1960. Spatial variation. Stochastic models and their application to some problems in forest surveys and other sampling investigations. Meddelanden Fran Statens Skogsforskningsinstitut, Band49, Nr5. Stockholm.

7. Olkin, I.; Gleser L. J. and Derman, C. 1980. Probability models and applications. N.Y.: Macmillan Publishing Co., Inc.

8. Smith, D.C. 1982. Waferboard press closing strategies. Forest Prod. J. 32(3):40-45.

9. Suchsland, O. 1959. An analysis of the particle board process. Michigan Quarterly Bulletin. 42(2):350-372.

10. _____. 1962. The density distribution in flake boards. Michigan Quarterly Bulletin. 45(1):104-121.

11. _____ and H. Xu. 1989. A simulation of the horizontal density distribution in a flakeboard. Forest. Prod. J. 39(5):29-33.

12. _____ and ______. 1991. Model analysis of flakeboard variables. For. Prod. J. 41(11/12):55-60.

13. Vanmarcke, E. 1983. Random fields: Analysis and synthesis. Cambridge: The MIT Press.

Table 1. Comparison of the variances of density averages in different-size zones (Flake: $\lambda=83.8$ mm, $\omega=9.31$ mm, $\tau=0.8$ mm and $D_f=0.4$ g/cm^3; flakeboard: $T_b=5$ mm and $CR=1.6$).

Zone size (mm^2)	Experiment	Simulation ((g/cm^3)^2)	Prediction
1x1	0.0444	0.0416	0.0392
5x5	0.0368	0.0336	0.0320
10x10	0.0292	0.0264	0.0244
25x25	0.0176	0.0136	0.0116

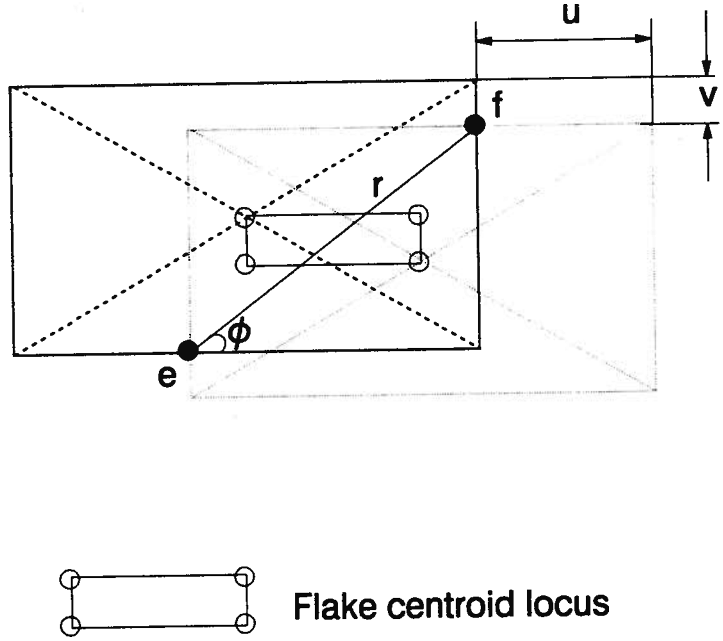

Figure 3.1 (b) Schematic diagram of the centroid locus of a flake to cover both points e and f.

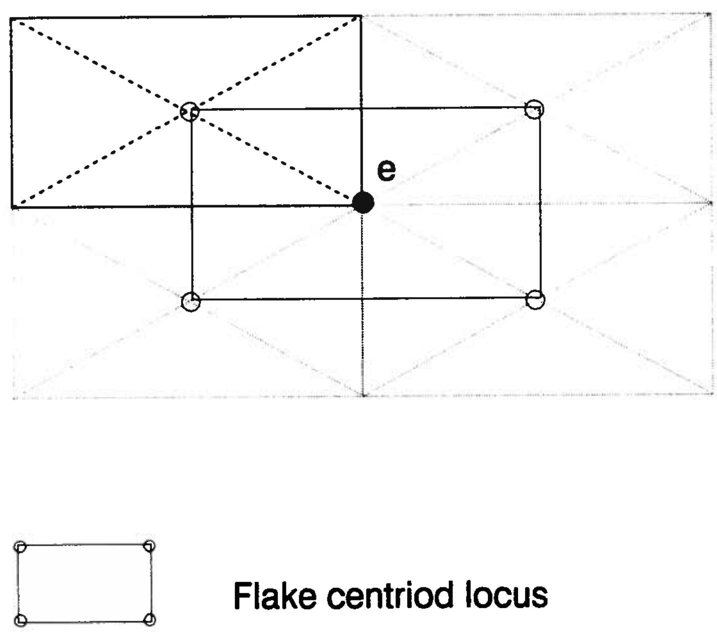

Figure 3.1 (a) Schematic diagram of the centriod locus of a flake to cover only one point e.

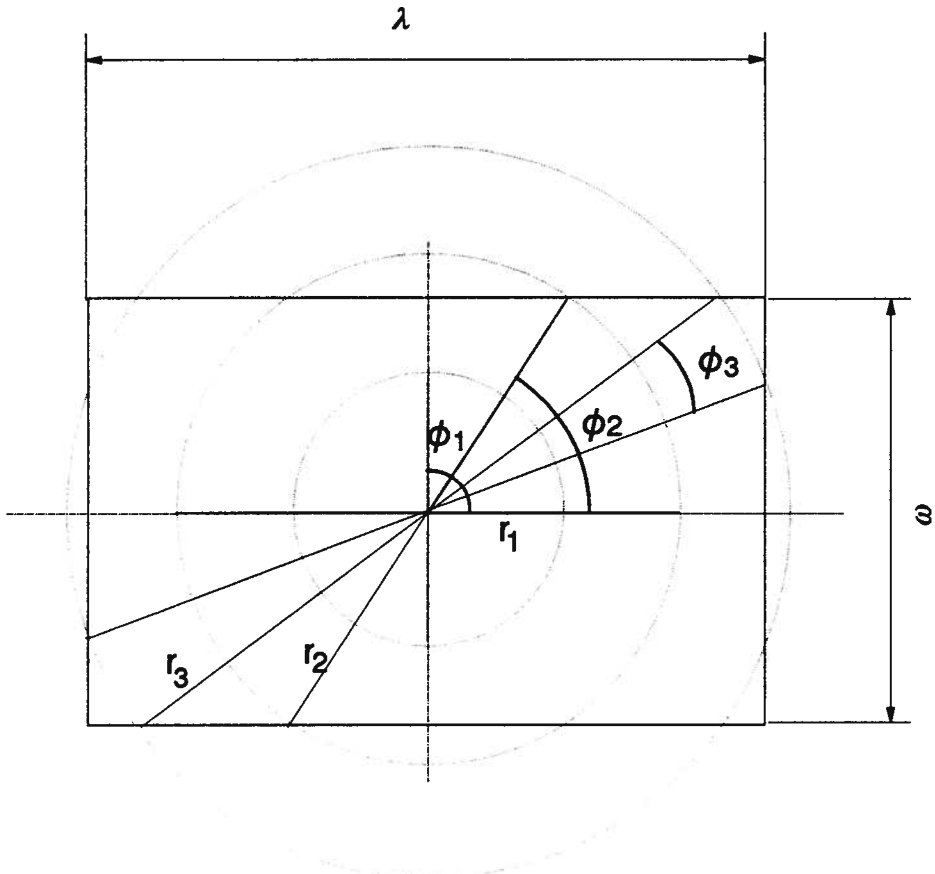

Figure 3.2 Schematic diagram of the integral range ϕ as related to the distance r in a flake.

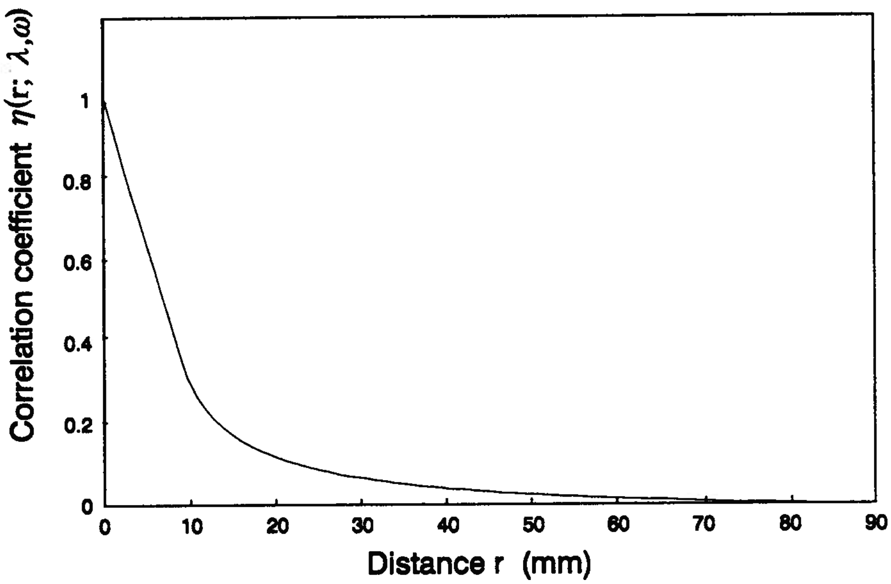

Figure 3.3 A typical predicted correlation coefficent as a function of the distance between two locations. (Flake length 85 mm and width 10 mm)

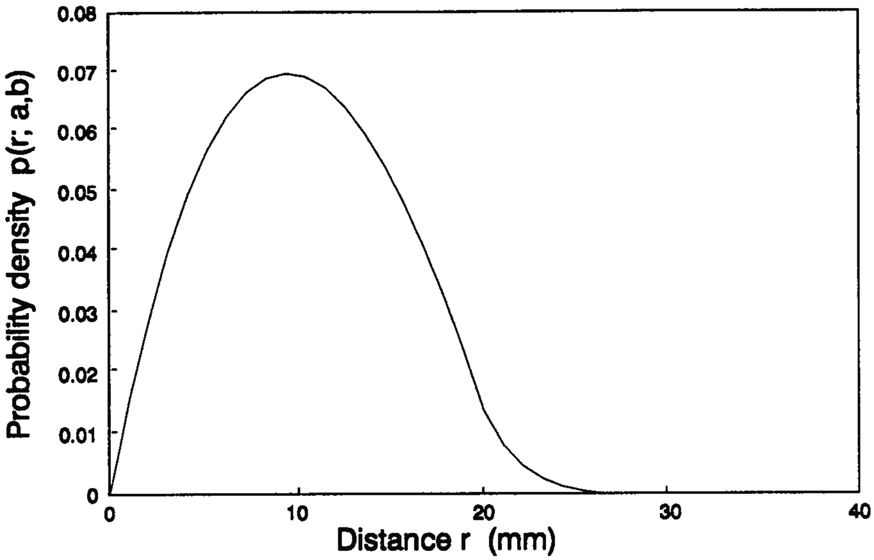

Figure 3.4 Probability density p(r; a,b) as a function of the distance between two locations in a 20mm x 20mm square.

Figure 3.5 Computer simulated image of horizontal density variation in a random flakeboard panel. (a). Flake: λ=85 mm, ω=10 mm, and τ=0.8mm; (b). Flake: λ=85 mm, ω=5 mm, and τ=0.8 mm; (c). Flake: λ=85 mm, ω=10 mm, and τ=1.2 mm; Other conditions: D_f=0.4 g/cm^3; board: CR=1.6 and T_b=10 mm.

Legend

color	density (g/cm^3)
green	0.2 - 0.4$^-$
blue	0.4 - 0.6$^-$
red	0.6 - 0.8$^-$
pink	0.8 - 1.0$^-$
yellow	1.0 - 1.2$^-$

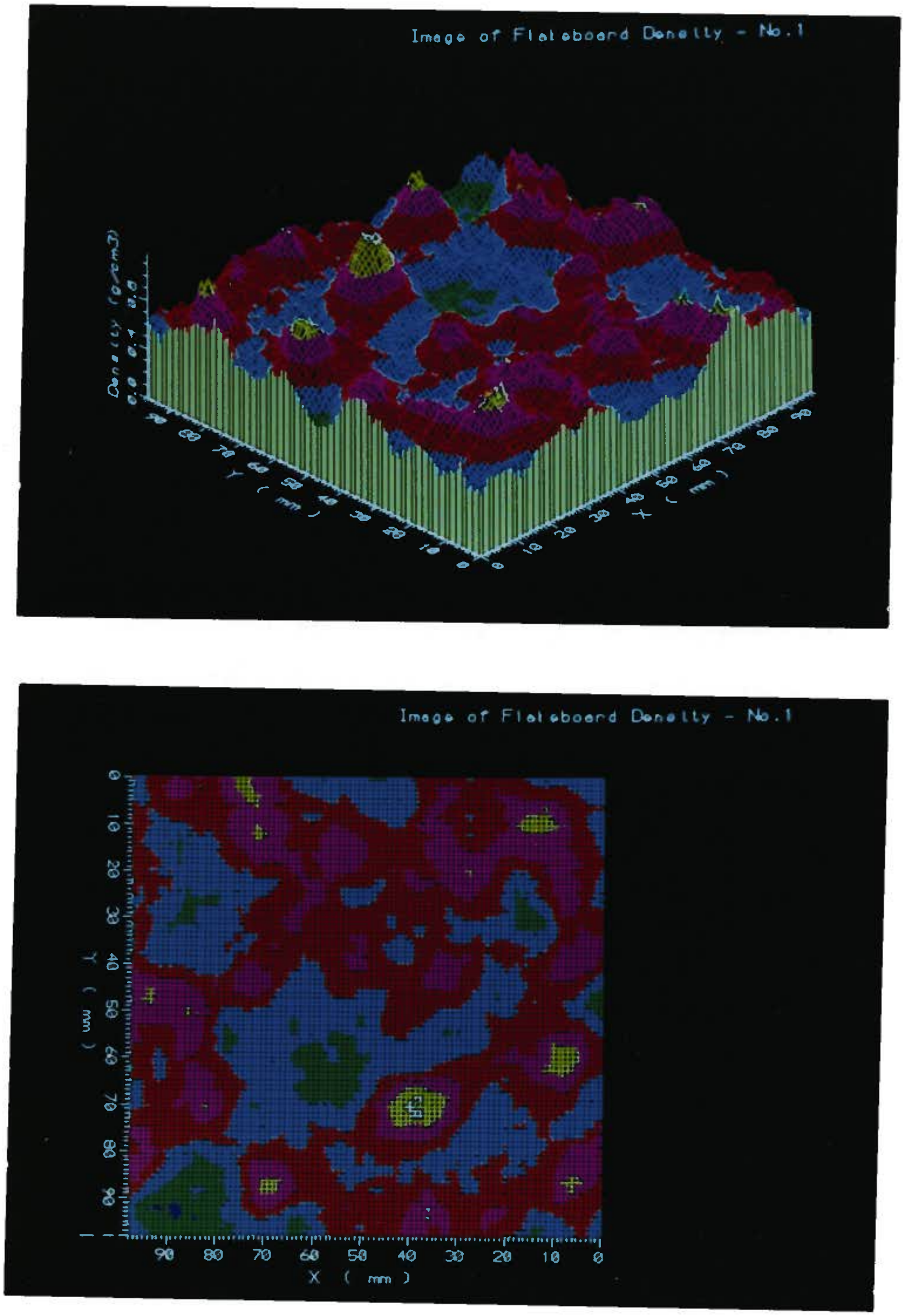
Image of Flakeboard Density - No.1
Y (mm)
X (mm)
Image of Flakeboard Density - No.1
0 10 20 30 40 50 60 70 80 90
Y (mm)
90 80 70 60 50 40 30 20 10 0
X (mm)

Figure 3.5 a

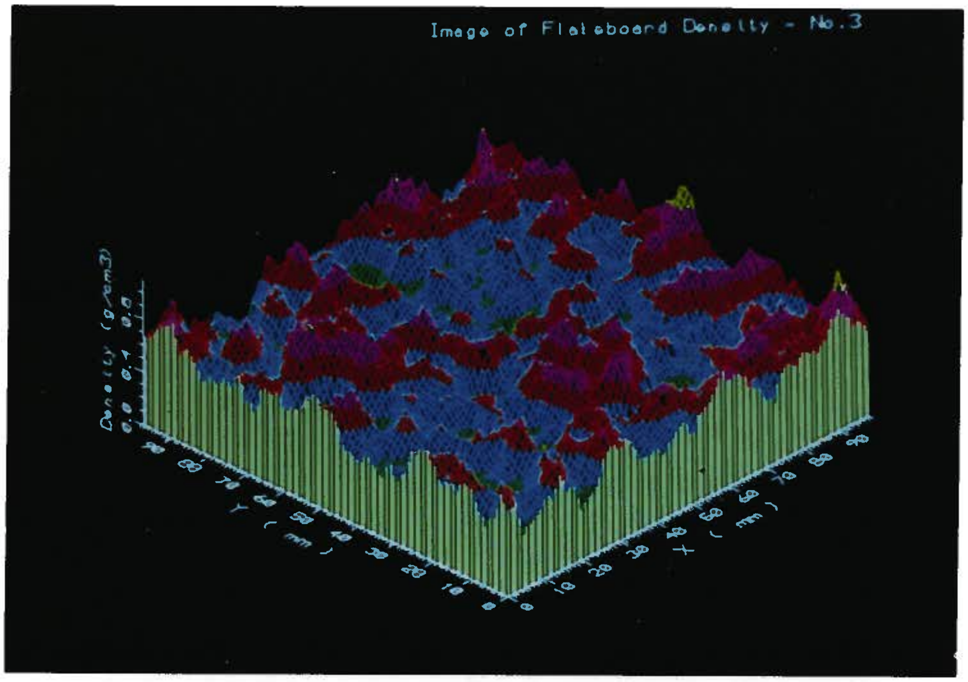
Image of Flatboard Density - No.3
Density (g/mm3)
Y (mm)
X (mm)

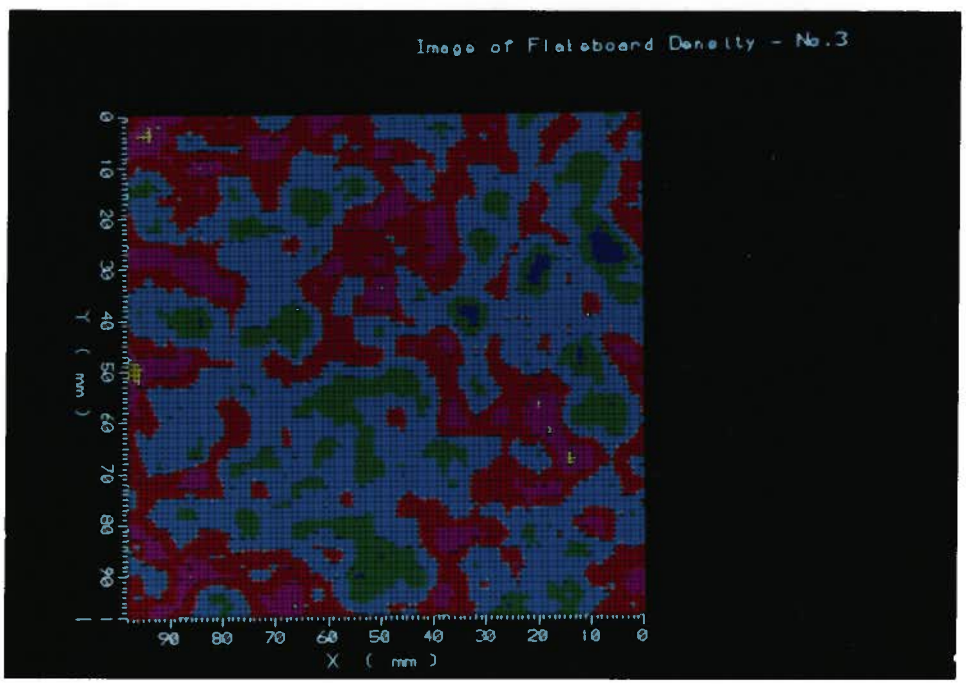
Image of Flatboard Density - No.3
Y (mm)
0
10
20
30
40
50
60
70
80
90
90 80 70 60 50 40 30 20 10 0
X (mm)

Figure 3.5 b

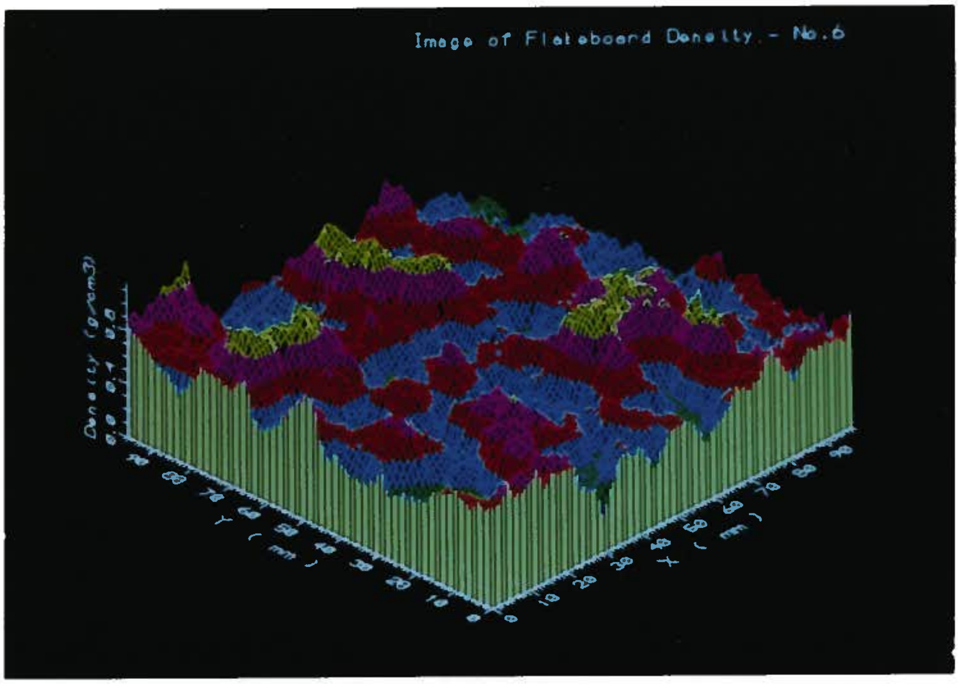
Image of Flakeboard Density - No.6
Density (g/cm3)
Y (mm)
X (mm)

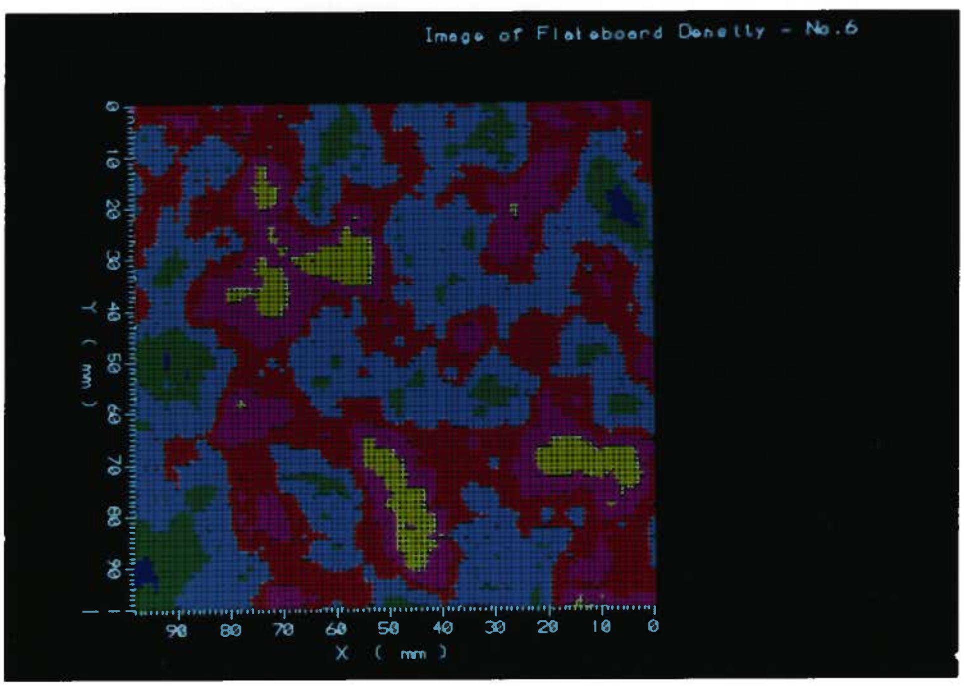
Image of Flakeboard Density - No.6
Y (mm)
X (mm)
90 80 70 60 50 40 30 20 10 0

Figure 3.5 c

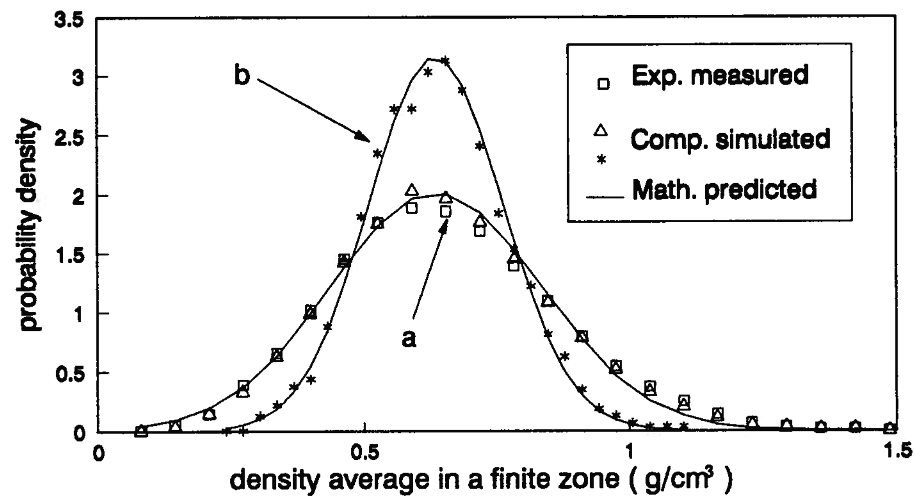

Figure 3.6 Distribution of flakeboard density averages in a finite zone as experimentally measured, computer simulated and mathematically predicted. (a) Zone size: 1x1 mm^2, and mean flake coverage: μ_f=10; (b) zone size: 5x5 mm^2, and mean flake coverage: μ_f=20. Flake: λ=83.8 mm, ω=9.31 mm and τ=0.8 mm; δ=0.4 g/cm^3. Board CR=1.6.

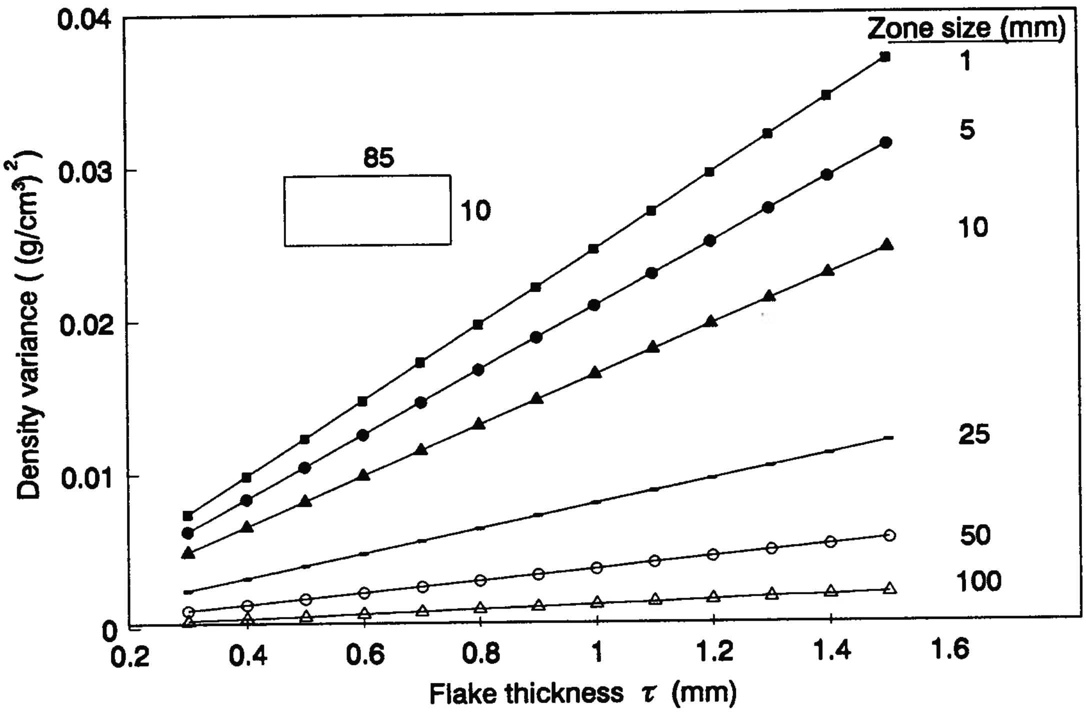

Figure 3.7a

Figure 3.7 Predicted effect of flake size on horizontal density variation in a random flakeboard. (a). Effect of flake thickness, λ=85 mm and ω=10 mm, (b). Effect of flake width, λ=85 mm, and τ=0.8 mm and (c) Effect of flake length, ω=10 mm and τ=0.8 mm. Side length of sampling zone $a=b$. Other conditions as in Fig. 3.6.

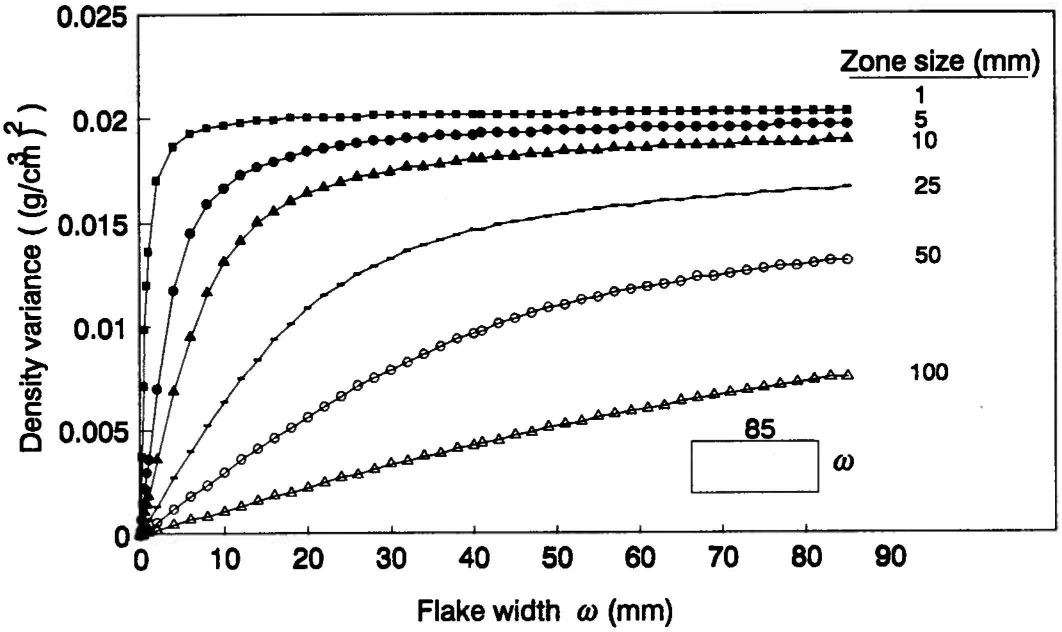

0.025
0.02
0.015
0.01
0.005
0
Density variance ((g/cm^3)^2)
0
10
20
30
40
50
60
70
80
90
Flake width ω (mm)
Zone size (mm)
1
5
10
25
50
100
85
ω

Figure 3.7b

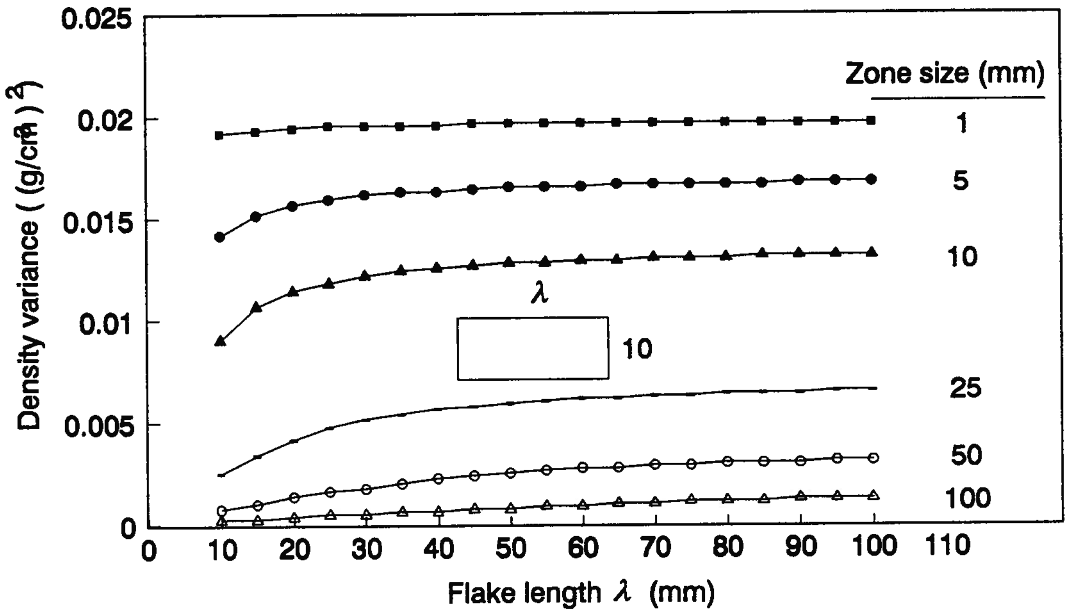

0.025
0.02
0.015
0.01
0.005
0
Density variance ((g/cm^3) ^{2})
Zone size (mm)
1
5
10
25
50
100
λ
10
0
10
20
30
40
50
60
70
80
90
100
110
Flake length λ (mm)

Figure 3.7c

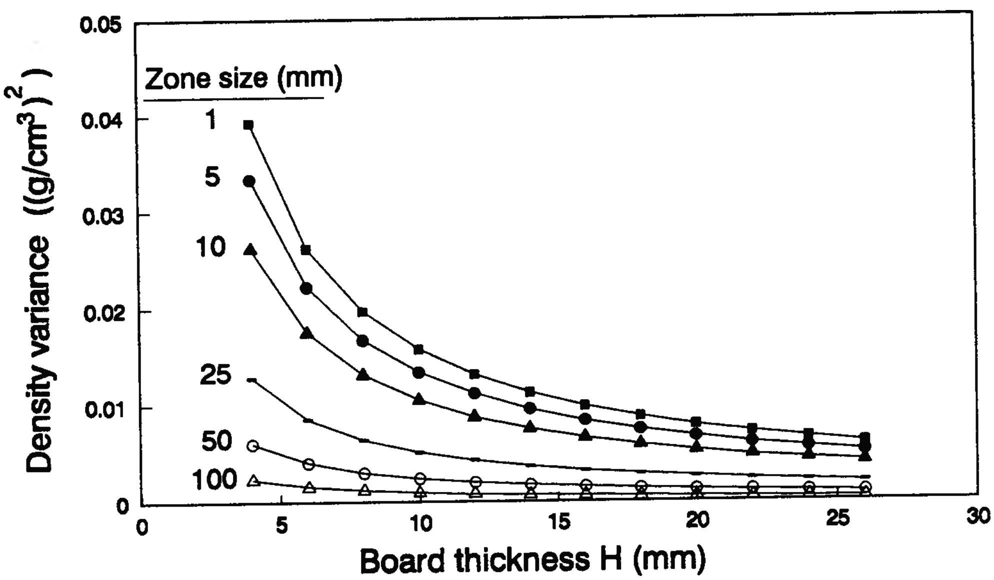

Figure 3.8 Predicted effect of board thickness on horizontal density variation in a random flakeboard.

Conditions as in Fig.3.6.

CHAPTER IV. COMPRESSION BEHAVIOUR OF RANDOMLY-FORMED WOOD FLAKE MATS

ABSTRACT. A theoretical model for predicting the compression response of a randomly-formed wood flake mat is developed. The model rigorously relates the overall mat response to local mat structure and individual flake properties. The compression behaviour of single flakes, flake columns and random flake mats is experimentally determined. Satisfactory agreement is found between the predicted and experimentally obtained results. Equations are also derived for the calculation of the relative volumetric change of between- and within-flake voids in a mat and the change of relative flake-to-flake bonded area during the course of mat densification. Typical predictive outputs are presented and discussed.

4.1 INTRODUCTION

In the next two chapters, the mat structure model developed in Chapter II will be further applied to formulate the compression behaviour of a flake mat in cold pressing based on the mechanical properties of original wood flakes. In doing so, a mathematical relationship between the marco-behaviour of a flake mat, its localized responses and the solid flake properties will be established. Chapter IV will be concerned with instantaneous responses and Chapter V will examine time-dependent properties.

From a material science standpoint, significant differences exist between production of wood and non-wood composite materials. Wood composites are typically manufactured by first applying relatively small quantities of adhesive to wood elements, mechanically forming these constituents into a loose mat structure and then consolidating the mat under heat and pressure. Development of adequate strength properties requires application of pressure which densifies the loose structure and results in permanent wood deformation. In contrast, non-wood composite materials usually consist of reinforcing elements dispersed in large quantities of resin matrix. Effective bonding of this structure is achieved without densification. Therefore, the compression behaviour of the mat structure of wood constituents, in the form of flakes, particles or fibres, is critical to wood composite manufacture.

Other important aspects of mat compression behaviour of flake mats related to wood composite processing and performance characteristics can be summarized as follows:

1. Changes in internal structure, such as void volume reduction and wood densification which occur during mat compression, strongly affect heat and mass transfer processes during hot-pressing (Humphrey and Bolton, 1989; Kamke and Wolcott, 1991);

2. The physical, chemical and mechanical interactions between mat compression, heat and moisture variation and adhesive cure can result in a non-uniform densification through the thickness of the manufactured panel, often referred to as the vertical density distribution (Suchsland, 1962; Harless et al, 1987; Wolcott et al, 1990);

3. Due to a random variation in mat structure as discussed in Chapter II and Chapter III, highly localized wood compression stresses and densification result from overall mat compression (Suchsland, 1962; Bolton et al, 1989;

Smith, 1980);

4. Upon press opening the compressed wood composites can springback and also exhibit non-reversible excessive dimensional change as a result of varying moisture conditions (Suchsland, 1973; Beech, 1975; Liu and McNatt, 1991).

Realizing the importance of the above, it is surprising to learn of the limited published information on compression behaviour of wood flake or fibre mats. Even for solid wood, little is known about transverse compression and viscoelasticity at the loading levels and over the ranges of moisture contents and temperatures that are encountered during wood composite manufacture (Humphrey and Bolton, 1989).

Suchsland (1959, 1962) appears to be the only researcher to study this wood composite mat behaviour. In his analysis, a random flake mat was treated as a system of independent, horizontally-stacked flake columns with varying flake content. The compression stresses developed in individual flake columns within the pressed mat were shown to be very high, and were a function of transverse compression stress-strain relationships of solid wood. Although the analysis was not mathematically rigorous, it provided a valuable insight into the flakeboard manufacturing process. Kunesh (1961) experimentally investigated the inelastic behaviour of solid wood under conditions of perpendicular-to-grain compression similar to the hot-pressing operation in wood composite manufacture. More recently, the transverse compression behaviour and viscoelasticity of wood blocks and wood flakes has been tested and modelled by Kasal (1989) and Wolcott (1990) using theories of cellular solids.

Knowledge about the compression behaviour of wood generally contributes to understanding such mat-compression-related product properties as panel density variation, springback on press opening and thickness swelling. However, it is unsuitable for quantitative analysis of wood composite manufacturing processes unless the relationship between individual wood constituent properties, spatial arrangement of wood elements in a mat and overall mat response is explicitly established. With the development of a random mat structure model (Chapter II), it is now possible to derive such a relationship.

Within this context, the objectives of the present work are:

1. To develop a theoretical model which predicts the overall pressure-deformation relationship of random flake mats in compression based on solid flake compression properties and mat structure;
2. To experimentally test the compression behaviour of wood flakes and flake mats, and compare these measurements with results predicted from the model; and
3. To quantitatively describe changes of mat internal structural properties, such as between-flake void volume and flake-to-flake bonded area, during compression.

4.2 THEORY

A uni-directional compression of a mat of materials such as natural or synthetic fibres, particles or flakes can simultaneously result in bending, shear, friction and compression responses in the constituents. Among these stress modes, bending stress is the dominant component at the early stage of mat compression when low pressure is applied. At higher pressure the mat constituents are mainly subject to transverse compression (Jones, 1963; Ellis et al, 1983; van Wyk, 1946). The latter scenario appears to be encountered in wood composite manufacture where the densification pressure can range as high as 4 to 7 MPa. Thus, in the following analysis, bending and other possible stresses are ignored, and the whole flake mat is treated as a system of compression units, which are the elements of flake columns. The flake mat formation is also assumed to be strictly random with regards to individual flake positions and orientations.

4.2.1 Compression Stress-strain Relationship of Flakes

Wood, as a natural cellular material, exhibits a unique mechanical behaviour when subjected to high compression in the perpendicular-to-grain direction. Because of the cellular structure, a typical complete deformation process goes sequentially through three stages: initial linear cell wall bending, non-linear cellular structure collapse and final cell wall densification (Gibson and Ashby, 1988). The linear and nonlinear stress-strain relationship of wood can be modelled by a modified Hooke's Law (Rusch, 1969; Wolcott, 1990):

$$\sigma=\varphi(\varepsilon)E\varepsilon \tag{4.1}$$

where

σ = stress, MPa.

ε = strain.

E = Young's modulus, MPa.

$\varphi(\varepsilon)$ = nonlinear strain function.

The function $\varphi(\varepsilon)$ equals unity when ε is in the initial linear compression range, then, it starts to monotonically decrease and reaches a minimum when the cell wall totally collapses, and finally increases to infinity as the cell wall starts to densify.

For most synthetic polymer foams (Meinecke and Clark, 1973) and wood (Wolcott, 1990), the strain function $\varphi(\varepsilon)$ is independent of the properties of matrix material or cell wall and depends only on the cellular structure. Therefore, effect of loading conditions, temperature and moisture content should not influence the strain function $\varphi(\varepsilon)$, but only Young's modulus E.

4.2.2 Pressure-thickness Relationship of Flake Mats

The flake compression stress σ, as defined by Eq. (4.1), depends on the corresponding strain ε. Even under the same overall mat compression, the strain ε of individual flakes at different locations in a mat can be substantially different. Similar strain variations can also exist within one flake of finite dimension. This unique behaviour is solely a result of the non-uniform mat structure which, for a randomly-formed flake mat, is explicitly known in the previous chapters.

A force F, applied on a random flake mat causes the mat to deform to thickness H. Because of the random distribution of flake number in columns, F can be only supported by those flake columns with flake count i greater than H/τ (τ: average flake thickness), or:

$$F=\sum_{i=H/\tau}^{\infty}\sigma_i a_i \tag{4.2}$$

where σ_i is the flake stress in columns with i flakes.

As mentioned in Section 2.2.2, the probability that any point in a mat is covered by i flakes, $p_f(i)$, can be referred to as the fractional mat areas, a_i/A, in which the number of flakes overlapping is i. Thus, combining Eqs.(4.1) and (2.2) with Eq.(4.2), the nominal overall compression stress, σ_n, which equals the applied pressure, can be obtained by:

$$\begin{aligned}\sigma_n &= \frac{F}{A}\\ &= \sum_{i=H/\tau}^{\infty}\sigma_i\frac{a_i}{A}\\ &= Ee^{-\gamma\lambda\omega}\sum_{i=H/\tau}^{\infty}\varphi(\varepsilon_i)\,\varepsilon_i\frac{(\gamma\lambda\omega)^i}{i!}\end{aligned} \tag{4.3}$$

where ε_i is the flake strain in columns with i flakes, and is determined by:

$$\varepsilon_i=\frac{\tau-H/i}{\tau}=\frac{i\tau-H}{i\tau} \tag{4.4}$$

So far, a theoretical model for predicting the mat pressure-deformation relationship is developed using fundamental mathematical and mechanical concepts. This theory can further be applied to calculate relative void volume and flake-to-flake bonded area changes with mat thickness during the course of densification.

4.2.3 Void Volume Change

Assuming wood cell wall density δ_o (typically 1.5 g/cm^3), the total void volume content VC_t is readily given by:

$$VC_t = 1 - \frac{D_m}{\delta_0} = 1 - \frac{W}{1000\ H\ A\ \delta_0} \tag{4.5}$$

where D_m and W are the overall mat density (g/cm^3) and weight (g), respectively.

Considering wood as a porous material, the total void volume in a loose flake mat may be classified into two components: between-flake voids and within-flake voids. Differentiation between the two types of void appears to be necessary since the environmental conditions inside flakes may not always be equilibrated with conditions between flakes during hot-pressing (Kamke and Wolcott, 1991). This may not be achieved without taking into account the horizontal flake coverage variation.

At any mat thickness H, between-flake voids can only occur in the columns with flake count less than H/τ. Thus, neglecting the lateral expansion in compressed flakes, the between-flake void volume content VC_{bf} is obtained by:

$$\begin{aligned} VC_{bf} &= \frac{1}{H\ A} \sum_{i=0}^{H/\tau} (H - i\tau)\, a_i \\ &= \sum_{i=0}^{H/\tau} \left(1 - \frac{i\tau}{H}\right) \frac{a_i}{A} \\ &= e^{-\gamma\lambda\omega} \sum_{i=0}^{H/\tau} \left(1 - \frac{i\tau}{H}\right) \frac{(\gamma\lambda\omega)^i}{i!} \end{aligned} \tag{4.6}$$

since a_i/A is known by Eq.(2.2)

The within-flake void volume content VC_{wf} is merely given by subtracting the between-flake void volume from the total void volume, or:

$$VC_{wf} = VC_t - VC_{bf} \tag{4.7}$$

4.2.4 Inter-flake Bonded Area Change

It seems clear that the only purpose of highly compacting flake mats during the manufacture of wood composites is to increase flake-to-flake contact and promote bonding. Thus, it is of great importance to predict how the inter-flake contact area relates to mat compaction. The maximum inter-flake bonded area BA_{max} of a flake mat resulting from an ideal complete mat compaction has been given by Eq.(2.20).

For a partially compacted mat at thickness H, the actual bonded area is always less than BA_{max} because effective flake-to-flake contact can only occur in columns with total solid-flake thickness greater than H. As such, the relative bonded area RBA can be defined by:

$$\begin{aligned} RBA &= \frac{1}{BA_{\max}} \sum_{i=H/\tau}^{\infty} (i-1)\, a_i \\ &= \frac{e^{-\gamma\lambda\omega}}{\gamma\lambda\omega-1} \sum_{i=H/\tau}^{\infty} (i-1) \frac{(\gamma\lambda\omega)^i}{i!} \end{aligned} \tag{4.8}$$

4.3 EXPERIMENT

The following experiment was designed to provide a data base for estimating the parameters of model input and to verify the proposed model. It consists of determining: perpendicular-to-grain compression stress-strain relationships for single flakes and flake columns, and pressure-deformation relationship of random flake mats.

4.3.1 Materials

Aspen (*Populus tremuloides*) veneers of thickness 0.79 mm were prepared by slicing along the grain direction. The veneers were cut into 25x25 mm^2 square flakes and rectangular flakes with average length 37.51 mm and width 6.09 mm. The flakes were then conditioned to a 9.1% moisture content at 20°C. Square flakes were used for single flake compression tests and also randomly selected to form 6-, 10-, 14-, and 18-flake columns for column compression tests.

All flake mats were prepared by hand felting 72 g of rectangular flakes into a forming box with inside area 152x152 mm^2. A highly compressible foam wall was placed around the mat perimeter to contain the flakes during testing. Efforts were made to ensure the randomness of mat formation during each packing process.

To compare compression responses of mats constructed from different sizes of flakes, the 37.51x6.09 mm^2 flakes were further cut in half either along length or width to give two different sizes: 37.51x3.05 mm^2 and 18.76x6.09 mm^2.

4.3.2 Procedures

All tests were conducted on a computerized, hydraulic press interfaced with an MTS (Material Test System) controller at an ambient temperature of about 20°C. The computer control and monitoring system allowed the complete testing procedure to be programmed and compression pressure and deformation data to be acquired in real time.

Prior to testing the samples, the machine compliance was measured and the pressure-deformation of the platens was found to be linear. This deformation was subtracted from the overall gross displacement to obtain the real compression of samples. Samples of single and multi-flake columns were compressed at a loading rate of 0.5 mm/min while 25 mm/min was used for flake mats.

4.4 RESULTS AND DISCUSSION

4.4.1 Flake Compression Modulus and Strain Function

Considerable variation is found among the compression responses of individual flakes (Fig.4.1). This may result from wood heterogeneity and the variance induced by the flake preparation process, namely, the effects of the principal material orientation (tangential and radial) (Bodig, 1963), sapwood-to-heartwood and earlywood-to-latewood ratio (Kennedy, 1968) and thickness variation and surface roughness (Wolcott et al, 1989). However, such effects are dramatically reduced when flake columns are compressed (Fig.4.2). The exact reason for such variation reduction is unknown. A universal statistical law relevant to this phenomenon is that the variance of an average value of several independent variables is always smaller than that of individual variables. In this regard, the stress-strain relationship of a flake column is indeed an average response of all flake elements of which the column is made, and should accordingly vary less.

In evaluating the average compression modulus E and the nonlinear strain function

$\varphi(\varepsilon)$ of flakes, 10-flake column data is used. E is estimated at approximately 25 MPa, which is much less than the corresponding modulus of a wood block. This seems to be a result of the dominance of surface roughness effects as the specimen thickness becomes very small (Wolcott et al, 1989). However, this deviation may not invalidate the use of the modified Hooke's law (Eq.4.1) for this application. $\varphi(\varepsilon)$ can be obtained by determining the constants in the following equation through a computer program:

$$\varphi(\varepsilon) = \sum_{i=0}^{10} b_i \varepsilon^i \tag{4.9}$$

The results of b_i are listed in Table 4.1. It should be noted that this estimation involves an approximation in designating $\varphi(\varepsilon)$ equal to unity in the linear range, as both Fig.4.1 and Fig.4.2 show slight nonlinearity of the stress-strain curves prior to the beginning of linear range. It appears that this discrepancy has little impact on the prediction accuracy, especially for higher mat compression regions where the induced error accounts for a negligible portion of total predicted stresses.

4.4.2 Compression Response of Flake Mats

Validation of the Model

Based on the estimated flake compression modulus and strain function, the mat compression response can be predicted using Eqs.(4.3) and (4.4). As shown in Fig.4.3, a close agreement is found between the predicted response and experimental measurement, except at pressure less than 1.5 MPa. This discrepancy seems to relate to the fact that the pressure against a flake mat during the initial compression stage is mainly resisted through flake bending, not transverse compression. A prediction of initial flake bending stresses could be made by treating the whole mat as a system of bending units with the span of each unit being determined by the distribution of free flake length, i.e., the distance along a flake between adjacent contacts with other flakes as defined in Section 2.2.3. This calculation is not considered here since our present interest lies in mat compression ranges of greater than 2 MPa, which is normally seen in the hot-pressing of wood composites.

According to Eq.(4.3), for a randomly-formed flake mat, compression response depends on the flake size only through the total coverage area content $\gamma\lambda\omega$. Thus, it is not affected by any change of flake length λ or width ω as long as the total flake coverage area is kept constant. This has been demonstrated experimentally by determining the compression pressure-deformation relationship of mats of flakes with different sizes (Fig.4.4). Again the region of initial discrepancy arises because the early compression pressure on a mat is dominated by flake bending resistance, not flake compression. The bending response is strongly affected by the flake slenderness ratio (ratio of length to width) (Jones, 1963).

Effect of Flake Properties

An important feature of the proposed model is that it establishes an explicit relationship between individual flake compression properties and overall mat response, as well as a relationship between local compression strain and stress and overall mat densification. According to Eq.(4.3), the mat densification response is a linear function of flake compression modulus E, as presented in Fig.4.5 which indicates the relationship between the applied pressure and compaction ratio (ratio of mat density to flake density). For a given species and flake thickness in a mat, the modulus E, during hot-pressing, is a temporal and spatial function of temperature and moisture content inside the mat. Therefore, with the development of this model, the success of predicting the vertical density profile of flakeboard may be achieved by incorporating a heat and mass transfer model (e.g., Humphrey and Bolton, 1989) and the compressive viscoelasticity of flakes (Wolcott, 1990) into Eq.(4.3).

Local Stress Distribution

At any given mat densification (or mat thickness H), the distribution of local compression stresses can be obtained by incorporating the compression stress-strain relationship of flakes in Eq.(4.1) into the Poisson distribution of flakes counts in individual columns (Eq.2.2). As shown in Fig.4.6, local stresses can vary markedly from as small as zero to as high as more than 40 MPa, with the variances increasing as applied pressure on mat increases. This is a characteristic stemming from the parentage of the Poisson distribution.

The level and variability of local stresses will directly relate to the severity of residual stresses in the compressed panel. The residual stresses, in turn, determine the minimum pressing time needed to give the panel an acceptable internal bond strength, and affect the springback and thickness swelling (Bolton et al, 1989). Furthermore, since such a wide distribution of local stresses is transferred to flake interfaces during pressing, the flake-resin bond development within the composite varies (Humphrey and Ren, 1989). As a result, a distribution of localized bonding strength in the final board is expected. Therefore, a quantitative characterization of the local stresses in the pressed mat may lead to the prediction of optimum pressing time and variability of board properties.

4.4.3 Predicted Results of Internal Mat Structure Change

Void Volume Content

Figure 4.7 shows a typical result of predicted (Eqs.4.5, 4.6, 4.7) total void volume content VC_t, the between-flake void volume content VC_{bf} and the within-flake void volume content VC_{wf} during the course of mat densification. While VC_t linearly decreases with the compaction ratio *CR*, the two components VC_{bf} and VC_{wf} exhibit markedly different patterns. Without doubt, the absolute volume of both between- and within-flake voids always decreases with an increase in *CR*. The initial rapid increase in VC_{wf} is merely a result that rate of decease in within-flake void volume with *CR* is much less than that of total mat volume. According to this prediction, less than 10% of between-flake void volume likely exits in random flakeboards, where the core *CR* is usually greater than 1.

Inter-Flake Bonded Area

As discussed previously, mat compression response is independent of flake length and width. For the same reason, any change in flake length and width should not affect the relative flake bonded area for a randomly-formed flake mat.

The predicted relative flake-to-flake bonded area, *RBA*, with mat densification with respect to flake thickness is displayed in Fig.4.8. It is interesting to note that an increase in flake thickness results in higher *RBA* at lower *CR* while a less important role is played by flake thickness at higher *CR*. This result may shed some light on how flake thickness affects the development of internal bond strength in flakeboard. Increasing the flake thickness appears beneficial for enhancing panel bond strength, not only by increasing areal resin concentration but also by promoting flake-to-flake contact, especially for low density products (Suda et al, 1987).

4.5 SUMMARY AND CONCLUSIONS

In modelling the compression behaviour of a randomly-formed flake mat, the mat structure is viewed as a system of horizontally arranged flake columns with infinitely small cross-sectional area. Pressure applied on the mat is primarily resisted through transverse compression of flakes in those columns with total solid-flake thickness greater than current mat thickness. With prior knowledge of the Poisson distribution of column flake count, a model has been developed to predict the mat compression response based on the compression characteristics of flakes.

Because variations in single flakes are much greater than flake columns, a more accurate estimation of flake compression stress-strain relationship as model input parameters, is provided by the flake column data. The model prediction is in good agreement with experimental results except at pressure less than 1.5 MPa. The predicted mat compression response is not affected by flake length and width.

With the development of this model, a quantitative relationship between individual flake compression properties and overall mat response as well as the relationship between local compression and stresses and overall mat densification are established. This essentially provides a new approach to investigating the role played by individual flakes in defining overall flakeboard properties and how localized material properties affect overall panel behaviour.

Equations are also derived for the calculation of relative volumetric changes of total, between- and within-flake voids, and relative flake-to-flake bonded area during mat densification. A quantitative description of internal mat structure change is necessary to fully understand the mechanism of heat and mass transfer and the development of internal bond strength during the hot-pressing operation. The establishment of the present model may also provide a basis for predicting such flakeboard properties as vertical density distribution, springback on press opening and even thickness swelling. To achieve this, further work is needed to extend the present model to incorporate viscoelasticity of the mat under compression at loading levels and over ranges of temperature and moisture content experienced during hot-pressing.

REFERENCES

1. Beech, J. C. 1975. The thickness swelling of wood particleboard. Holzforschung 29: 11-18.

2. Bodig, J. 1963. The effect of anatomy on the initial stress-strain relationship in transverse compression. For. Prod. J. 15(5): 197-202.

3. Bolton, A.J., P.E. Humphrey and P.K. Kavvouras. 1989. The hot pressing of dry-formed wood-based composites Part VI. The importance of stresses in the pressed mattress and their relevance to the minimisation of pressing time, and the variability of board properties. Holzforschung 43: 406-410.

4. Ellis, E. R., K. B. Jewett, W. H. Ceckler, and E. V. Thompson. 1983. Dynamic compression of paper: III. Compression equation for cellulose mats. AIChE Symposium Series. 232(80): 1-7.

5. Gibson, L. J., and M. F. Ashby. 1988. Cellular solids: structure and properties. Pergamon Press. N. Y. 357 pp.

6. Harless, P. E., F. G. Wagner, P. H. Short, R. D. Seale, P. H. Mitchell, and D. S. Ladd. 1987. A model to predict the density profile of particleboard. Wood Fibre Sci. 19: 81-92.

7. Humphrey, P. E., and A. J. Bolton. 1989. The hot pressing of dry-formed wood-based composites: Part II. A simulation model for heat and moisture transfer, and typical results. Holzforschung. 43(3): 199-206.

8. ____, and S. Ren. 1989. Bonding kinetics of thermosetting adhesive systems used

in wood-based composites: the combined effect of temperature and moisture content. J. Adhesive Sci. Technol. 3(5): 397-413.

9. Jones, R. L. 1963. The effect of fibre structural properties on compression response of fibre beds. Tappi. 46(1): 20-27.

10. Kamke, F. A., and M. P. Wolcott. 1991. Fundamentals of flakeboard manufacture: wood-moisture relationships. Wood Sci. Technol. 25: 57-71.

11. Kasal, B. 1989. Behaviour of wood under transverse compression. Master's Thesis, VPI&SU. Blacksburg, VA.

12. Kennedy, R. W. 1968. Wood in transverse compression: Influence of some anatomical variables and density on behaviour. For. Prod. J. 18(3): 36-40.

13. Kunesh, R. H. 1961. The inelastic behaviour of wood: a new concept for improved panel forming process. For. Prod. J. 9: 395-406.

14. Liu, J. Y., and J. D. McNatt. 1991. Thickness swelling and density variation in aspen flakeboards. Wood Sci. Technol. 25: 73-82.

15. Meincke, E.A., and R.C. Clark. 1973. Mechanical properties of polymeric foams. Technomic Publishing. Westport, Conn. 105 pp.

16. Rusch, K. C. 1969. Load-compression behaviour of flexible foams. J. Appl. Polym. Sci. 13: 2297-2311.

17. Smith, D. C. 1980. Waferboard press closing strategies. For. Prod. J. 32(3): 40-45.

18. Suchsland, O. 1959. An analysis of the particleboard process. Michigan Quarterly Bulletin 42(2): 350-372.

19. ____. 1962. The density distribution in flake boards. Michigan Quarterly Bulletin 45(1): 104-121.

20. ____. 1973. Hygroscopic thickness swelling and related properties of selected commercial particleboards. For. Prod. J. 23(7): 26-30.

21. Suda, H., S. Kawai and H. Sasaki. 1987. Production technology for low-density particleboard III. Effect of particle geometry on board properties. Japan Wood Res. Soc. J. 33(5): 376-384.

22. van Wyk, C. M. 1946. Note on the compressibility of wool. J. Textile Inst. 37: 285-292.

23. Wolcott, M. P. 1990. Modelling viscoelastic cellular materials for the pressing of wood composite. Ph.D. dissertation, VPI&SU. Blacksburg, VA.

24. ____, F. A. Kamke, and D. A. Dillard. 1990. Fundamentals of flakeboard manufacture: viscoelastic behaviour of the wood composite. Wood Fibre Sci. 22(4): 345-361.

25. ____, B. Kasal, F. A. Kamke, and D. A. Dillard. 1989. Testing small wood specimens in transverse compression. Wood Fibre Sci. 21(3): 320-329.

Table 4.1. The regression results for strain function $\varphi(\varepsilon)$

strain (ε)	strain function ($\varphi(\varepsilon)$)	
0 - 0.16	1	
> 0.16	Eq. 12	
	i	b_i
	0	-18.41
	1	455.24
	2	-4361.09
	3	21797.65
	4	-57902.60
	5	54472.87
	6	131405.66
	7	-512553.08
	8	748850.68
	9	-541248.47
	10	160504.47

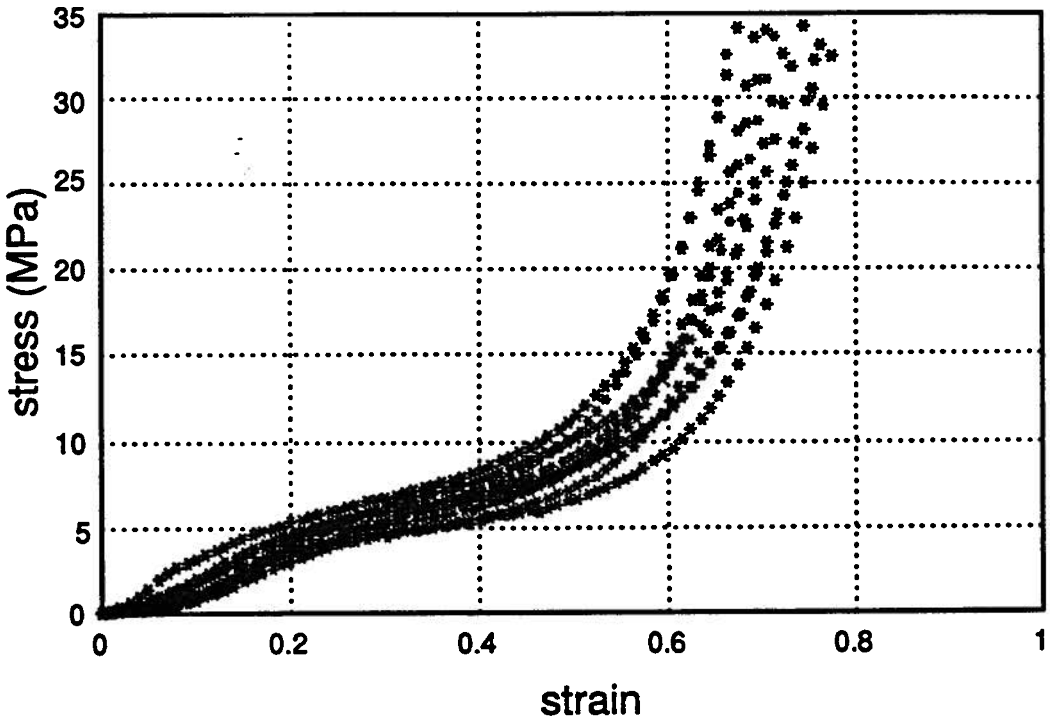

Figure 4.1 Experimentally measured stress-strain relationship for single aspen flakes under transverse compression. Flake size: 25mm x 25mm x 0.79mm, 9.1%MC, 20°C, and 0.5 mm/min loading rate.

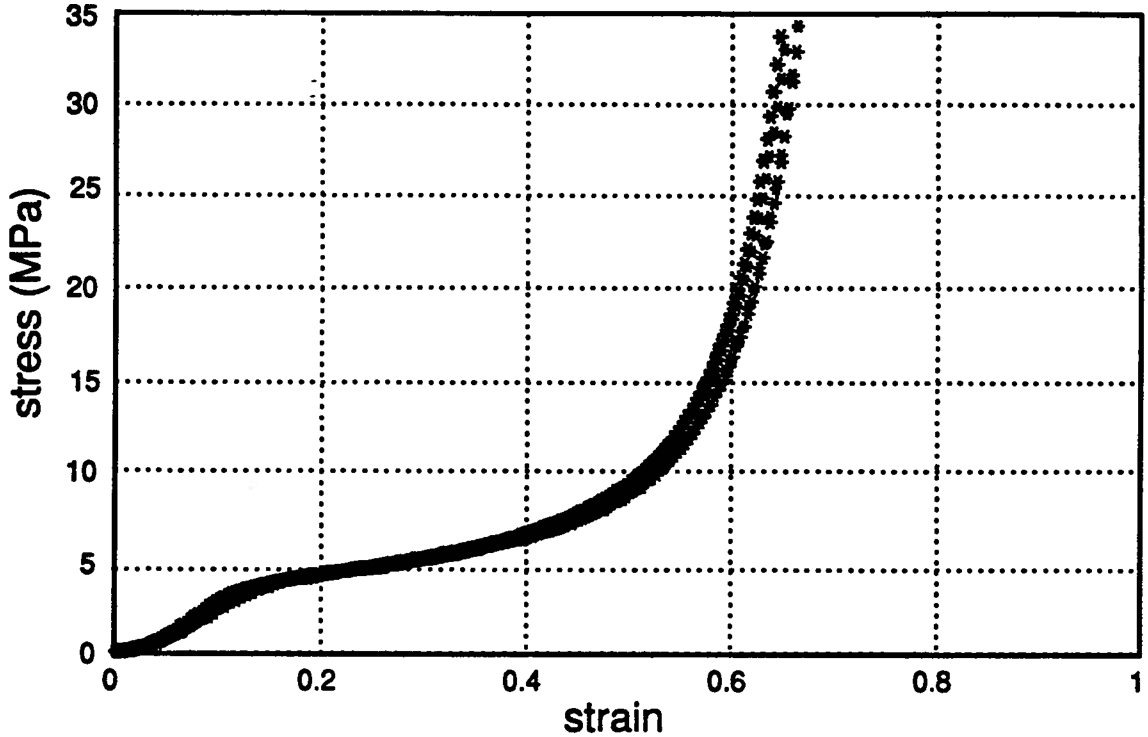

Figure 4.2 Experimentally measured compression stress-strain relationship for aspen flake columns (10-flake). Other conditions as in Fig.4.1.

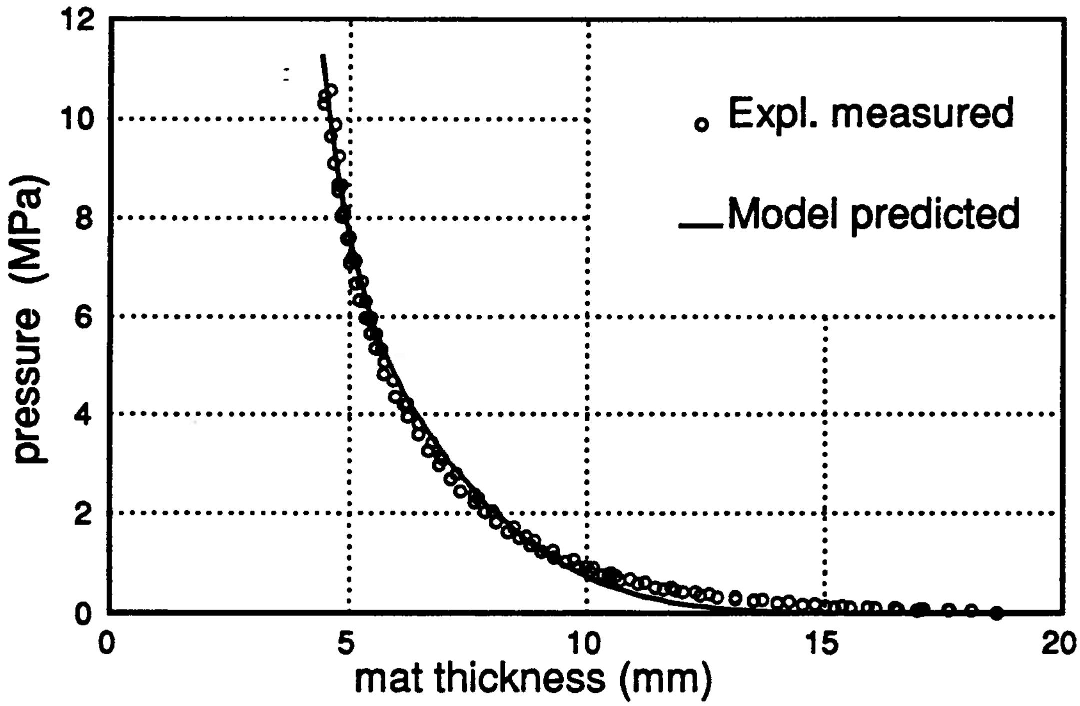

Figure 4.3 Comparison between experimental measurements and model prediction of pressure-mat thickness relationship of a randomly-formed flake mat in compression . Flake size: 37.51mm x 6.09mm x 0.79mm, total flakes: 72g. 9.1%MC, 20°C and 25mm/min loading rate.

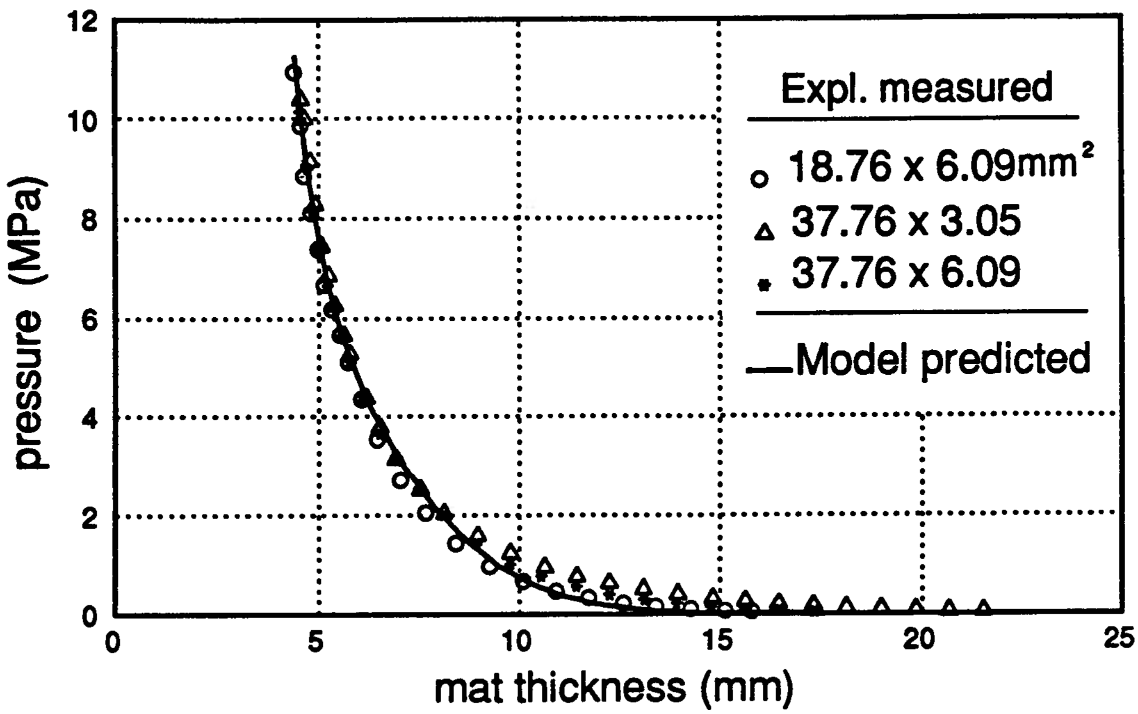

Figure 4.4 Experimentally measured pressure-mat thickness relationship for flake mats of different flake sizes compared to model prediction. All flake thickness: 0.79mm and other conditions as in Fig.4.3.

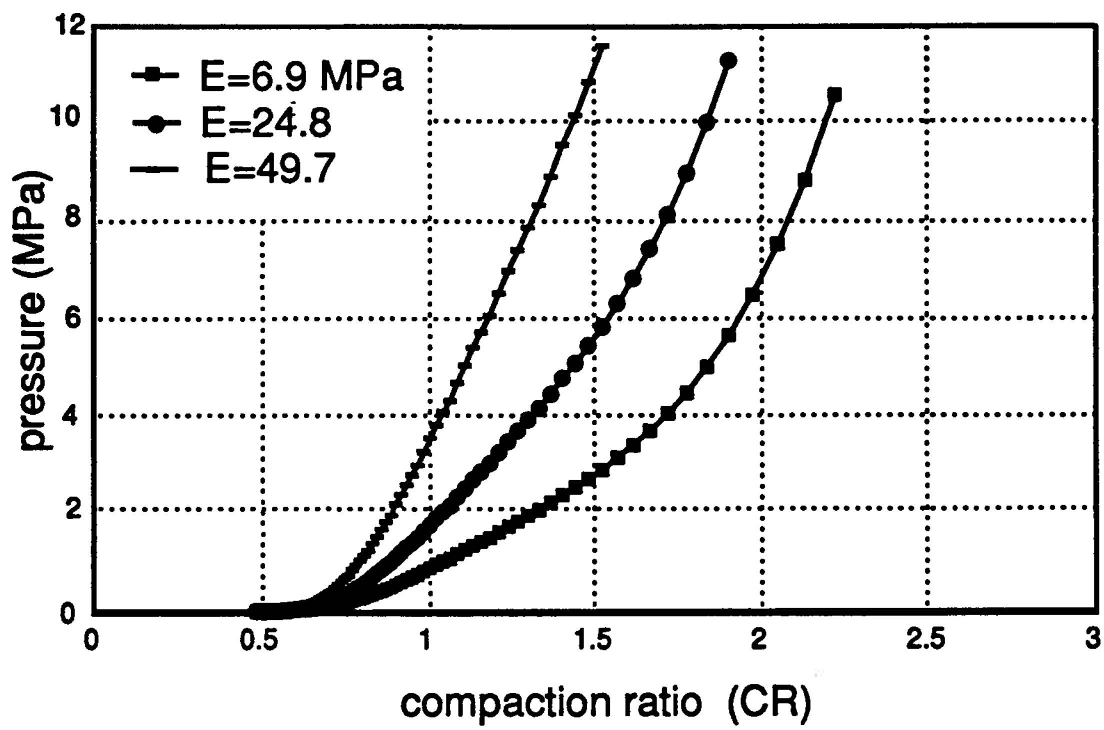

Figure 4.5 Predicted compression response of a random flake mat as affected by flake compression modulus. Flake size and other conditions as in Fig.4.3.

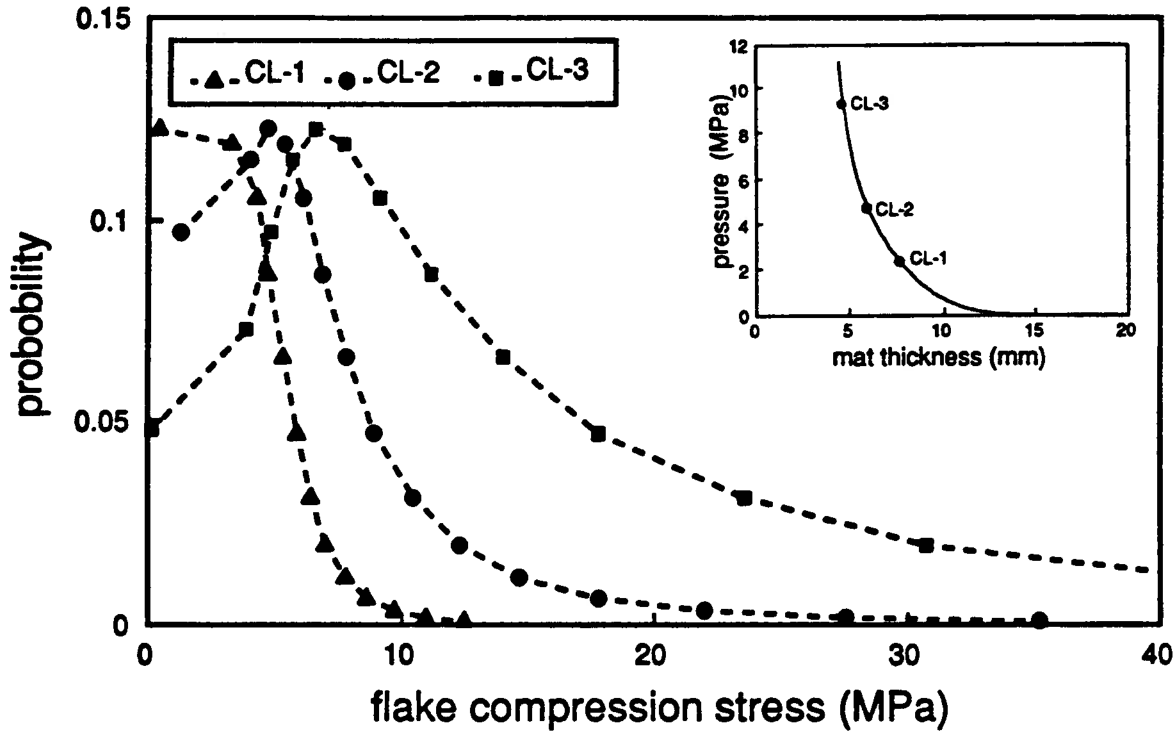

Figure 4.6 Predicted local stress distribution of a flake mat under three different compression levels. Conditions as in Fig.4.3.

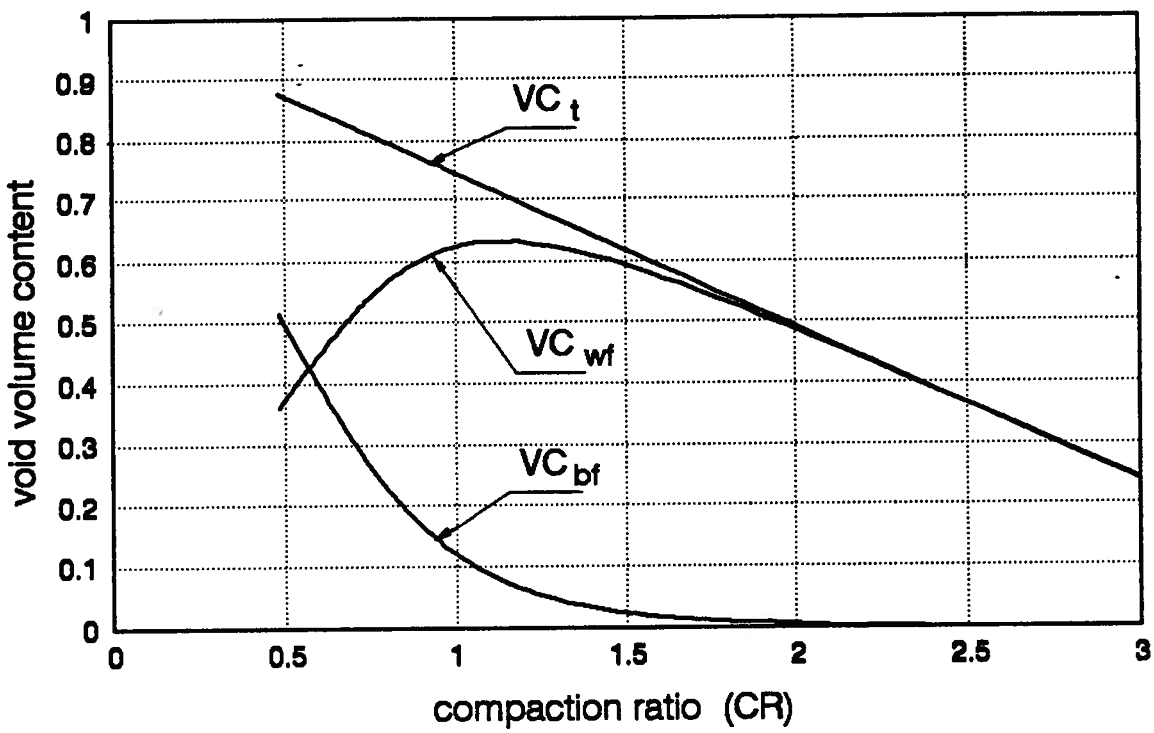

Figure 4.7 Predicted relative volumetric change of total, between- and inside-flake voids in an aspen flake mat under compression. Flake density: 0.38 g/cm^3 and other conditions as in Fig.4.3.

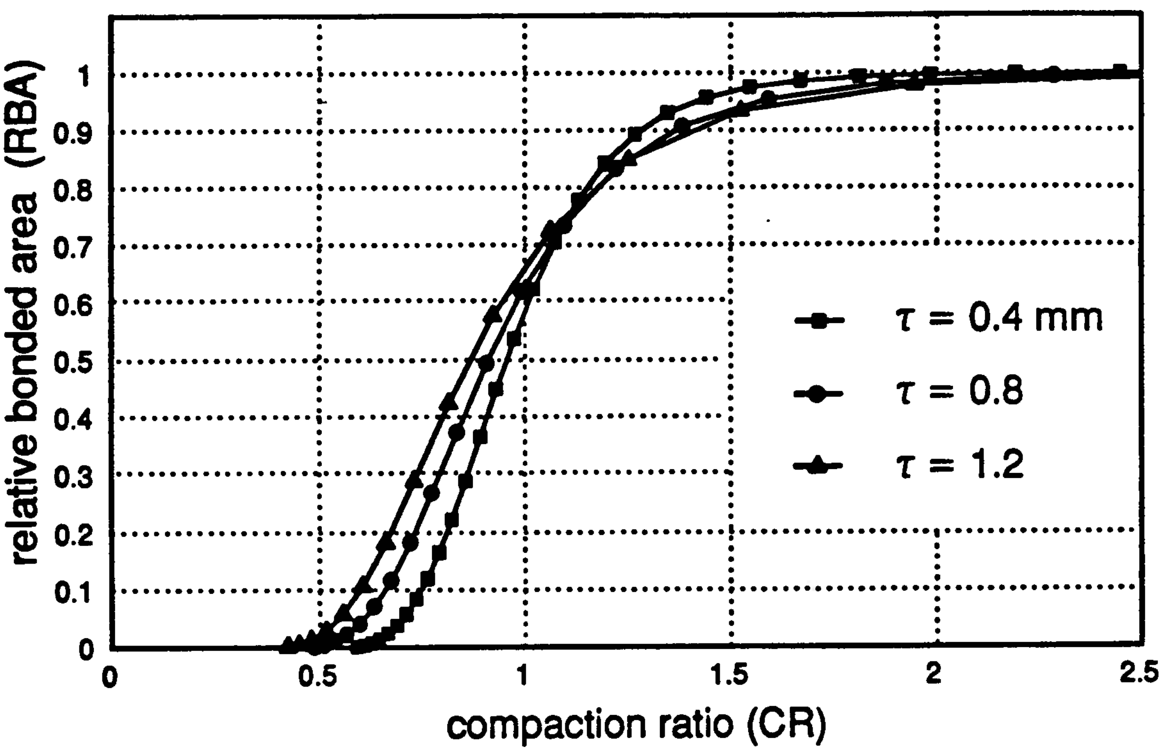

Figure 4.8. Predicted relative change of flake-to-flake bonded area in a flake mat under compression as affected by flake thickness. Other conditions as in Fig.4.3.

CHAPTER V. VISCOELASTICITY OF RANDOM WOOD-FLAKE MATS DURING PRESSING

5.1 INTRODUCTION

In the preceding chapter, the unique compression behavior of a flake mat has been proved to be a combined result of the nonlinear mechanical response of wood under perpendicular-to-grain compression and the random mat structure. Like many other natural or synthetic polymers, wood is a viscoelastic material. Hence a wood-flake mat subjected to compression pressure will also exhibit time-dependent load-deformation characteristics. Mat viscoelasticity affects the vertical density formation in a wood composite panel, and presumably the springback upon press opening and thickness swelling as related to changing moisture conditions.

The main objective of this chapter is to develop a viscoelasticity model for a flake mat in compression. To derive such a model, one could use either a phenomenological approach or a structural approach. While the phenomenological constituent equations are based solely on experimental observations where the material is treated as a continuum, the structural ones are obtained from the structure model and the constituent properties. In the following analysis, the structural procedure is applied and the mat viscoelasticity model is based on the known mat structure and the nonlinear viscoelastic properties of wood flakes. Such a model offers a structure-properties relationship.

5.2 BACKGROUND

5.2.1 Viscoelasticity of Wood and other Cellular Materials

The viscoelasticity of wood has long been recognized as one of the most important properties in structural applications where wood is under long term static loading, or in the press drying process where wood is under a static pressure and subject to high temperature and humidity. In these situations, wood can be adequately treated as a linear viscoelastic material, because the applied load is under certain limits within the linear range. A considerable literature has accumulated on linear viscoelasticity of wood, which is represented in several good reviews (Schniewind, 1968; Pentoney and Davidson, 1962; Bodig and Jayne, 1982; Holzer et al, 1989).

During the production of non-veneer wood composites, wood elements coated with thermosetting adhesives are compressed under high pressure to form an integrated panel. Such high pressure in combination with the random mat structure results in a highly nonlinear and nonuniform mechanical response of the flake components.

Youngs (1957) and Kunesh (1961) are two of the earliest researchers who investigated the nonlinear viscoelastic behavior of wood under perpendicular-to-grain compression. Such important phenomena as the time-dependent stress-strain relationship, instantaneous and delayed strain recovery, permanent deformation, and temperature and moisture dependent stress relaxation were observed. These phenomena were related to the destruction of cellular structure within the wood samples. Bolton and Breese (1987) attempted to interpret viscoelastic behavior of wood loaded at right angles to the grain by relating strain development to microstructural change in cell wall material. They concluded that the majority of strain development involved bond breakage and reformation in regions containing less ordered cellulose, hemicellulose and lignin.

The relationship of the nonlinear viscoelastic behavior of wood to its corresponding cellular structure also has been readily observed in other natural and synthetic cellular materials (e.g., Gibson and Ashby, 1988; Meinechke and Clark, 1973; Rusch, 1969). The nonlinearity was attributed to the interaction between linear viscoelastic response of cell wall polymers and geometric nonlinearities of cellular collapse (Meinechke and Clark, 1973; Rusch, 1969). This interpretation along with the relevant nonlinear viscoelasticity model was adopted by Wolcott (1990) to explain response of wood flakes during the pressing of wood composites.

According to these researchers, the nonlinear stress relaxation modulus $E(t)$ of synthetic cellular polymers and wood was adequately predicted by multiplying the linear response of the polymer, $E'(t)$, by nonlinear strain function, $\varphi(\varepsilon)$, or:

$$E(t)=\varphi(\varepsilon)E'(t)=\varphi(\varepsilon)Kt^{-\xi} \tag{5.1}$$

where the strain function, $\varphi(\varepsilon)$, depends only on strain ε but not on time t. The constant K is the relaxed modulus of the material at a certain time (usually 1 sec.). The constant ξ is the slope in the double logarithmic plot of modulus $E(t)$ versus time elapsed t, which is indicative of the rate of stress relaxation. It depends only on the cell wall polymer.

The usefulness of Eq.(5.1) implied a possibility of extending the linear Boltzmann superposition principle to modelling the response of nonlinear cellular material to successive loads, provided that the stress-relaxation rate ξ was not too large (Meinecke and Clark, 1973). The stress at any time t was then given by:

$$\sigma(t)=\varepsilon_0 E(t)+\varphi(\varepsilon)\int_0^t E(t-t')\frac{d\varepsilon(t')}{dt'}dt' \qquad (5.2)$$

where ε_0 and $\varepsilon(t)$ are the initial strain and the strain at time t, respectively.

Compared with stress relaxation, the nonlinear creep response of cellular materials seems much more complicated. So far, according to the available literature, there has been very limited success in developing a compression creep model for wood (Wolcott, 1990) or other cellular materials (Meinecke and Clark, 1973; Gibson and Ashby, 1988). Under this circumstance, the focus of model development in the present work will be on stress relaxation, whereas the creep response of wood flakes and mats will be experimentally measured and compared.

5.2.2 Rheological Behavior of Wood Composite Mats

Despite its critical importance to the formation of composite boards, the rheological behavior of wood-furnish mats in compression has only been investigated to a very limited extent. Wolcott (1990) used theories of the viscoelastic behavior of amorphous polymers (Ferry, 1980) to explain the vertical density profile formation in flakeboard. The glass transition temperature of the lignin component in wood was estimated from experimentally measured temperature and vapour gas pressure at different locations inside the flake mat during hot-pressing. Mat strain development was related to the external pressure profile through the difference between the actual flake temperature and the calculated glass transition temperature. The information provided from this analysis is insightful but only qualitative. A quantitative prediction of density gradient formation in wood composites certainly requires a more comprehensive treatment of wood viscoelasticity.

More recently, the thermo-hydro rheological behavior of randomly-formed wood fiber mats was experimentally investigated by Ren (1991). Samples were measured under a wide range of temperature and moisture content conditions encountered in a typical wood composite hot-pressing process. The data was then fit to a five-element "spring and dashpot" model. The model parameters were determined as functions of the temperature, moisture content conditions inside the mat, and the mat density. Such a model has an immediate capability for predicting compression strain development in fiber mats of the same structure and constituents as the tested samples. However, the model's predictability for other types of wood furnish mats is doubtful because wood furnish type and mat structure can strongly affect the mechanical response of the mat. To incorporate the effects of such mat production factors as wood element geometry, orientation and species, a more rigorous and integrated approach is needed.

5.3 A STRUCTURAL MODEL OF FLAKE-MAT STRESS RELAXATION

As discussed in section 4.2.3, the total stresses imposed on a mat with thickness of H, σ_n, are supported only by a part of the mat areas, where the effective flake coverage count i is greater than H/τ (τ: flake thickness). Similar to Eq.(4.5), the relationship between the time-dependent mat stresses, $\sigma_n(t)$, and the stresses shared by local flake columns, $\sigma_i(t)$, is given by the following expression:

$$\sigma_n(t) = \sum_{i=H/\tau}^{\infty} \sigma_i(t) p_f(i) \tag{5.3}$$

where the relative area of i-flake columns, $p_f(i)$, is a Possion variable given by Eqs.(4.2) and (4.3).

For a standard relaxation test in which a compression deformation is suddenly applied to a flake mat, the mechanical responses of supporting flake columns take place simultaneously, i.e., the column stress $\sigma_i(t) = 0$, for $t < 0$ and $\sigma_i(t) = \sigma_{i\,max}$ for $t > 0$. The stress relaxation in individual flake columns is then given by Eq.(5.1). Thus the mat stress relaxation can be further defined by substituting $p_f(i)$ and $\sigma_i(t)$ in Eq.(5.3) with Eqs.(4.2) and (5.1), respectively, i.e.,

$$\sigma_n(t) = Ke^{-\gamma\lambda\omega} \sum_{i=H/\tau}^{\infty} \frac{\varphi(\varepsilon_i)\,\varepsilon_i\,(\gamma\lambda\omega)^i}{i!}\, t^{-\xi_i} \tag{5.4}$$

During hot-pressing, compression load is usually applied successively onto the mat. The strain histories of individual flake columns in a mat vary in accordance with their flake coverage counts. The higher the flake count, the sooner the column areas come under compression. To calculate the compression stresses in flake columns produced under the linear loading strain histories as shown in Fig.5.1, we need to resort to the extended Boltzmann superposition principle as given by Eq.(5.2). But first, the strain and time parameters pertinent to the loading histories need to be determined.

The maximum strain in the highest effective flake columns, ε_N, is given by:

$$\varepsilon_N=\frac{N\tau-H}{N\tau} \tag{5.5}$$

where N is the number of flakes contained in the highest effective flake columns. It can be estimated by designating $p(i)=0.001$ in Eq.(3.1) and solving the equation for i ($=N$).

Likewise, the maximum compression strain in i-flake columns, ε_i, is given by:

$$\varepsilon_i=\frac{i\tau-H}{i\tau} \tag{5.6}$$

If a flake mat is compressed with constant crosshead speed V during the initial loading period, the time required for all supporting flake columns to reach their maximum strain, t_0, is determined by:

$$t_0=\frac{N\tau-H}{V} \tag{5.7}$$

The time period from the external load being applied onto the mat to i-flake columns coming under compression, t_i', is given by:

$$t_i'=\frac{N\tau-i\tau}{V} \tag{5.8}$$

The time taken for i-flake columns to reach their maximum strain, t_i, is obtained by:

$$t_i=\frac{i\tau-H}{V} \tag{5.9}$$

Thus the strain history in i-flake columns can be described by the following expression:

$$\begin{aligned} \varepsilon_i(t) &= 0 && (t<t_i') \\ \varepsilon_i(t) &= \frac{t-t_i'}{t_i}\varepsilon_i && (t_i'<t<t_0) \\ \varepsilon_i(t) &= \varepsilon_i && (t>t_0) \end{aligned} \tag{5.10}$$

Taking derivative of $\varepsilon_i(t)$ with respect to t in Eq.(5.10) and substituting ε_i and t_i with Eq.(5.6) and (5.9) yields:

$$\begin{aligned} \frac{d\varepsilon_i(t)}{dt} &= \frac{V}{i\tau} && (t_i'<t<t_0) \\ \frac{d\varepsilon_i(t)}{dt} &= 0 && otherwise \end{aligned} \tag{5.11}$$

Now, we can use the extended Boltzmann superposition integral to calculate the flake column stresses. Since the stress of wood flakes under a standard relaxation test is given by Eq.(5.1), the integral (Eq.(5.2)) for determining the stress under successive loading strain histories as described by Eq.(5.10) and Eq.(5.11) then becomes, in the range $t < t_0$,

$$\begin{aligned} \sigma_i(t) &= 0+\varphi(\varepsilon_i)\int_{t_i'}^{t} K(t-t')^{-\xi_i}\frac{V}{i\tau}dt' \\ &= \frac{KV\varphi(\varepsilon_i)}{i\tau(1-\xi_i)}(t-t_i')^{1-\xi_i} \end{aligned} \tag{5.12}$$

For $t \geq t_0$, the integral becomes:

$$\begin{aligned} \sigma_i(t) &= 0+\varphi(\varepsilon_i)\int_{t_i'}^{t_0} K(t-t')^{-\xi_i}\frac{V}{i\tau}dt' \\ &= \frac{KV\varphi(\varepsilon_i)}{i\tau(1-\xi_i)}\left[(t-t_i')^{1-\xi_i}-(t-t_0)^{1-\xi_i}\right] \end{aligned} \tag{5.13}$$

Substituting $\sigma_i(t)$ in Eq.(5.3) with Eqs.(5.12) and (5.13) and $p_f(i)$ with Eq.(4.2) yields:

$$\sigma_n(t) = \frac{KVe^{-\gamma\lambda\omega}}{\tau} \sum_{i=H/\tau}^{\infty} \frac{\varphi(\varepsilon_i)(\gamma\lambda\omega)^i}{i(1-\xi_i)\,i!} (t-t_i')^{1-\xi_i}$$
$$(t<t_0)$$
$$\sigma_n(t) = \frac{KVe^{-\gamma\lambda\omega}}{\tau} \sum_{i=H/\tau}^{\infty} \frac{\varphi(\varepsilon_i)(\gamma\lambda\omega)^i}{i(1-\xi_i)\,i!} [(t-t_i')^{1-\xi_i} - (t-t_0)^{1-\xi_i}] \tag{5.14}$$
$$(t \geq t_0)$$

5.4 MATERIALS AND EXPERIMENTAL PROCEDURE

The objectives of this experiment are fourfold to test the viscoelasticity of wood flakes under transverse compression to develop a database needed for predicting mat stress relaxation, to measure the stress relaxation of flake mats and compare with model prediction, and to relate the creep response of flake mats to that of wood flakes.

All mat samples were hand-felt and made of aspen (*Populus tremuloides*) flakes with average length 37.51 mm, width 6.09 mm and thickness 0.79 mm. Each sample weighed 72 g and was of 152 mm by 152 mm square. For testing the viscoelastic properties of wood, 25 mm by 25 mm square flakes with thickness 0.79 mm were hand-cut. To reduce the effect of wood variation, the samples were prepared by randomly selecting six flakes and stacking them together. A more detailed description of sample preparation procedures was presented in Section 4.3.1.

All samples were conditioned to a 9.1% moisture content at 20 °c before being tested on a MTS testing system at room temperature and humidity conditions. Stress and strain were measured and acquired in real time through a computer data acquisition system.

The stress relaxation tests on wood flakes were conducted by suddenly imposing strain on a 6-flake stack and then maintaining this strain for 10 minutes. Several strain levels were chosen to represent different stress-strain characteristics. During the mat stress relaxation tests, a crosshead loading speed of 5 mm/sec was used.

To test the creep response of wood flakes, pre-determined stress levels were suddenly applied to 6-flake stacks and maintained for 10 minutes. The flake mat creep tests were carried out by first imposing pre-defined stresses at a constant rate of 5 MPa/sec and then maintaining the stress levels for 10 minutes.

5.5 RESULTS AND DISCUSSION

5.5.1 Flake Stress Relaxation

The stress-strain curve of wood in perpendicular-to-grain compression is generally nonlinear. Thus the stress relaxation modulus $E(t)$ is not only time dependent but also strain dependent. This nonlinear stress relaxation behavior was evaluated by testing the relaxed modulus $E(t)$ at different strain levels, as shown in Fig.5.2a. The double logarithmic plots of modulus $E(t)$ versus time were straight lines with varying slopes (Fig.5.2b). Therefore, the modulus $E(t)$ model as given by Eq.(5.1) is generally valid and the stress relaxation rates as indicated by slopes of the lines in Fig.5.2 vary with the strain levels. The former finding agrees with the results reported by many other researchers (Youngs, 1957; Kunesh, 1961; Rosa and Fortes, 1988; Wolcott, 1990). However, the latter one, although suggested by the observations from Youngs (1957) and Kunesh (1961), is not consistent with the results cited by Rosa and Fortes (1988) and Wolcott (1990).

The fact that stress relaxation rate varies with the strain level may be explained using free volume theory in polymers (Ferry, 1980). This theory states that the viscoelasticity of a polymer is ultimately attributed to the presence of free volume, which may be present as holes of the order of molecular dimensions or smaller voids associated with packing irregularities. In the case of wood, such free volume exists in the amorphous sites in the cell walls. The amount of free volume in wood is affected by imposed stresses, which can results in bond breakage (Kauman, 1966; Bolton and Breese, 1987). The way stresses influence the formation of free volume depends on both the stress mode and magnitude. Generally, tensile, shear, bending and buckling stresses can promote the formation of free volume, whereas compression stresses hinder the development of free volume (Ferry, 1980). It is known that wood-cell-wall polymer subjected to transverse compression can sequentially experience three different stress modes: bending, buckling and compression (Gibson and Ashby, 1988). Accordingly, free volume in the cell wall polymer increases with loading strain during linear elastic, nonlinear elastic or plastic buckling ranges and decreases during the cell wall densification range. As a result, the compression stress relaxation rate increases with the strain level in the first two ranges and decreases in the last range (Fig.5.2).

5.5.2 Mat Stress Relaxation

It is known from Chapter IV that the stress-deformation relationship of a randomly formed flake mat in compression is nonlinear. The nonlinear stress relaxation of mats was determined by compressing the mat samples under sustained deformation at different loading levels, as indicated in Fig.5.3a. The log-log plots of the stress relaxation versus time are also straight lines (Fig.5.3b) and the line slopes indicating the stress-relaxation rates decrease with the loading levels. This macro-mechanical response of a mat appears to be related directly to the stress relaxation behavior of its constituents--wood flakes.

The stress relaxation relationship between a mat and flakes was examined by predicting the time-dependent stresses in the mat from the viscoelasticity of flakes. The log-log plots of the predicted mat stress relaxation versus time (Eq.5.14) are shown in Fig.5.4. The model prediction in trend follows the results from the experimental observation (compare Fig.5.3 with Fig.5.4). It should be noted that the flake stress relaxation rate ξ_i, an important input parameter to the model, was estimated from the limited experimental database obtained in this work. The heterogeneity of wood flakes and especially the variation of climatic conditions under which the tests were conducted, suggest more controlled tests are needed in order to more accurately determine the flake viscoelastic parameters. The lack of such controlled tests is believed to largely contribute to discrepancies in stress-relaxation rate between the model prediction (Fig.5.4) and the experimental observation (Fig.5.3).

One of the prediction capabilities of the proposed model is that it can calculate the effect of the loading rate (or press closing rate) on the time-dependent stresses in a mat. Figure 5.5, for example, shows that higher loading rate results in higher maximum stress in the mat for a given mat compression strain and consequently more stress relaxation. Despite the differences in the initial stress history, the asymptotic stress relaxation approaches a common level, which is a function of the mat strain level and independent of the loading strain rate.

5.5.3 Creep

The nonlinear creep behavior of flakes was tested by suddenly applying and maintaining different levels of stresses in 6-flake stacks which represented different characteristics of compression stress-strain relationship. The loading levels and their corresponding relative creep strain are shown in Fig.5.6. The highest creep strain is found to be associated with the cell wall yield point (Wolcott, 1991; Rosa and Fortes, 1988), where wood starts buckling. The extent to which flakes deform under sustained stresses, however, decreases as the stress level increases. The creep in both the linear range and the highly densified range is considerably lower than that in the cell wall buckling range.

While relative creep strain has been commonly used to describe creep behavior for wood and most other materials, it seems unsuitable for a highly porous flake mat. The mat creep described by the relative strain as shown in Fig.5.7 is almost an order less than that of solid wood flakes of which the mats are made. The small mat creep strain directly results from considerably higher initial deformation, which is, in turn, due to the loose mat structure.

To compare creep behavior between solid wood flakes and porous flake mats on the same density basis, a new term -- relative creep compaction ratio is used. Note that compaction ratio, *CR*, is the ratio of current material density to original wood density and is indicative of the material solidity. Thus, the relative creep compaction-ratio, *RCR*, is defined by:

$$RCR=\frac{CR(t)-CR(0)}{CR(0)} \tag{5.15}$$

where *CR(t)* and *CR(0)* are respectively the compaction ratio at time *t* and at time 0.

The relative creep compaction ratio of wood flakes and flake mats are compared in Fig.5.8, from which some noticeable changes as a result of using *RCR* evaluation can be seen. Firstly, the effect of loading stress levels on flake *RCR* is not the same as that on relative creep strain, for example, "line b" representing the highest relative creep strain in Fig.5.6b does not give the highest relative creep compaction ratio in Fig.5.8a. This is because the sensitivity of density change with compression deformation (neglecting the lateral expansion of compressed wood) is proportional to the initial material density. Higher loading stress levels result in higher mat density, therefore, the rate at which the mat density increases with further deformation becomes faster. Secondly, the creep behavior of flake mats in terms of *RCR* is quantitatively comparable to that of wood flakes (compare Fig.5.8a with Fig.5.8b). It appears that the macro-creep *RCR* of a mat in compression is an average response of its constituents under the same loading mode.

5.6 CONCLUSIONS

A structural model for predicting the stress relaxation of a flake mat in compression has been developed. This model explicitly relates the time-dependent stresses in a compressed mat to the nonlinear stress relaxation behavior of solid wood flakes. The predicted results agree generally with the experimental observations despite some quantitative discrepancies in the relaxation rates, which may be due to the lack of accurate estimation of original flake viscoelastic properties as the model input parameters.

The experimental results obtained in this work confirm that the double logarithmic relationship between flake stresses and time is linear. The relaxation rate varies with the loading strain levels. This phenomenon seems to be related to the free volume change in the cell wall polymers of wood flakes under different compression levels.

The creep behavior of wood flakes and flake mats was tested and compared. The comparable creep behavior between two materials is found by using the evaluation of relative creep compaction ratio instead of the more common relative creep strain. The creep of a flake mat seems to be affected by its constituents through their average viscoelastic responses.

REFERENCES

1. Bodig, J. and B. A. Jayne. 1982. Mechanics of wood and wood composites. Van Norstrand Reinhold company. New York. 712pp.

2. Bolton, A. J. and M. C. Breese. 1987. Time dependent strain development of wood loaded at right angles to the grain. Wood and Cellulosics. John Wiley and Sons. New York. 664pp.

3. Ferry, J. D. 1980. Viscoelastic properties of polymers. Third edition. John Wiley and Sons, Inc. New York. 641 pp.

4. Gibson, L. J. and M. F. Ashby. 1988. Cellular solids: Structure and properties. Pergamon press, New York. 357 pp.

5. Holzer, S. M., J. R. Loferski and D. A. Dillard. 1989. A review of creep in wood: concepts relevant to develop long-term behavior predictions for wood structures. Wood and Fiber Sci. 21(4): 376-392.

6. Kauman, W. G. 1966. On the deformation and setting of the wood cell wall. Holz als Roh- u. Werkstoff. 24(11): 551-556.

7. Kunesh, R. H. 1961. The inelastic behavior of wood: A new concept for improved panel forming processes. For. Prod. J. 9: 395-406.

8. Meincke, E. A. and R. C. Clark. 1973. Mechanical properties of polymer foams. Technomic. Westport. CT. 105 pp.

9. Pentoney, R. E. and R. W. Davidson. 1962. Rheology and the study of wood. Forest. Prod. J. 12(5): 243-248.

10. Ren, S. 1991. Thermo-hydro rheological behavior of materials used in the manufacture of wood-based composites. Ph.D. dissertation. Department of Forest Products, Oregon State University. 240 pp.

11. Rosa, M. E. and M. A. Fortes. 1988. Stress relaxation and creep of cork. J. Mat. Sci. 23: 35-42.

12. Rusch, K. C. 1969. Load-compression behavior of flexible foams. J. Appl. Polym. Sci. 13: 2297-2311.

13. Schniewind, A. P. 1968. Recent progress in the study of the rheology of wood. Wood Sci. and Technol. 2: 188-206.

14. Wolcott, M. P. 1990. Modelling viscoelastic cellular materials for the pressing of wood composites. Ph.D. dissertation. Department of Wood Science and Forest Products, Virginia Polytechnic Institute and State University.

15. Youngs, R. L. 1957. The perpendicular-to-grain mechanical properties of red oak as related to temperature, moisture content, and time. U.S. FPL. Report No. 2079.

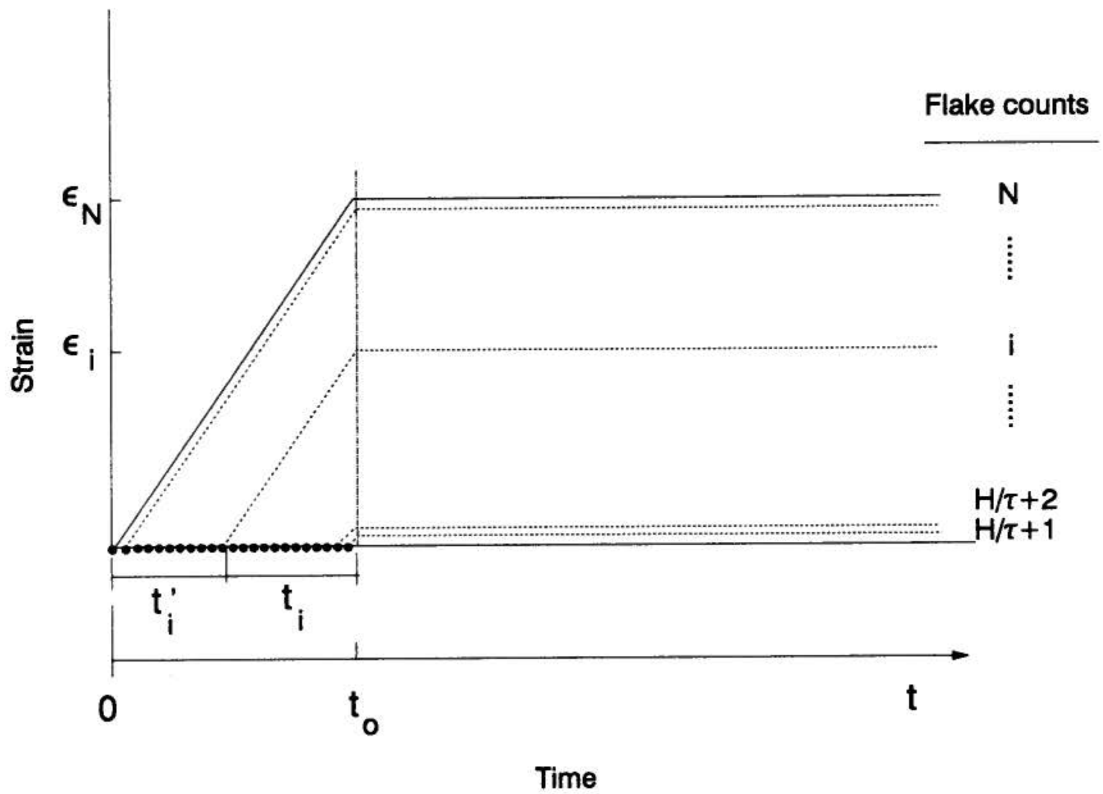

Figure 5.1 Linear loading strain histories of flake columns in a mat. t'_i = time elapsed before i-flake columns become under compression; t_i= time taken for i-flake columns to reach maximum strain ϵ_i.

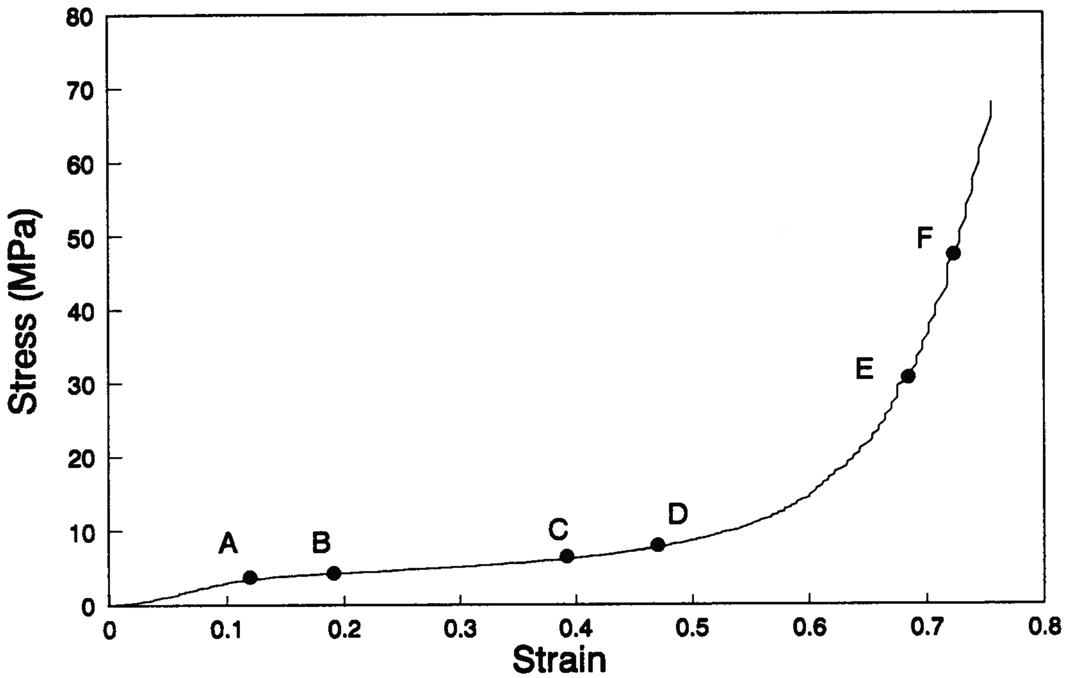

Figure 5.2 (a) The strain levels imposed during flake stress relaxation tests, as indicated in a stress-strain curve.

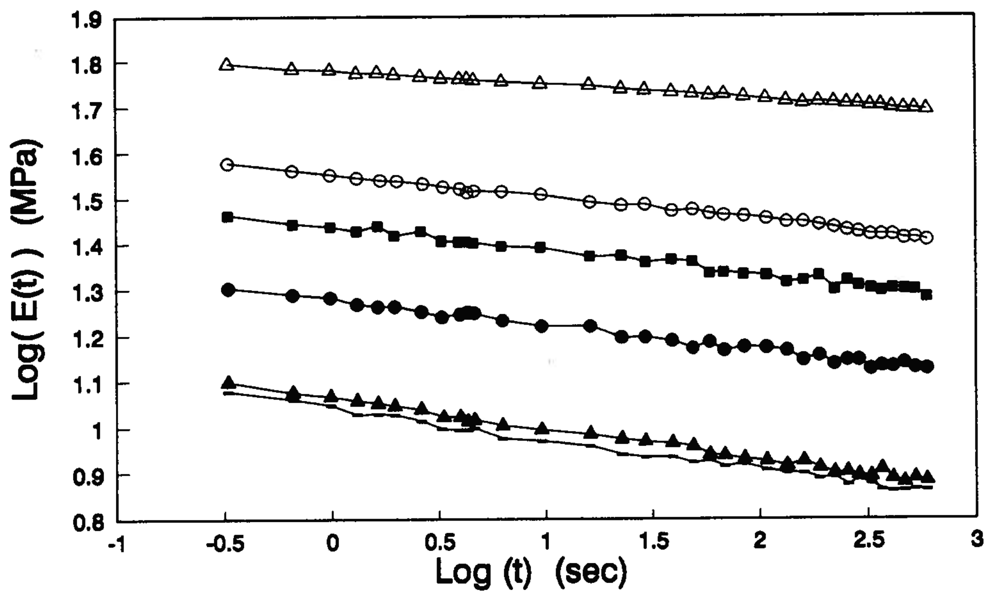

Legend	A	B	C	D	E	F
Slope	-.0554	-.0573	-.0645	-.0654	-.0528	-.0305

Figure 5.2 (b) Double logrithm plots of stress relaxation in 6-layer flake columns in compression.

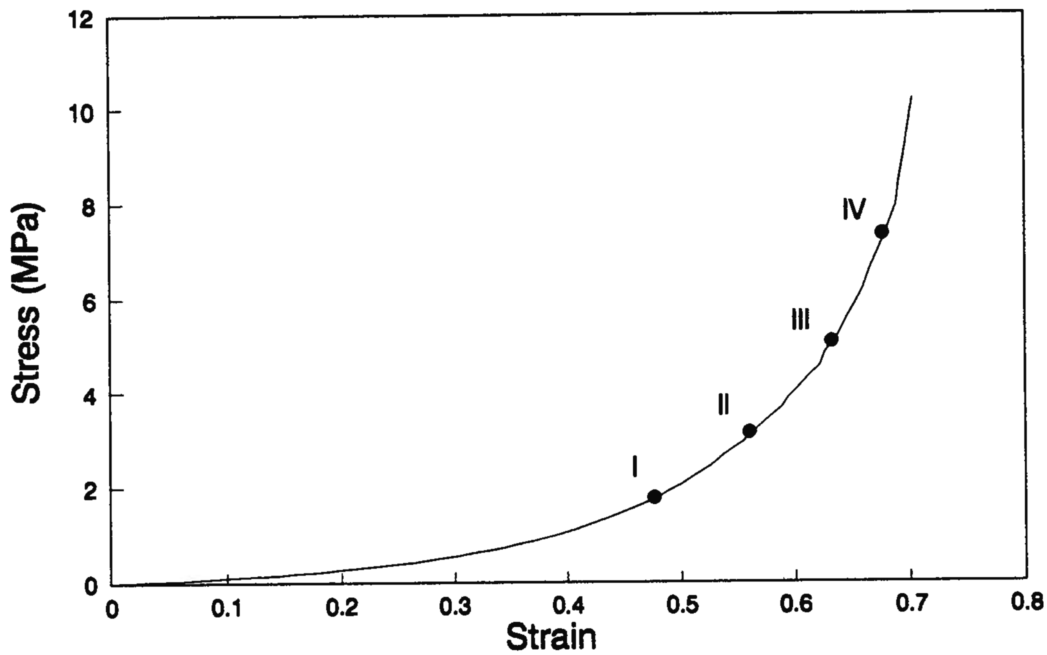

Figure 5.3 (a) The strain levels imposed during mat stress relaxation tests, as indicated in a stress-strain curve.

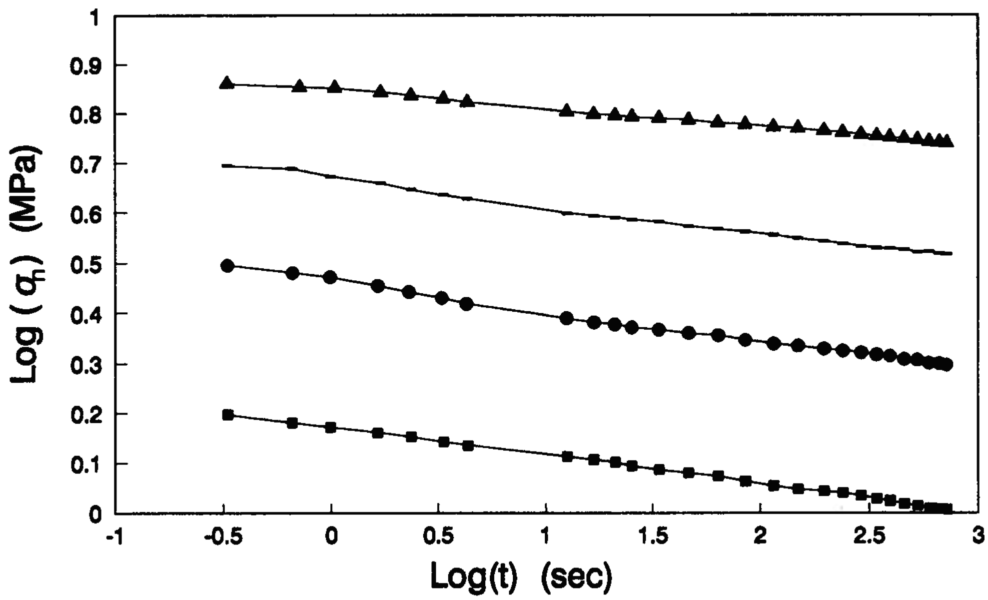

Legend	I	II	III	IV
Slope	-.0586	-.0572	-.0527	-.0377

Figure 5.3 (b) Double logrithm plots of experimentally measured stress relaxation in flake mats in compression.

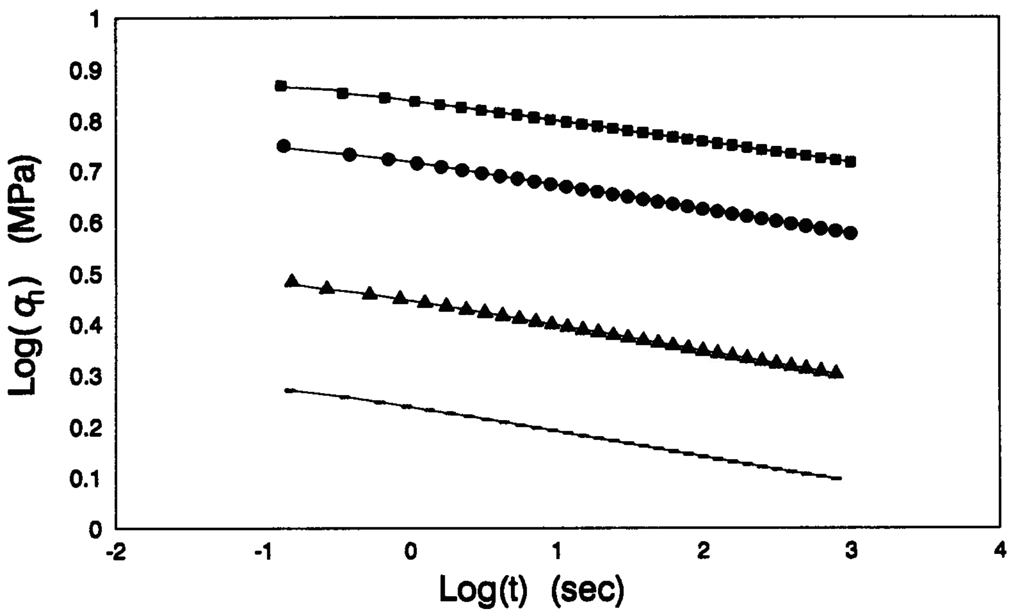

Legend	—	—▲—	—●—	—■—
Strain level	0.49	0.56	0.67	0.7
Slope	-.0483	-.0482	-.0456	-.0397

Figure 5.4 Double logrithm plots of predicted stress relaxation in flake mats in compression.

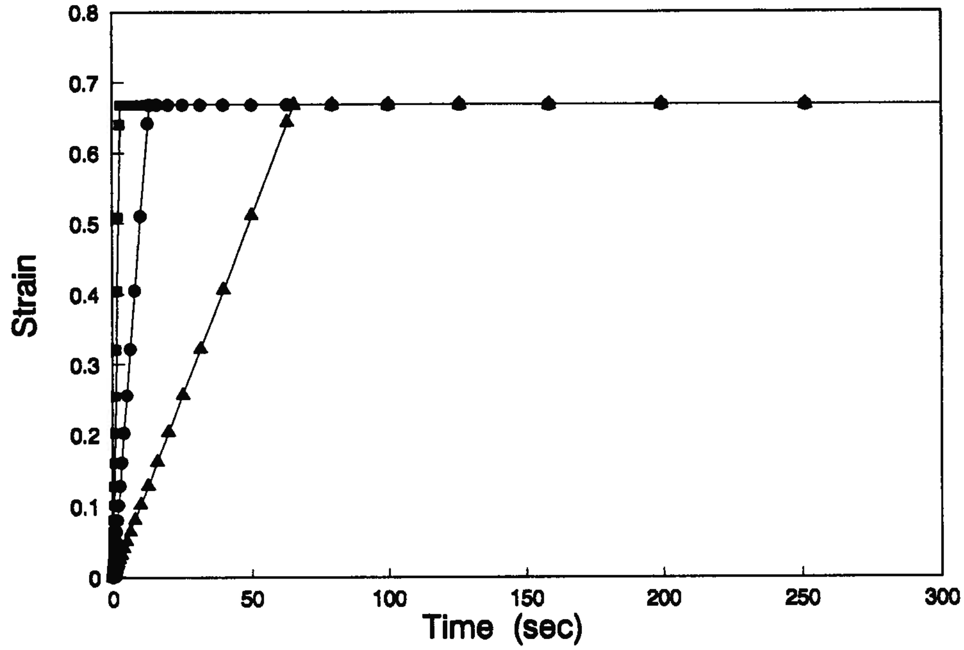

Figure 5.5 (a) Three strain histories in mat stress relaxation tests.

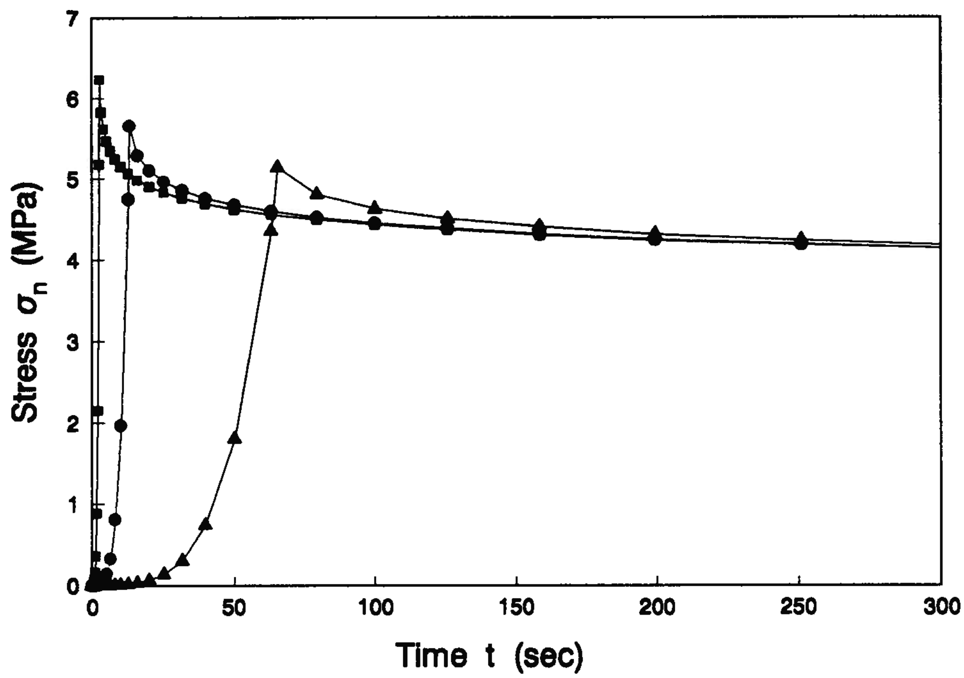

Figure 5.5 (b) Typical predicted time-dependent compression stresses in flake mats as affected by loading rate.

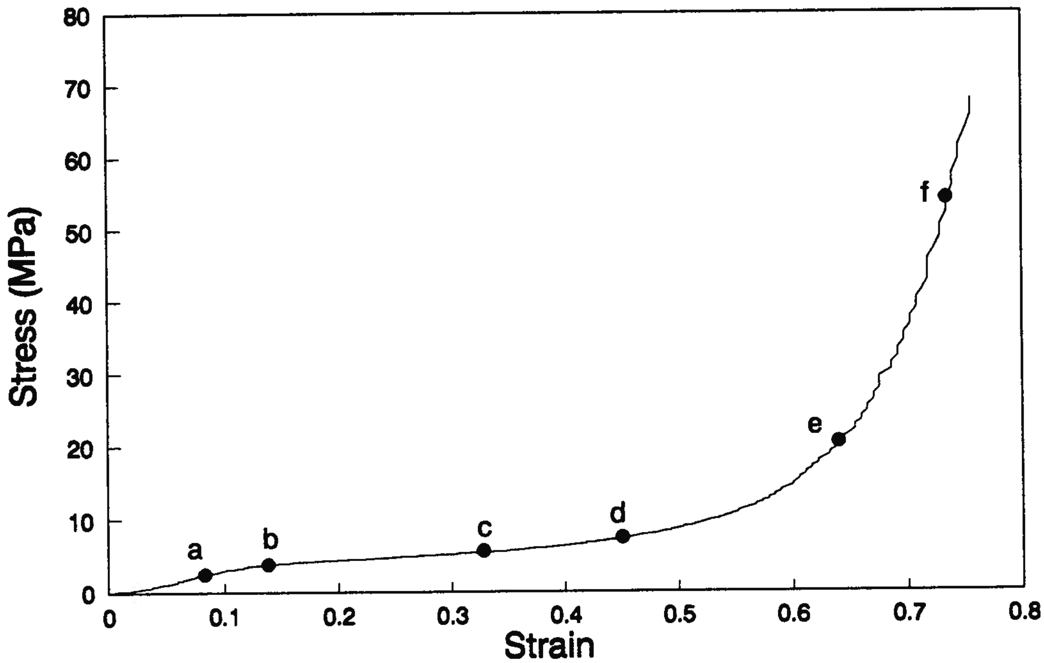

Figure 5.6 (a) The stress levels imposed during flake strain creep tests, as indicated in a stress-strain curve.

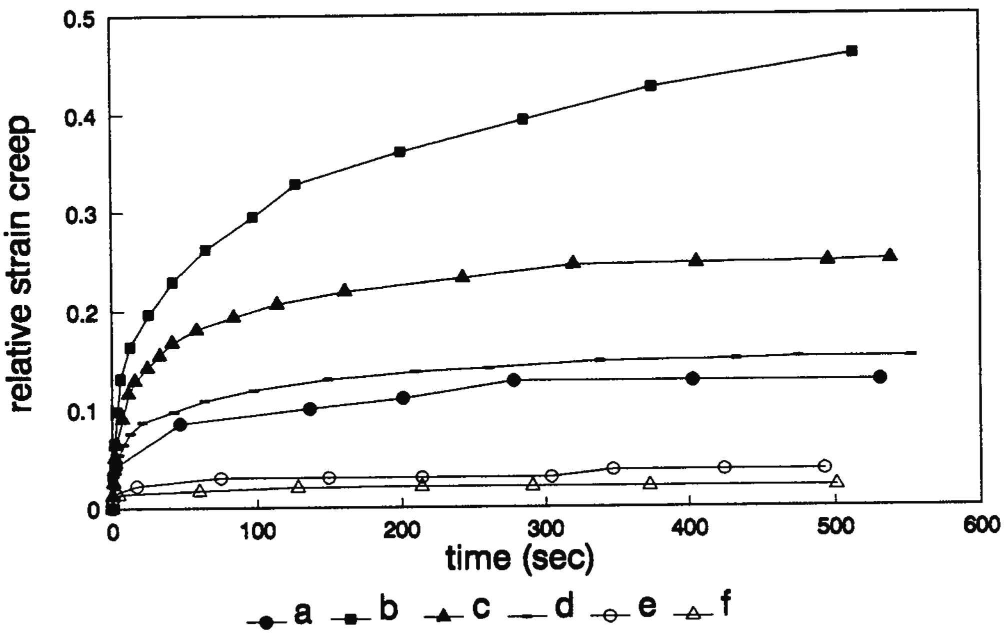

Figure 5.6 (b) Experimental results of relative creep strain ($(\epsilon(t)-\epsilon(0))/\epsilon(0)$) in 6-layer flake columns.

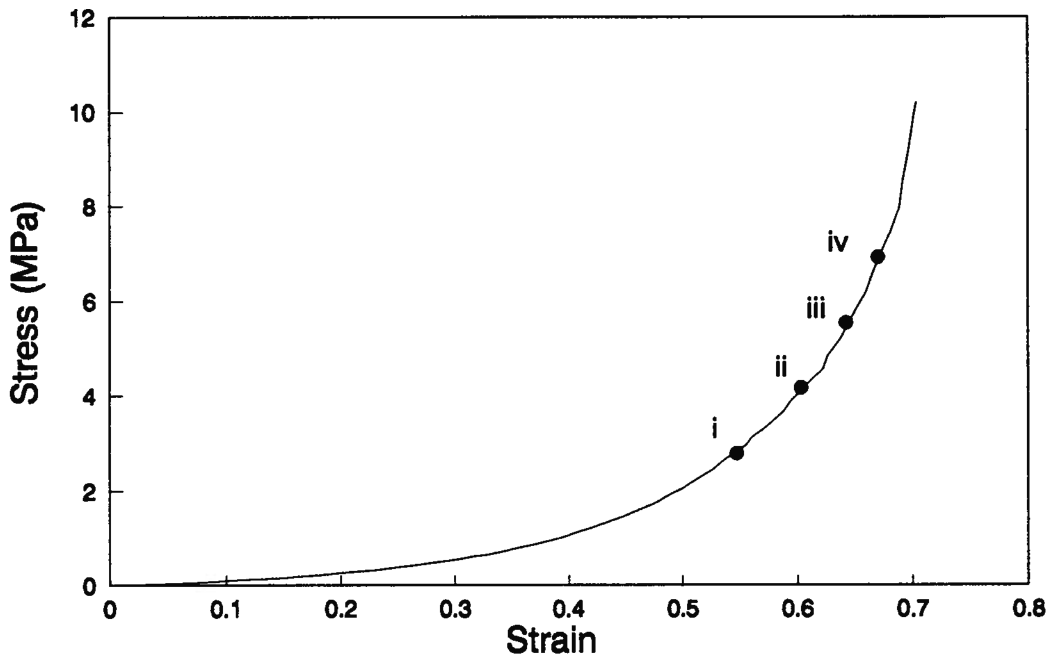

Figure 5.7 (a) The stress levels imposed during mat creep tests, as indicated in a stress-strain curve.

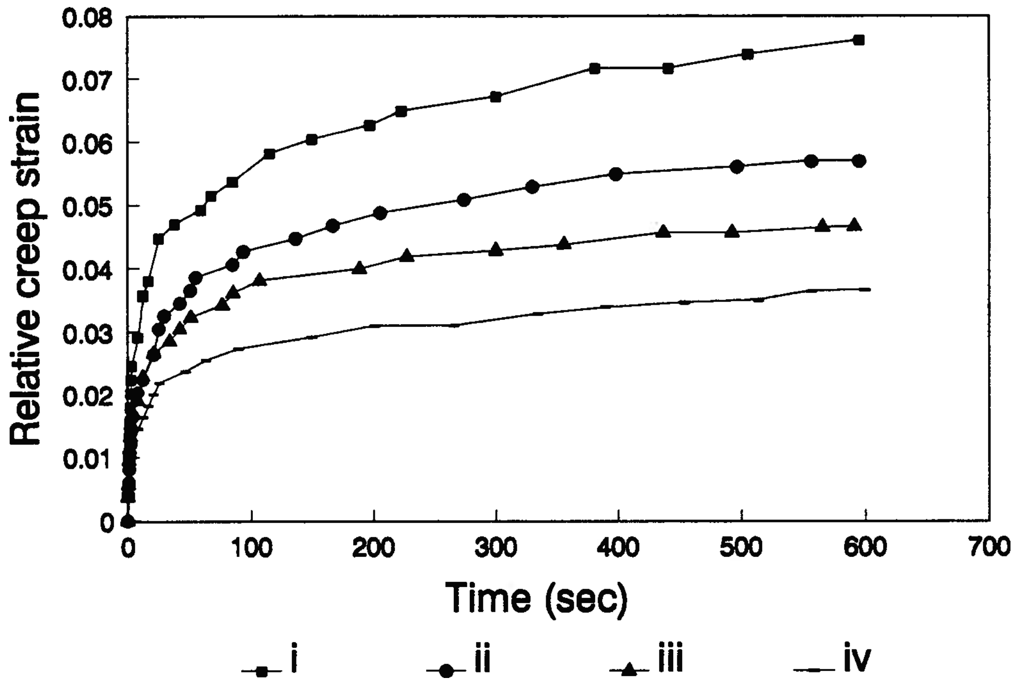

Figure 5.7 (b) Experimental results of relative creep strain ($(\epsilon(t)-\epsilon(0))/\epsilon(0)$) in flake mats.

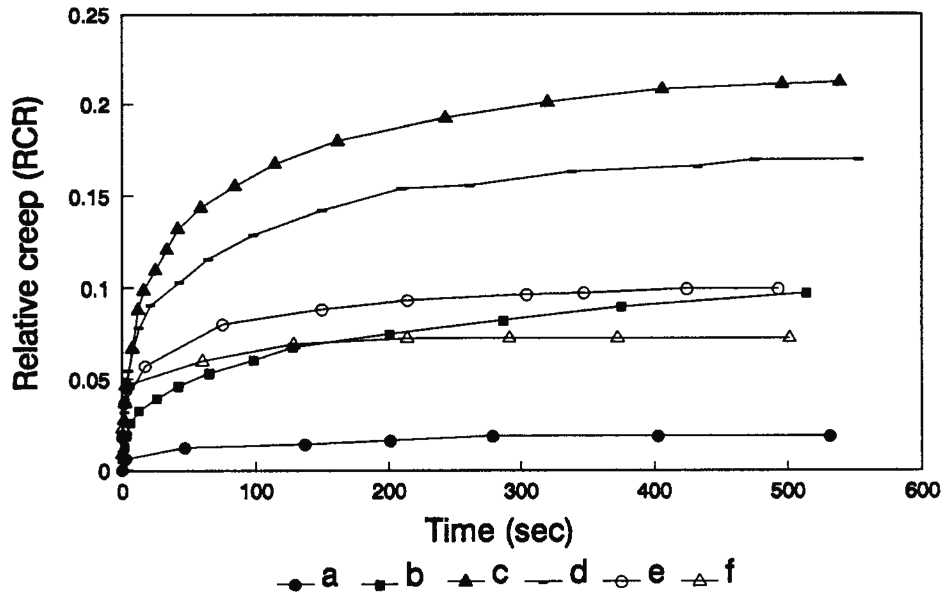

Figure 5.8 (a) Experimental results of relative creep compaction ratio ((CR(t)-CR(0))/CR(0)) in 6-layer flake columns, legends as in Fig.5.6.

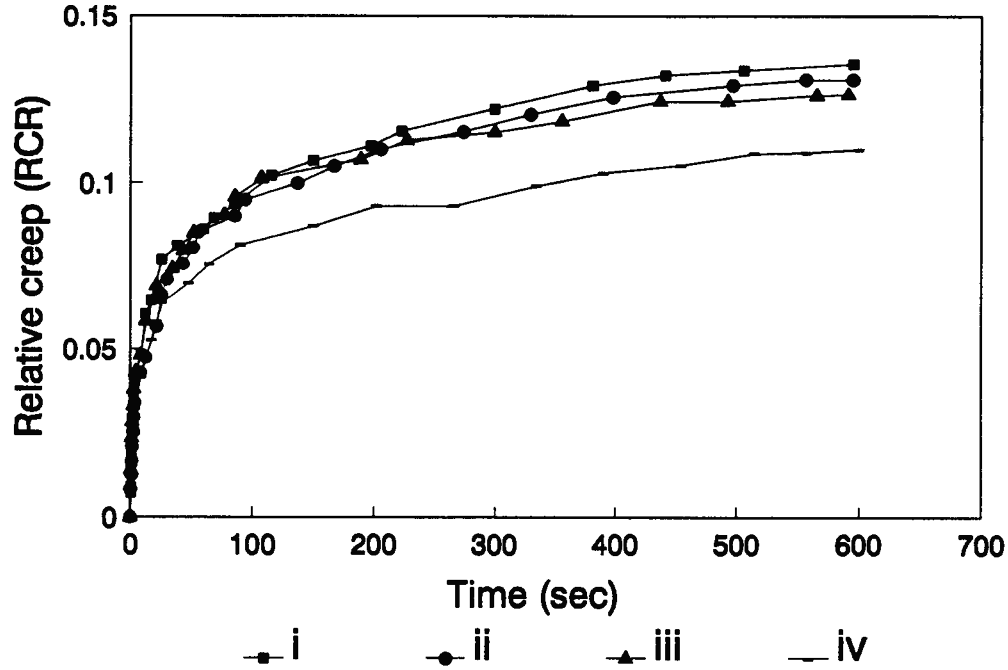

Figure 5.8 (b) Experimental results of relative creep compaction ratio ((CR(t)-CR(0))/CR(0)) in flake mats, legends as in Fig.5.7.

CHAPTER VI. CONCLUDING REMARKS

6.1 GENERAL REMARKS

The present work has, for the first time, developed a theoretical model of mat formation which describes the spatial configuration of wood flakes in a randomly-packed flake mat using the geometric probability theory. The validity of the model has been tested by direct experimental observations and numerical simulations. This model has been then applied to predict the consolidation behaviour of a mat during cold pressing, through which the overall compressive behaviour of a mat is explicitly related to properties of wood flakes and local mat response. This model provides a fundamental approach to correlating the product properties to its production variables and may thereby become a basis for a theory of the wood composite formation. Such a theory is believed to hold a significant promise in fully understanding the wood composite manufacturing process.

6.2 NATURE AND CONTRIBUTIONS OF THE MODEL

1). The commonly used term "random flake mat formation" is rigorously defined in terms of the randomness of flake centroid position and flake orientation. Such a random configuration is tested and verified through the direct measurement of hand-formed mats and, therefore, is legitimately assumed during the model derivation.

2). Flake elements with uniform geometry are considered to lie parallel to the surface of a mat. Such a mat structure best manifests itself in a two-dimensional geometric model.

3). The random mat structure is mathematically described on a probability basis under the assumptions 1) and 2). Flake centroids and flake areal coverage in mat field are found to be Poisson distributed, whereas size of between-flake voids in a multi-layered mat follows a modified exponential distribution.

4). A computer program for simulating and rapidly evaluating mat structural properties is developed using the Monte Carlo technique. The outputs, which is written in both numerical forms and colour image presentations, agrees well with the mathematical predictions. This computer package is believed to play a significant role in the further development of more comprehensive wood-composite formation models.

5). A mathematical model of horizontal density variation in a random flakeboard is presented using random fibre network theory. This model rigorously correlates the local flakeboard density variation to sampling zone size, flake geometry, original wood density, flakeboard compaction ratio and thickness. The information provided by this model may well lead to the prediction of variations of other physical and mechanical properties in a flakeboard panel.

6). A theoretical model for predicting compression behaviour of a randomly formed wood flake mat is also developed based on the prior knowledge of mat structure and fundamental mechanical concepts. The significance of this model is that overall flake mat behaviour is explicitly related to solid wood properties and local mat responses. In addition, equations are derived for calculating the changes of between- and within-flake void volume and inter-flake bonded areas in a mat during pressing. These parameters are useful for fully understanding the mechanism of the hot-pressing process.

7). The compressive viscoelasticity of a mat and solid wood flakes are experimentally tested and compared. A structural model of mat stress relaxation is established. The comparable creep behaviour between a flake mat and flakes is found using a new evaluation term - relative creep compaction ratio.

6.3 FURTHER RESEARCH WORK

Model Modification and Development

The present model has been developed under the assumption of uniform flake geometry and random flake orientation. Introducing a distribution or combination of flake sizes into the model can make it better representative of practical conditions. Changing the flake orientation from purely random to non-random distribution will enable the model to simulate the structure of such products as oriented strand board (OSB) and parallel strand lumber (Parallam). Further modelling effort can also be given to extend the present two-dimensional model to a three-dimensional one to improve the accuracy of characterizing between-flake void sizes in a mat.

The predictability of the mat compression model may be improved if the effect of flake bending stresses is incorporated. Further research is also needed to make the present mat viscoelasticity model a complete one.

Experimental Tests

Perhaps the bigger challenge in further studies in this area is to develop effective methodologies and tools to form and test the mat structure. In this regard, a robotic mat forming system combined with a X-ray detector and an image analyzer is believed to be very useful.

As for the mat compression behaviour, an environmental chamber, which can be mounted on a MTS controlled press, is essential for carrying out temperature-elevated sample tests. Both solid wood flakes and flake mats need to be tested under the same conditions in order to make quantitative comparisons.